

Short Term High Quality Studies to Support Activities under the Eastern Partnership

HiQSTEP PROJECT

STUDY ON THE EFFECT OF THE PLACEMENT OF SOLAR PANELS ON BUILDINGS TO INCREASE ENERGY SECURITY AND ENERGY EFFICIENCY AND DEVELOP CLEAN ENERGY IN THE EASTERN PARTNERSHIP COUNTRIES

Component 3 Report:

Quantification of the Potential of Building PVs in Georgia and other Eastern Partner Countries

September 2017

This report has been prepared by the KANTOR Management Consultants Consortium. The findings, conclusions and interpretations expressed in this document are those of the Consortium alone and should in no way be taken to reflect the policies or opinions of the European Commission

List of abbreviations

AM	Armenia
ANRE	The National Regulatory Authority for Energy in Moldova
AREA	Azerbaijan State Agency on Alternative and Renewable Energy Sources
AZ	Azerbaijan
BAPVs	Building Applied Photovoltaics
BIPVs	Building Integrated Photovoltaics
BY	Belarus
CBA	Cost Benefit Analysis
CEER	Council of European Energy Regulators
DGPV	Distributed Generation from Photovoltaics
EaP	Eastern Partnership
EC	European Commission
ECT	Energy Community Treaty
EU	European Union
EUD	EU Delegation
GE	Georgia
GEDF	Georgian Energy Development Fund
GWNERC	Georgian Water and Energy Regulatory Commission
HiQSTEP	Short term high quality studies to support activities under the Eastern Partnership
HVAC	Heating, Ventilation and Air conditioning
MD	Moldova
NEURC	National Energy and Utilities Regulatory Commission of Ukraine
PSRC	Public Services Regulatory Commission of the Republic of Armenia
PV	Photovoltaic(s)
R2E2	Armenia Renewable Resources and Energy Efficiency Fund
RES	Renewable Energy Sources
SAEEE	State Agency on Energy Efficiency and Energy Saving of Ukraine
STL	Study Team Leader
T&D	Transmission and Distribution
TOR	Terms of Reference
UA	Ukraine
MS	Member State
SPE	Solar Power Europe
ROO	Renewable Obligation Order

Table of Contents

Table of Contents

Preamble	1
1 Introduction	3
1.1 Estimation of the PV energy potential of the built-up area: The theoretical background	5
1.1.1 Data	5
1.1.2 Methodologies	12
1.1.3 Proposed methodology - Case studying - Results - Accuracies	14
1.2 Estimation of the rooftop solar potential	22
1.2.1 Methodological approach	22
1.2.2 First task - Classification of the examined roofs	22
1.2.3 Second task - Estimation of solar suitable rooftop areas	23
1.2.4 Third task - Potential photovoltaic capacities within cities and solar energy simulations	24
1.3 PV technology overview	28
2 Eastern Partner Countries situation review	35
2.1 Availability of GIS Data – Quantification of solar potential	35
2.1.1 Armenia	37
2.1.2 Azerbaijan	41
2.1.3 Belarus	45
2.1.4 Georgia	49
2.1.5 Moldova	55
2.1.6 Ukraine	59
3 Rooftop solar potential	67
3.1 Assumptions	67
3.2 Armenia	70
3.2.1 Yerevan	70
3.2.2 Vanazdor	71
3.2.3 Gyumri	71
3.3 Azerbaijan	72
3.3.1 Baku	72
3.3.2 Sumgait	73
3.3.3 Ganja	73
3.4 Belarus	74
3.4.1 Minsk	74
3.4.2 Mogilev	75
3.4.3 Vitebsk	75

3.5	Georgia.....	76
3.5.1	Tbilisi	76
3.5.2	Batumi	77
3.5.3	Kutaisi.....	78
3.5.4	Rustavi.....	79
3.6	Moldova	80
3.6.1	Chisinau.....	80
3.6.2	Balti	80
3.6.3	Cahul	81
3.7	Ukraine	81
3.7.1	Kyiv.....	82
3.7.2	Odesa.....	83
3.7.3	Lviv	84
3.7.4	Zaporizhia.....	85
4	PV energy supply.....	87
4.1	Assumptions	87
4.1.1	Orientation and inclination.....	87
4.1.2	Assessment of the temperature impact.....	88
4.2	Armenia	89
4.3	Azerbaijan.....	93
4.4	Belarus	96
4.5	Georgia.....	100
4.6	Moldova	105
4.7	Ukraine	109
4.8	Aggregated results.....	114
5	Assessment of the electricity production and the grid supply.....	116
5.1	Assumptions	116
5.2	Armenia	117
5.3	Azerbaijan.....	117
5.4	Belarus	117
5.5	Georgia.....	118
5.6	Moldova	118
5.7	Ukraine	118
5.8	Peak load mitigation strategies	119
6	Synopsis and Conclusions	122
7	References	123
8	Annex: Summary of surface-related findings.....	128

List of Tables

Table 1. Examined orientation - inclination scenarios.....	26
Table 2. Input data for the solar energy simulations	27
Table 3. Typical types and sizes of PV systems.....	28
Table 4. Common roof suitability coefficients for all the examined rooftop areas.....	67
Table 5. Solar suitability coefficient for flat roofs.....	68
Table 6. Types of roofs and the gross available rooftop areas within the city of Yerevan	70
Table 7. Solar suitable rooftop areas and the potential PV capacities in the city of Yerevan	71
Table 8. Types of roofs and the gross available rooftop areas within the city of Vanadzor	71
Table 9. Solar suitable rooftop areas and the potential PV capacities in the city of Vanadzor ..	71
Table 10. Types of roofs and the gross available rooftop areas within the city of Gyumri	72
Table 11. Solar suitable rooftop areas and the potential PV capacities in the city of Gyumri	72
Table 12. Types of roofs and the gross available rooftop areas within the city of Baku	72
Table 13. Solar suitable rooftop areas and the potential PV capacities in the city of Baku	73
Table 14. Types of roofs and the gross available rooftop areas within the city of Sumgait	73
Table 15. Solar suitable rooftop areas and the potential PV capacities in the city of Sumgait... 73	73
Table 16. Types of roofs and the gross available rooftop areas within the city of Ganja.....	74
Table 17. Solar suitable rooftop areas and the potential PV capacities in the city of Ganja	74
Table 18. Types of roofs and the gross available rooftop areas within the city of Minsk	74
Table 19. Solar suitable rooftop areas and the potential PV capacities in the city of Minsk	75
Table 20. Types of roofs and the gross available rooftop areas within the city of Mogilev	75
Table 21. Solar suitable rooftop areas and the potential PV capacities in the city of Mogilev ...	75
Table 22. Types of roofs and the gross available rooftop areas within the city of Vitebsk.....	75
Table 23. Solar suitable rooftop areas and the potential PV capacities in the city of Vitebsk....	76
Table 24. Types of roofs and the gross available rooftop areas within the city of Tbilisi	76
Table 25. Solar suitable rooftop areas and the potential PV capacities in the city of Tbilisi	77
Table 26. Types of roofs and the gross available rooftop areas within the city of Batumi	77
Table 27. Solar suitable rooftop areas and the potential PV capacities in the city of Batumi	78
Table 28. Types of roofs and the gross available rooftop areas within the city of Kutaisi.....	78
Table 29. Solar suitable rooftop areas and the potential PV capacities in the city of Kutaisi.....	78
Table 30. Types of roofs and the gross available rooftop areas within the city of Rustavi.....	79
Table 31. Solar suitable rooftop areas and the potential PV capacities in the city of Rustavi....	79
Table 32. Types of roofs and the gross available rooftop areas within the city of Chisinau.....	80
Table 33. Solar suitable rooftop areas and the potential PV capacities in the city of Chisinau..	80
Table 34. Types of roofs and the gross available rooftop areas within the city of Balti.....	80
Table 35. Solar suitable rooftop areas and the potential PV capacities in the city of Balti.....	81
Table 36. Types of roofs and the gross available rooftop areas within the city of Cahul	81
Table 37. Solar suitable rooftop areas and the potential PV capacities in the city of Cahul	81
Table 38. Types of roofs and the gross available rooftop areas within the city of Kyiv.....	82
Table 39. Solar suitable rooftop areas and the potential PV capacities in the city of Kyiv.....	82
Table 40. Types of roofs and the gross available rooftop areas within the city of Odesa	83
Table 41. Solar suitable rooftop areas and the potential PV capacities in the city of Odesa	84
Table 42. Types of roofs and the gross available rooftop areas within the city of Lviv	84
Table 43. Solar suitable rooftop areas and the potential PV capacities in the city of Lviv	85
Table 44. Types of roofs and the gross available rooftop areas within the city of Zaporizhia....	85
Table 45. Solar suitable rooftop areas and the potential PV capacities in the city of Zaporizhia	86
Table 46. Examined orientation - inclination scenarios.....	88

Table 47. Climatic data of the examined cities of Armenia	89
Table 48. Solar energy production of a PV system in south orientation and optimal inclination in the examined cities of Armenia	91
Table 49. Climatic data of the examined cities of Azerbaijan.....	93
Table 50. Solar energy production of a PV system in south orientation and optimal inclination in the examined cities of Azerbaijan.....	94
Table 51. Climatic data of the examined cities of Belarus	96
Table 52. Solar energy production of a PV system in south orientation and optimal inclination in the examined cities of Belarus	98
Table 53. Climatic data of the examined cities of Georgia.....	100
Table 54. Solar energy production of a PV system in south orientation and optimal inclination in the examined cities of Georgia.....	103
Table 55. Climatic data of the examined cities of Moldova	105
Table 56. Solar energy production of a PV system in south orientation and optimal inclination in the examined cities of Moldova	107
Table 57. Climatic data of the examined cities of Ukraine	109
Table 58. Solar energy production of a PV system in south orientation and optimal inclination in the examined cities of Ukraine	112

List of Figures

Figure 1. Example of GIS Data Layers.....	6
Figure 2. Example of aerial image covering the city of Thessaloniki, Greece	6
Figure 3. Example of LIDAR data covering the city of Thessaloniki, Greece	7
Figure 4. Example of WorldView-2 image (B,G,NIR) covering the municipality of Kalamaria (Thessaloniki, Greece).....	10
Figure 5. Example of QuickBird-2 image (B,G,NIR) covering the village of Kalampaki (Kavala, Greece).....	10
Figure 6. Example of Ikonos-2 image covering the city of Thessaloniki, Greece	11
Figure 7. <i>Example of Landsat-7 image (B,G,NIR) covering the city of Thessaloniki, Greece....</i>	12
Figure 8. <i>GIS Layer combination for the city of Patras</i>	15
Figure 9. <i>Combination of Building and Block Layers for Patras city centre.....</i>	16
Figure 10. <i>True colour, bands 1,2,3</i>	17
Figure 11. <i>2006 IKONOS Patras Classification results. Upper- Red: Built-up areas, Green: Green spaces, Grey: Open spaces, Down- The original Ikonos image of the same area.....</i>	18
Figure 12. <i>Class: Buildings</i>	19
Figure 13. <i>Class: Open spaces.....</i>	19
Figure 14. <i>Class: Green spaces.....</i>	19
Figure 15. <i>True colour, bands 1, 2, 3 the study area in yellow frame.....</i>	19
Figure 16. <i>Class: Buildings</i>	20
Figure 17. <i>Class: Open spaces.....</i>	20
Figure 18. <i>Class: Green spaces.....</i>	20
Figure 19. <i>General methodology.....</i>	21
Figure 20. A flat roof can be totally utilised for photovoltaics	23
Figure 21. Dual-pitched (left) and hipped (right) roof solar suitability	23
Figure 22. Historical evolution of technology market share and future trends.....	24
Figure 23. Monocrystalline Silicon solar cell.....	25
Figure 24. Polycrystalline Silicon solar cell.....	25
Figure 25. Perspective of existing state of the art flat roof mounted PV systems.....	29

Figure 26. Perspective of existing state of the art PV installations mounted on pitched roofs ...	30
Figure 27. Perspective of existing state of the art façade mounted PV systems	30
Figure 28. Perspective of existing state of the art flat and curved roof BIPV systems.....	31
Figure 29. Perspective of existing state of the art “standard in-roof” systems (left image) and solar shingles or tiles	31
Figure 30. Perspective of existing state of the art semi-transparent BIPV skylight systems.....	32
Figure 31. Perspective of existing state of the art curtain wall glazing systems with semi-transparent modules	32
Figure 32. Perspective of existing state of the art PV parapets with semi-transparent PVs	33
Figure 33. Perspective of existing state of the art cladding BIPV systems and opaque PV parapets (PV database - Urban Scale Photovoltaic Systems).....	34
Figure 34. Perspective of existing state of the art fixed BIPV shading devices	34
Figure 35. Perspective of existing state of the art sun-tracking BIPV shading devices	34
Figure 36. <i>Sample National Report</i>	35
Figure 37. <i>Yerevan: True colour, bands 1, 2, 3 the study area in yellow frame</i>	38
Figure 38. <i>Yerevan: Zoom in the study area</i>	38
Figure 39. <i>Yerevan: The results of the classification process</i>	38
Figure 40. <i>Vanadzor: True colour, bands 1, 2, 3 the study area in yellow frame</i>	39
Figure 41. <i>Vanadzor: Zoom in the study area</i>	39
Figure 42. <i>Vanadzor: The results of the classification process</i>	39
Figure 43. <i>Gyumri: True colour, bands 1, 2, 3 the study area in yellow frame</i>	40
Figure 44. <i>Gyumri: Zoom in the study area</i>	40
Figure 45. <i>Gyumri: The results of the classification process</i>	40
Figure 46. <i>Baku: True colour, bands 1, 2, 3 the study area in yellow frame</i>	42
Figure 47. <i>Baku: Zoom in the study area</i>	42
Figure 48. <i>Baku: The results of the classification process</i>	42
Figure 49. <i>Sumgait: True colour, bands 1, 2, 3 the study area in yellow frame</i>	43
Figure 50. <i>Sumgait: Zoom in the study area</i>	43
Figure 51. <i>Sumgait: The results of the classification process</i>	43
Figure 52. <i>Ganja: True colour, bands 1, 2, 3 the study area in yellow frame</i>	44
Figure 53. <i>Ganja: Zoom in the study area</i>	44
Figure 54. <i>Ganja: The results of the classification process</i>	44
Figure 55. <i>Minsk: True colour, bands 1, 2, 3 the study area in yellow frame</i>	46
Figure 56. <i>Minsk: Zoom in the study area</i>	46
Figure 57. <i>Minsk: The results of the classification process</i>	46
Figure 58. <i>Mogilev: True colour, bands 1, 2, 3 the study area in yellow frame</i>	47
Figure 59. <i>Mogilev Zoom in the study area</i>	47
Figure 60. <i>Mogilev The results of the classification process</i>	47
Figure 61. <i>Vitebsk: True colour, bands 1, 2, 3 the study area in yellow frame</i>	48
Figure 62. <i>Vitebsk: Zoom in the study area</i>	48
Figure 63. <i>Vitebsk: The results of the classification process</i>	48
Figure 64. <i>The Cadastral System of Georgia</i>	50
Figure 65. <i>Extracts from Cadastral System of Georgia</i>	52
Figure 66. <i>Evaluation of the quality of the Cadastral System of Georgia</i>	54
Figure 67. <i>The Cadastral System of Moldova</i>	58
Figure 68. <i>General city plan of Kyiv</i>	60
Figure 69. <i>General city plan of Lviv</i>	61
Figure 70. <i>General city plan of Odesa</i>	62
Figure 71. <i>Kyiv: True colour, bands 1, 2, 3 the study area in yellow frame</i>	63

Figure 72. <i>Kyiv: Zoom in the study area</i>	63
Figure 73. <i>Kyiv: The results of the classification process</i>	63
Figure 74. <i>Odesa: True colour, bands 1, 2, 3 the study area in yellow frame</i>	64
Figure 75. <i>Odesa: Zoom in the study area</i>	64
Figure 76. <i>Odesa: The results of the classification process</i>	64
Figure 77. <i>Lviv: True colour, bands 1, 2, 3 the study area in yellow frame</i>	65
Figure 78. <i>Lviv: Zoom in the study area</i>	65
Figure 79. <i>Lviv: The results of the classification process</i>	65
Figure 80. Example of PV arrays positioned on a flat roof with the appropriate distance between them, in order to eliminate mutual shadings	68
Figure 81. Calculating PV array spacing	68
Figure 82. Dual-pitched (left) and hipped (right) roof solar suitability	69
Figure 83. Solar energy production for all simulation scenarios in Armenia.....	92
Figure 84. Solar energy production for all simulation scenarios in Azerbaijan	95
Figure 85. Solar energy production for all simulation scenarios in Belarus	99
Figure 86. Solar energy production for all simulation scenarios in Georgia	105
Figure 87. Solar energy production for all simulation scenarios in Moldova.....	109
Figure 88. Solar energy production for all simulation scenarios in Ukraine.....	114
Figure 89. Solar energy production for all orientation-inclination scenarios in all examined cities	114

Preamble

The present report is a deliverable of the “Study of the Effect of the Placement of Solar PV on Buildings in the EaP Countries” carried in the framework of the EU-funded project “High Quality Studies to Support Activities under the Eastern Partnership - HiQSTEP” (EuropeAid/132574/C/SER/Multi). The study covers all six Eastern Partner Countries, namely Armenia, Azerbaijan, Belarus, Georgia, Moldova and Ukraine.

The overall objective of the study is to address the effect of the placement of solar panels on buildings in Eastern Partner countries for the purpose of increasing energy security and energy efficiency and developing clean energy sources.

The specific objectives of the study are the following:

- To present EU policies, rules, regulations, tools and schemes towards the promotion of solar panels on buildings;
- To assess existing policies, rules, regulations and tools towards promotion of solar panels on buildings in the six Eastern Partner countries;
- To develop cost-benefit analysis for the staged development of building PVs in all Eastern Partner countries;
- To formulate recommendations on how to enhance PV penetration in the six Eastern Partners;
- To quantify the impact of building PV penetration to the overall energy mix and on the energy security of each country and to quantify the impact of PV generated energy to greenhouse gas emission reduction.

The present Study was implemented by a Study Team headed by Mr. Nikos Turlis, Study Team Leader and composed of:

Mr. Vassilis Papandreou – Energy Expert, Coordinator of Component 1

Mr. Matteo Leonardi – Energy Expert, Coordinator of Component 2

Prof. Agis Papadopoulos – Solar Energy Expert, Coordinator of Component 3

Prof. Petros Patias - Rural and Surveying Engineering Expert

Ms. Chiara Candelise – Energy Expert, Coordinator of Components 4 & 5

Mr. Nikos Turlis - Grid Expert

Mr. Armen Gharibyan - Local Energy Expert Armenia

Mr. Jahangir Efandiyev - Local Energy Expert Azerbaijan

Mr. Andrei Malochka - Local Energy Expert Belarus

Ms. Nino Maghradze – Local Energy Expert Georgia

Mr. Andrei Sula – Local Energy Expert Moldova

Mr. Kostiantyn Gura - Local Energy Expert Ukraine

Special thanks to the Study’s counterparties in the Eastern Partner Countries for their support and useful guidance throughout the elaboration of the study including the field missions. In particular the Study Team wishes the best with the future implementation of buildings’ solar PV programmes to:

- The Ministry of Energy and Natural Resources of Armenia, represented by Mr. Tigran Melkonyan;

- The Agency for Renewable Energy of Azerbaijan (AREA), represented by Mr. Jamil Malikov;
- The Department of Energy Efficiency in National Standardisation Authority of Belarus, represented by Mr. Andrey Minekov and Mr. Vladimir Shevchenok;
- The Ministry of Energy of Georgia, represented by Ms. Margalita Arabidze and Ms. Natali Jamburia;
- The Ministry of Economy of Moldova, represented by Mr. Denis Tumoruc;
- The State Agency for Energy Efficiency of Ukraine (SAEE), represented by Mr. Sergeiy Savchuk;

1 Introduction

As a deliverable of the third component of the study the present report comprises an assessment of technical potential of PV in buildings for selected cities in all six Eastern Partner Countries. Whereas the selection of cities in Georgia was provided for in the study's ToR and included Tbilisi, Batumi, Rustavi and Kutaisi, the selection of representative cities in other countries was based on a set of criteria. These included size, which in all cases was best represented by the national capital, resource and data/information availability as well as participation in the Covenant of Mayors initiative.

The technical potential assessment presented in this report comprises two major stages in terms of its development. First it was the collection, verification and analysis of surface data i.e. the derivation of areas in each cities built environment on which the placement of PV would be possible. Then, the second part of the assessment uses this gross area in order to come up with reasonable estimates on the PV capacities that would be able to be installed on the buildings. This step involves a series of constraints relative to the roof inclination, orientation, already captured roof space and shading obstructions. Although it is discussed from a planner's point of view we have deliberately not included grid constraints in this technical potential assessment. Grid impact in respect of distributed generation brings both benefits and costs which are meant to be dealt with in the Cost-Benefit Analysis part of the study. Having the capacities defined, an annual simulation for the derivation of the specific annual yield is used for the translation of the capacity estimates to energy. In view of the requirements of the Cost-Benefit Analyses which are planned later on this study capacity and energy figures are presented for two market segments. Due to their characteristics the market segments are either small residential systems or bigger buildings which include multi-family apartment buildings, commercial and industrial applications.

The identification (location, distribution and size) of the built-up area is of major importance in urban, suburban and agricultural studies. The calculation of its change throughout the time to the detriment of the non-built-up area constitutes a highly important indicator of urban change and environmental degradation (Xian and Crane, 2006; Kaufmann et al., 2007; Xu, 2008; Melesse et al., 2007; Weng, 2008).

Urban texture reconstruction and modelling as well as spectral and meteorological performance of the urban fabric are attractive research areas. However, this assumes availability of a vast amount of detailed data regarding mainly the existing buildings, which in many cases is not trivial.

In many countries, this assumption is covered by detailed cadastral data, but in a large number of cases either this data is not available, accessible or up to date. In all such cases, the only remaining source of data is remotely sensed images, either air- or space- borne and the only sustainable and cost-effective methodology is the automatic extraction of building footprints.

However, algorithms introduced over the years are (i) – for both macro scale and for micro scale – missing the urban district in the middle (Jochem et al., 2009; Carneiro et al., 2009); (ii) site specific (Kassner et al., 2008); (iii) involving strict requirements pertinent to the data quality and required expertise (Wiginton et al., 2010; Levinson et al., 2009) or (iv) vague and hence impossible to adapt elsewhere.

Scaling site assessment has been one of the major barriers and it is currently accomplished manually at high cost (i.e. time and expense) or via crude drawing on Google Earth visualisations. None of the current practices is scalable and more over they are not directly applicable in cases where both high quality and low cost are required at a GigaWatt (GW) scale (Gadsden et al., 2003; Ghosh and Vale, 2006; Ryatt et al., 2001).

As a result, several considerations must be made in order to compute the roof area available. The number and height of the buildings and the construction typologies influence the built-up surface area. Additionally, having obtained total roof area for a region, it is necessary to reduce this area to that which is available for solar photovoltaic applications, in order to determine potential power output. There are many factors which influence the fraction of available roof area, including: (1) shading, from other parts of the roof or from neighbouring buildings and trees; (2) other competing uses (such as other installations e.g. solar thermal systems, elevators, roof terraces or penthouses); (3) the orientation and inclination of the roofs; and (4) the installation and racking of the PV panels themselves (Wiginton et. a.; 2010).

In designing a method to estimate the available roof area, the following considerations should be taken into account (Izquierdo, et. al. 2008):

- be accurate;
- be reliable, with the possibility of computing or bounding the error of the roof area estimation; be inexpensive (low cost);
- be efficient (low calculation times);
- require few, global, available and standard input data;
- produce geo-referenced results;
- be scalable from local to global scales;
- be structured and flexible, so that new or unforeseen aspects can be introduced,
- be able to be used for the estimation of the long-term evolution of available roof surfaces.

And as stated:

“... One of the most important aspects to be considered is the size of the area being studied. Very often the same techniques cannot be applied at local and regional or world scales.

For instance, it may be possible to quantify the shadowing effects among buildings with a digital 3D model of a city (Robinson, 2006), but this is not a practical option when the scope of a study is a whole continent.

For similar reasons, homogeneous or average data is usually considered as first approach (Sorensen, 2001) for large-scale studies, which is obviously inaccurate but inexpensive indeed...”.

Due to these difficulties, some researchers, instead of estimating the roof and facade areas available for solar use, they rely on descriptions of the correlation between solar usable areas and population's density (e.g. Lehmann and Peter, 2003), since it is acceptable that roof area shares a correlation with population (Ghisi, 2006; Izquierdo et al., 2008; Kumar, 2004; Lehmann & Peter, 2003; Naroll, 1962; Pillai & Banerjee, 2007; Pratt, 1999; Taubenbock et al., 2008). In fact, Guindon et al. (2004) confirm a "high correlation" between building density and population density. Needless to say that such an assumption, being rather crude, cannot guarantee accurate results, at least not to the level required by this study.

1.1 Estimation of the PV energy potential of the built-up area: The theoretical background

1.1.1 Data

1.1.1.1 GIS data

Over the last few years, there was an exponential increase of consumer demand for geospatial information along with the necessary tools to manipulate and graphically display such datasets. Geospatial information is data referenced to a place - a set of geographic coordinates -, which can often be gathered and displayed in real time while the main tool for all actions connected to the particular set of information, the Geographic Information System (GIS) is a computer data system capable of capturing, storing, analysing, and displaying geographically referenced information. The power of GIS is the ability to combine geospatial information in unique ways - by layers or themes - and extract something new.

The attributes of different types of geospatial data -such as land ownership, roads and bridges, buildings, lakes and rivers, counties, or city districts- can each constitute a layer or theme in GIS a schematic representation of which can be found in Figure 1. GIS has the ability to link and integrate information from several different data layers or themes over the same geographic coordinates, which is very difficult to do with any other means. For example, GIS could combine a major road from one data layer as the boundary dividing land zoned for commercial development with the location of wetlands from another data layer. Precipitation data, from a third layer, could be combined with a fourth data layer that shows streams and rivers. GIS could then be used to calculate where and how much runoff might flow from the commercial development into the wetlands. Thus, the power of GIS analysis can be used to create a new way to interpret information that would otherwise be very difficult to visualise and analyse.

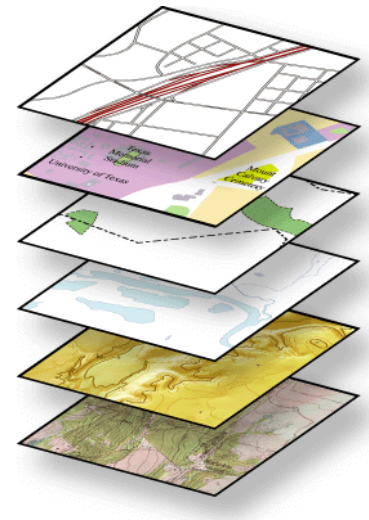
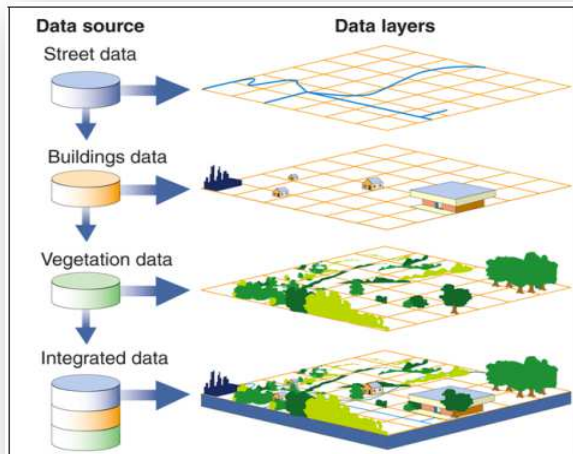


Figure 1. Example of GIS Data Layers

1.1.1.2 Aerial imagery

Today, a wide variety of sensors and platforms is available, providing many choices for high resolution imagery and complementary data, such as Digital Surface Models (DSMs) that are suitable for the detection of buildings. Such high resolution sensors can be divided into two broad categories: air-borne and space-borne.

Concerning air-borne sensors for very high resolution imagery, digital aerial cameras are the standard choice.

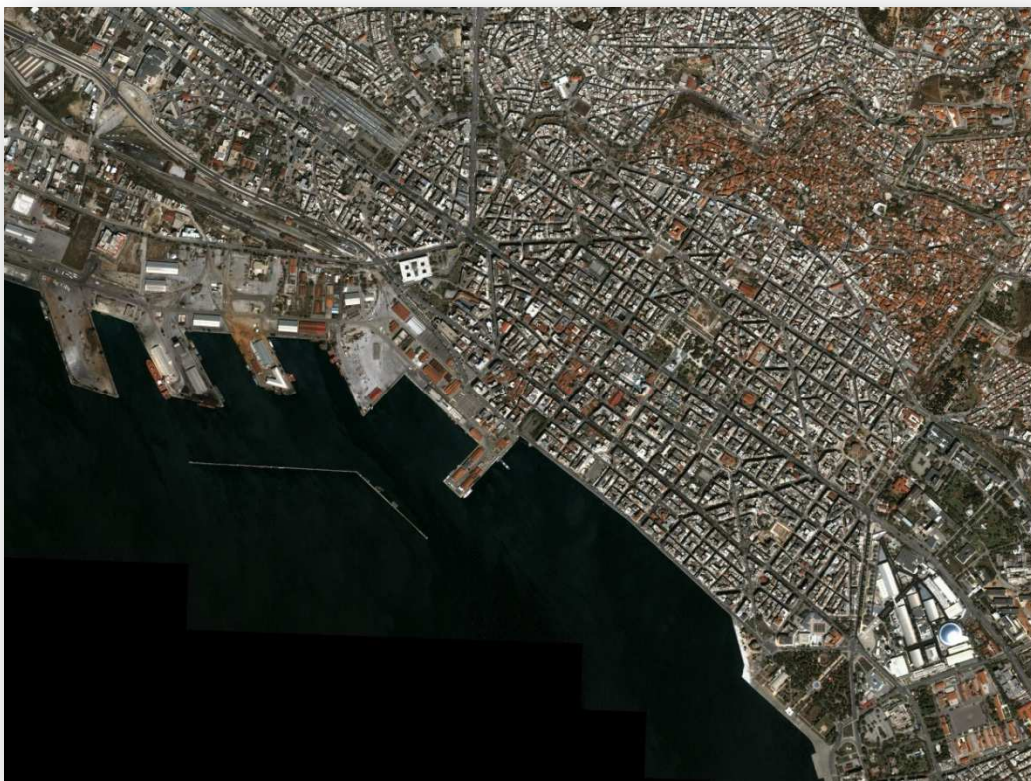


Figure 2. Example of aerial image covering the city of Thessaloniki, Greece

The rather recent availability of air-borne laser scanning technology can increase the degree of automation, accuracy, efficiency and adaptability (e.g. Pfeifer, M., Rutzinger, et al., 2007; Dorninger, Pfeifer, et al., 2008; Jochem, Hofle, et al., 2009). A systematic combination of aerial photos, building footprints and Light Detection and Ranging (LiDAR) backscatter can process twice the size of urban space involving trees and roof configurations of various levels of complexity in half the time (Nguyen, Pearce, et al., 2012). In case LIDAR data are available, they can be combined with building footprint data (e.g. Gagnon et. al., 2016, Lukac et. al. 2013), in order to calculate in more detail, the shading, tilt and azimuth of roof tops and achieve more accurate determination of the PV suitability estimates.



Figure 3. Example of LIDAR data covering the city of Thessaloniki, Greece

1.1.1.3 Satellite imagery

Space-borne sensors are also a good source for high-resolution data. Satellite images may have lower ground resolution than aerial images, but, in general, they are more cost-efficient in cases where the area of interest is considerably large.

High spatial resolution remotely sensed data, are the primary source for providing detailed imagery of the complex and heterogeneous urban environment. Until recently, satellite-based remote sensing techniques for land-use studies, with the spectral resolution contained in four spectral channels, were sufficient to discriminate between broadly differentiated land cover classes in urban settings. With the launch of WorldView-2, 8-band multispectral imagery has enhanced even more the feature extraction and takes the land use/ land cover beyond this level by extracting features like roof types and road conditions.

Very high-resolution space-borne imaging systems like IKONOS, KOMPSAT and CartoSat provide panchromatic images of 1m ground resolution and multi-spectral channels with 4m resolution. QuickBird and EROS offer even better ground sampling distance of 0.6–0.7m, whereas WorldView and GeoEye offer 0.5m resolution in panchromatic imagery. Technical specifications details are summarised in following table.

Satellite	Sensor	Band	Spectral Range (μm)	Scene Size (km x km)	Pixel Resolution
WorldView-2	Multi-spectral	1=Costal	400 - 450	16.4 X 16.4	1.84 m
		2=Blue	450 - 510		
		3=Green	510 - 580		
		4=Yellow	585 - 625		
		5=Red	630 - 690		
		6=Red Edge	705 - 745		
		7=NIR-1	770 - 895		
		8=NIR-2	860 - 900		
	Panchromatic	Pan	450 - 800		0.46 m
QuickBird-2	Multi-spectral	1=Blue	450 - 520	16.5 X 16.5	2.44 - 2.88 m
		2=Green	520 - 600		
		3=Red	630 - 690		
		4=NIR	760 - 900		
	Panchromatic	Pan	760 - 850		0.61 - 0.72 m
Orbview-3	Multi-spectral	1=Blue	450 - 520	8 X 8	4 m
		2=Green	520 - 600		4 m
		3=Red	625 - 695		4 m
		4=NIR	760 - 900		4 m
	Panchromatic	Pan	450 - 900		1 m
IKONOS-2	Multi-spectral	1=Blue	455 - 520	11 X 11	4 m
		2=Green	510 - 600		
		3=Red	630 - 700		
		4=NIR	760 - 850		

	Panchromatic	Pan	760 - 850		1 m
SPOT-5	Multi-spectral	1=Green	500 - 590	60 x 60	10 m
		2=Red	610 - 680		10 m
		3=NIR	780 - 890		10 m
		4=SWIR	1580 - 1750		20 m
	Panchromatic	Pan	480 - 710	2.5 m	
ASTER	Multi-spectral	VNIR	0.52 - 0.86	120 X 150	15 m
		SWIR	1.600 - 2.430		30 m
		TIR	8.125 - 11.65		90 m
Landsat-7	ETM+ multi-spectral	1,2,3,4,5,7	0.450 - 2.350	185 X 185	30 m
	ETM+ thermal	6.1, 6.2	10.40 - 12.50		60 m
	Panchromatic ETM+ thermal	8	0.52 - 0.90		15 m

- **WorldView-2**

WorldView-2, launched in October 2009, is the first high-resolution 8-band multispectral commercial satellite. Operating at an altitude of 770km, WorldView-2 provides 46cm panchromatic resolution and 1.84m multispectral resolution. The four primary multi-spectral bands include traditional blue, green, red and near-infrared bands. The four additional bands include a shorter wavelength blue band, centered at approximately 427 nm, called the coastal band for its applications in water colour studies; a yellow band centered at approximately 608 nm; a red edge band centered strategically at approximately 724 nm at the onset of the high reflectivity portion of vegetation response; and an additional, longer wavelength near infrared band, centered at approximately 949 nm, which is sensitive to atmospheric water vapor (Digital Globe, 2016). The new WorldView-3/4 satellite launched in 2016 provides a higher resolution of 31cm.



Figure 4. Example of WorldView-2 image (B,G,NIR) covering the municipality of Kalamaria (Thessaloniki, Greece).

- **QuickBird-2**

QuickBird-2, launched in October 2001, is the high-resolution 4-band multispectral commercial satellite. Operating at an altitude of 450km, QuickBird-2 provides 60-72cm panchromatic resolution and 2.44-2.88m multispectral resolution. The four multi-spectral bands include traditional blue, green, red and near-infrared bands (Digital Globe, 2016).



Figure 5. Example of QuickBird-2 image (B,G,NIR) covering the village of Kalampaki (Kavala, Greece).

- **OrbView-3**

OrbView-3, launched in June 2003, is the high-resolution 4-band multispectral commercial satellite. Operating at an altitude of 465 km, OrbView-3 provides 1 m panchromatic resolution and 4 m multispectral resolution. The four multi-spectral bands include traditional blue, green, red and near-infrared bands (Digital Globe, 2016).

- **Ikonos-2**

Ikonos-2, launched in September 1999, is the high-resolution 4-band multispectral commercial satellite. Operating at an altitude of 681km, Ikonos-2 provides 1m panchromatic resolution and 4m multispectral resolution. The four multi-spectral bands include traditional blue, green, red and near-infrared bands (Digital Globe, 2016).



Figure 6. Example of Ikonos-2 image covering the city of Thessaloniki, Greece

- **Spot-5**

Spot-5, launched in May 2002, is 4-band multispectral commercial satellite. Operating at an altitude of 832km, Spot-5 provides 5m (2.5m after optimisation) panchromatic resolution and 10m multispectral resolution (+1 band 20m in SWIR). The three primary multi-spectral bands include traditional G, R and NIR bands. The last band includes part of the Short Wave Infrared area (1.58-1.75 μ m) of the spectral (Satellite Imaging, 2016).

- **ASTER**

ASTER, launched in December 1999, is 14-band multispectral commercial satellite. Operating at an altitude of 705km, ASTER provides 15, 30 and 90m multispectral resolution. The three first multi-spectral bands include traditional G, R and NIR bands. The next five bands include parts of the Short Wave Infrared area (SWIR) of the spectral. The last five bands include parts of the Thermal IR area (TIR) of the spectral (Satellite Imaging, 2016).

- **Landsat-7**

Landsat ETM+, launched in April 1999, is 7-band multispectral commercial satellite. Operating at an altitude of 705.3km, Landsat ETM+ provides 15m panchromatic resolution and 30m multispectral resolution (+1 band 60m in TIR). The four primary multi-spectral bands include traditional B, G, R and NIR bands. The three additional bands include two parts of the Short Wave Infrared area (1.55-1.75 μ m and 2.08-2.35 μ m), and a part of the Thermal IR area (10.42-12.50 μ m) (Satellite Imaging, 2016).



Figure 7. Example of Landsat-7 image (B,G,NIR) covering the city of Thessaloniki, Greece

1.1.2 Methodologies

1.1.2.1 GIS based techniques

GIS techniques have been applied by several authors to study PV deployment and/or impervious urban fabric (Gadsden et al., 2003; Ghosh and Vale, 2006; Izquierdo et al., 2008; Kraines et al., 2001; Kraines and Wallace, 2003; Ryatt et al., 2001).

The level, scope and access of municipal GIS data depend on the technical sophistication and the policy of each city. A typical use of GIS involves the superimposition of various layers (e.g. cadastral map layers, building outlines, aerial or satellite images etc) and the estimation of the roof top areas.

However, it should be noted that normally (Gadsden, et. al., 2003a, 2003b) "... each building outline is formed from intersecting polylines (i.e. graphical objects with numerous line segments) distributed across several map layers. A closed polygon can be created by manually drawing round the visual outline of the footprint on an additional superimposed layer. This is, however, an extremely time-consuming exercise, rendering it impractical on a large scale..."

The following steps are typical in calculating the total area of the buildings in the city:

- Add field to use it in Dissolve function
- Field Calculator adds massively the same attribute to the features
- Dissolve using this field and aggregating the Area of buildings

The buildings are then extracted from the digital cadastral database and the built-up area is the aggregation of all individual building areas.

1.1.2.2 Air-borne imagery based techniques

Very often, the available GIS data is neither complete nor up to date. In such instances, GIS building layers are enhanced by air-borne imagery for the building rooftop extraction. In order to do this, the aerial imagery should be geometrically corrected for image, sensor and anaglyph distortions, and thus the produced Orthophoto is used.

Various researchers (e.g. Akbari, et. al., 2003, Psaltis and Ioannidis, 2008) have used either high resolution (50cm or better) aerial images (i.e. Black/White, Colour, or Infrared) or the finally produced orthophotos, in order to obtain accurate estimates of urban fabric.

However, as expected, the general conclusion is that "... However, all three bands are in the visible spectrum and, thus, do not cover the entire solar and thermal radiative ranges. For this reason, limited information can be acquired from this data type...".

There are several assumptions and constraints of the methodology:

- Manual building digitisation is both tedious and time consuming, while is bound by image resolution. For instance, as reported in (Nguyen et al, 2013) "Since supervision was required for every individual house concerning roof type, shaded portion, orientation and inclination, it takes about 2 weeks to process 0.5km² of urban space".
- Various distortion and multiple view problems are arising through merging big numbers of aerial photos into an orthophoto.
- In addition to the time and labour consumption, final results are dependent on the user's experience, which becomes another uncontrolled uncertainty.

1.1.2.3 Space-borne imagery based techniques

Remote sensing provides reliable scientific tools for the calculation of the built-up area, using inter-temporal satellite images and studying the multispectral space. Image recognition, both object-based and spectrally based, supervised and unsupervised, has been used as a means of studying urban fabric and determining roof area (Akbari et al., 2003; Guindon et al., 2004; Ratti and Richens, 1999; Taubentock et al., 2008).

The main techniques on the determination of the built-up area from satellite images utilise neural networks (Seto and Liu, 2003), supervised or unsupervised image classifications (Masek et al., 2000; Ward et al., 2000; Zhang et al., 2002; Xian and Crane, 2005; Yuan et al., 2005; Ioannidis et al., 2009; Lu and Weng, 2005; Yang, 2011; Ukwattage and Dayawansa, 2012), object-based classifications (Guindon et al., 2004; Zhou et al., 2012, Stamou et al, 2012, Stamou et al, 2013, Stamou et al, 2014a, Stamou et al, 2014b), support vector machines (Huang and Lee, 2004; Melgani and Bruzzone, 2004; Pal and Mather, 2005; Griffiths et al., 2010; Kamusoko et al., 2013) and Tasseled Cap transformation (Deng and Wu, 2012).

Generally, the methodologies proposed depend on the image scale. In small scales situations (e.g., city level), the problem is being addressed by various classification/segmentation techniques from the field of remote sensing.

Such techniques can be categorised as low-level, mid-level and high-level:

- Low-level techniques consider information at the pixel level to facilitate change, and include methods like image differencing, rationing and principal component analysis (PCA) (Pratt, 2001).
- Mid-level techniques, including object-oriented classification, feature and texture segmentation, are widely used today (Blaschke et al., 2000; Busch, 1998, Walter, 2004). These techniques are more robust than the low-level methods, as they use a more complex level of information to detect change.
- High-level techniques, also known as knowledge-based methods or expert systems, are currently the most frequently used techniques. They incorporate cognitive functions to improve image-scene analysis and make use of a wide variety of data.
- Finally, it must be noted that in automatic image classification, two types of problems are generally observed:
 - Errors of commission and omission: Building polygons that do not represent actual buildings and buildings not classified as actual buildings.
 - Over- and under-segmentation: Single buildings represented by more than one polygons and many buildings represented by only one polygon.

1.1.3 Proposed methodology - Case studying - Results - Accuracies

In order to arrive to an accurate and cost effective methodology applicable to city scale, a case study has been carried out for the city of Patras, Greece. The case study involves the use of detailed cadastral GIS building rooftop layer with an accuracy of better than 20cm. Based on this data, the total city (as defined by the administrative boundaries) building rooftop area has been calculated. This is then assumed the baseline, against which the relative areas estimated by satellite imagery (Ikonos and Landsat) of various resolutions are evaluated.

1.1.3.1 Total building rooftop area calculated by GIS data

Patras Metropolitan area is located in the administrative region of Western Greece with a total area of 738.9 km², while the actual municipal unit is limited to a total of 124.71 km² presented in Figure 8 below.

A complete and up to date Cadastral GIS system is available for the city, which served as the basis for the calculation of the total building rooftop area.

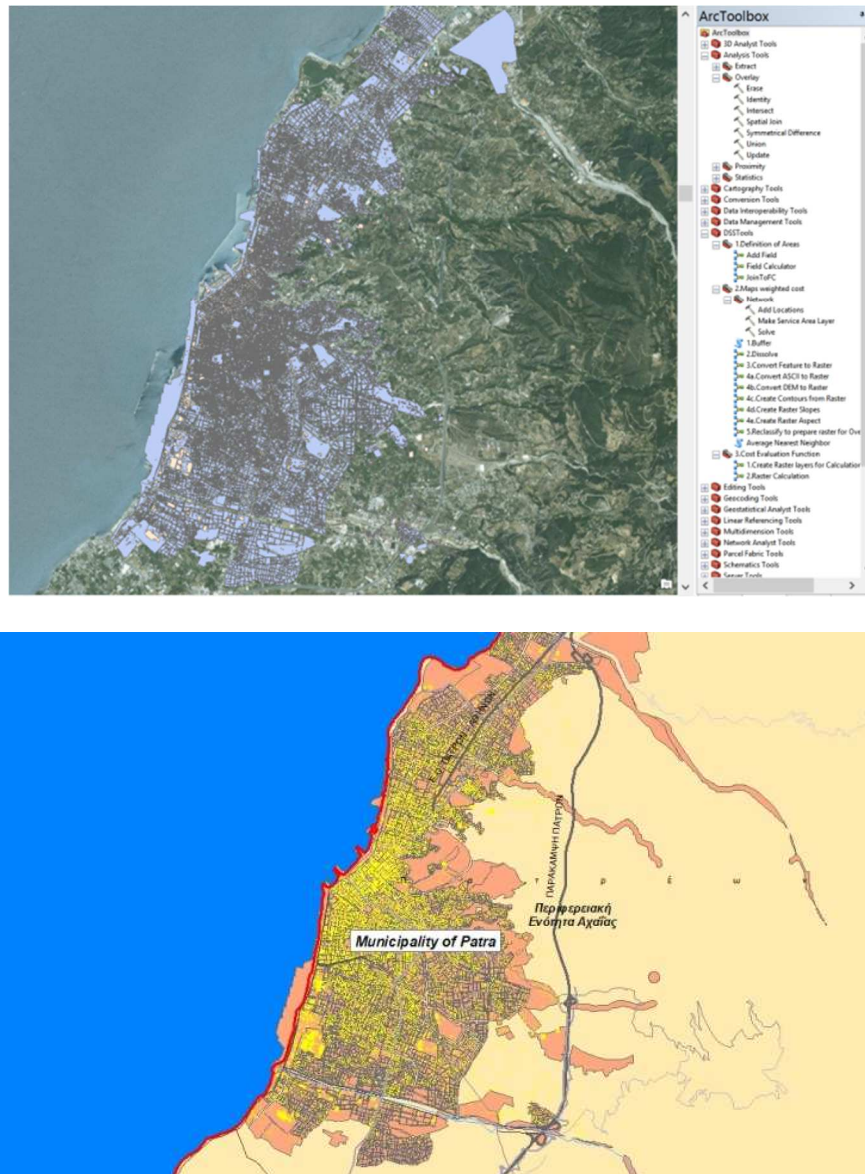


Figure 8. GIS Layer combination for the city of Patras

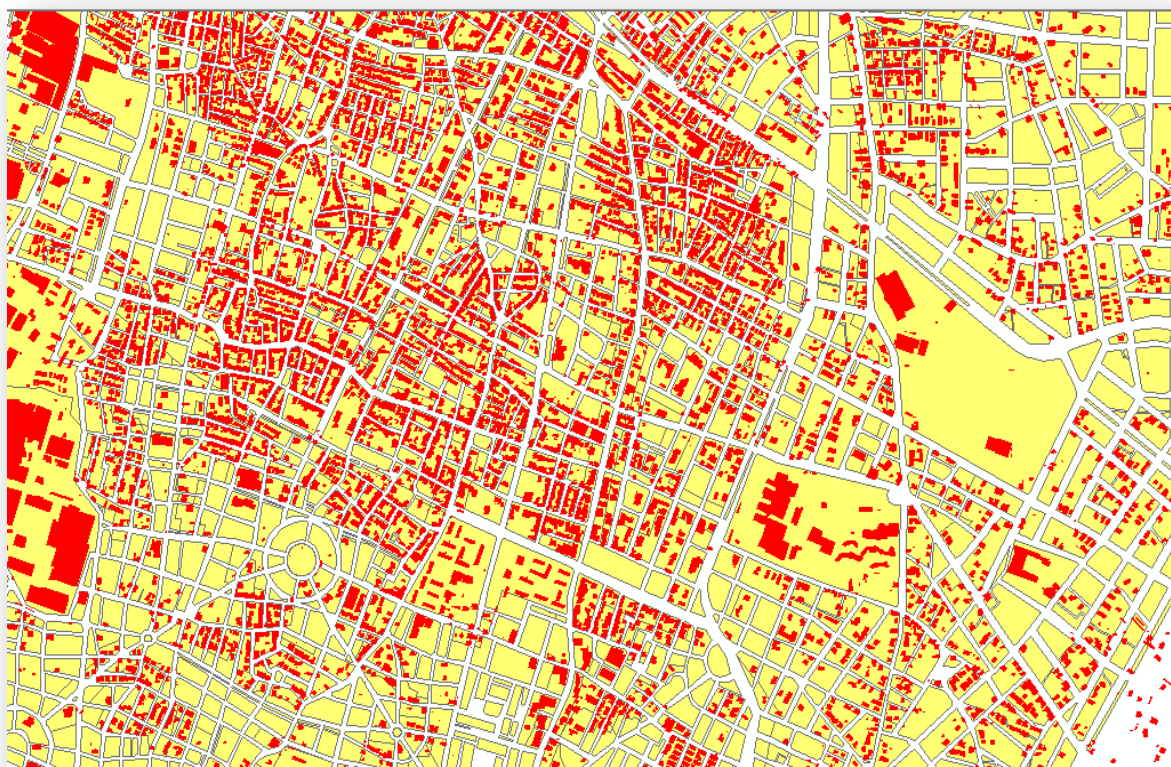


Figure 9. Combination of Building and Block Layers for Patras city centre

1.1.3.2 Total Building rooftop area calculated by Ikonos satellite imagery

Data: Ikonos 2 (R,G,B,NIR)

Date: 18 October 2007

Resolution: 1m



Figure 10. True colour, bands 1,2,3

Classification procedure:

In order to achieve rooftop extraction and further analysing the rooftop materials, a sequence of processes was executed. Initially, the panchromatic and the multispectral images were segmented into administrative boundaries, and the city area was extracted. The next step was to pan-sharpen the multispectral image, in order to obtain a high resolution multispectral image, and continue with the classification process.

Then, 100 classes have been used in automatic unsupervised classification and subsequently the information (i.e. buildings, green space, open space) included in each spectral class has been identified. The final general classes have been obtained by generalizing all relevant sub-classes (e.g. different building types). These were transformed to shapefiles and then introduced in a GIS environment for further processing. On the premises that the footprint of the buildings also depicts the rooftop area, a geodatabase of the study area containing information about the building stock was conducted. More specifically, this geodatabase includes information about the geographical distribution for every single building, the rooftop area and the surface material.

Results:

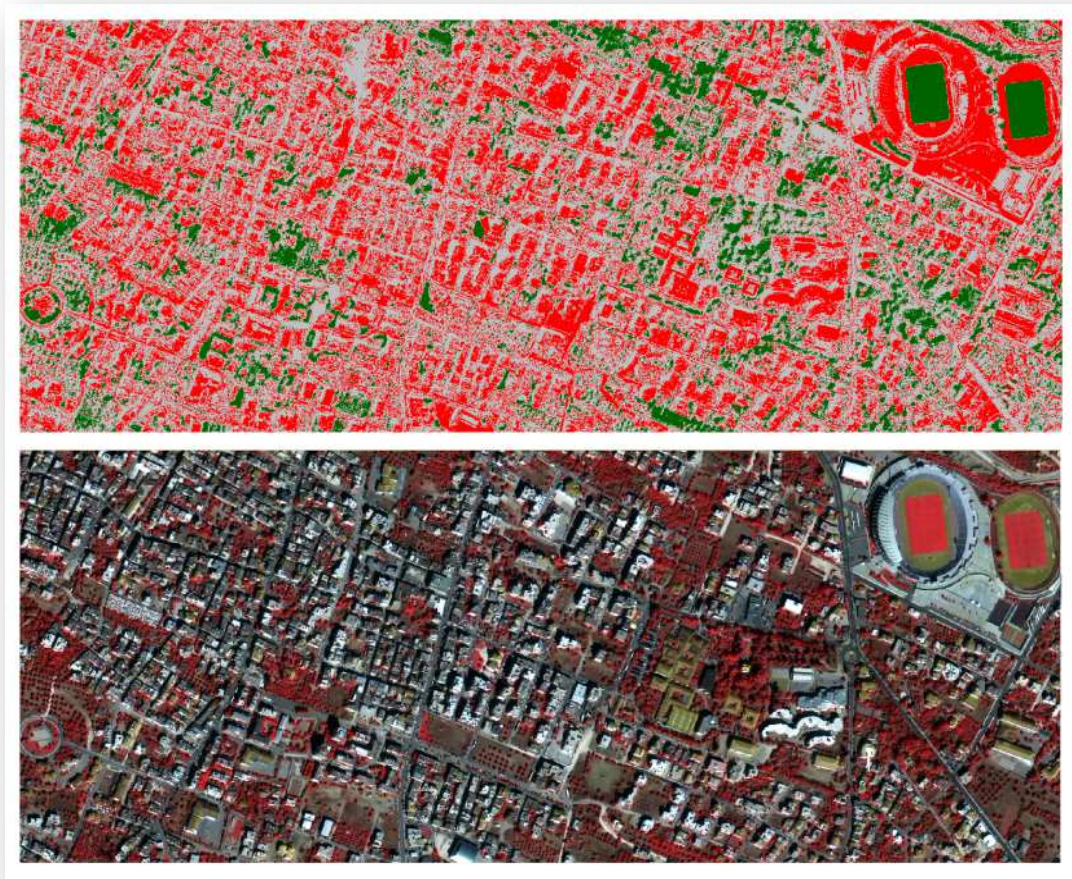


Figure 11. 2006 IKONOS Patras Classification results. Upper- Red: Built-up areas, Green: Green spaces, Grey: Open spaces, Down- The original Ikonos image of the same area

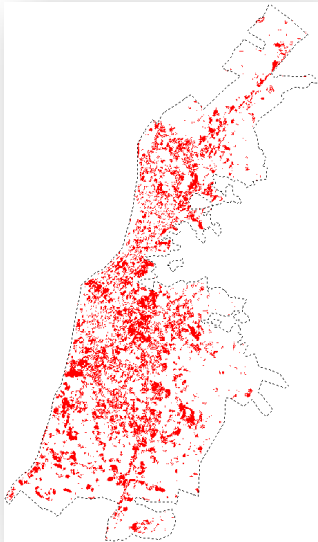


Figure 12. *Class: Buildings*



Figure 13. *Class: Open spaces*

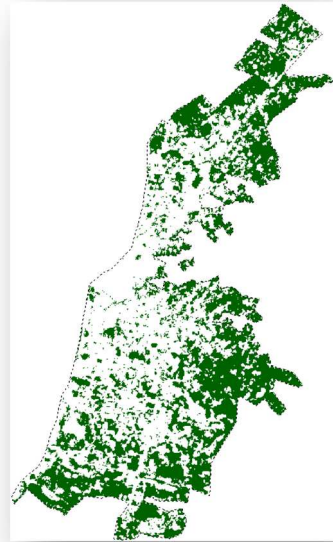


Figure 14. *Class: Green spaces*

1.1.3.3 Total Building rooftop area calculated by Landsat satellite imagery

Data: Landsat 7 ETM+, 220-337, free downloaded from <http://glovis.usgs.gov>

Date: 13 August 2005

Resolution: 15m Panchromatic, 30m Multispectral



Figure 15. *True colour, bands 1, 2, 3 the study area in yellow frame*

Classification procedure:

20 classes have been used in automatic unsupervised classification and subsequently the information (i.e. buildings, green space, open space) included in each spectral class has been identified. The final general classes have been obtained by adding and generalizing all relevant sub-classes (e.g. different building types). Again, these were transformed to shapefiles and introduced in the GIS environment for further processing.

Results:

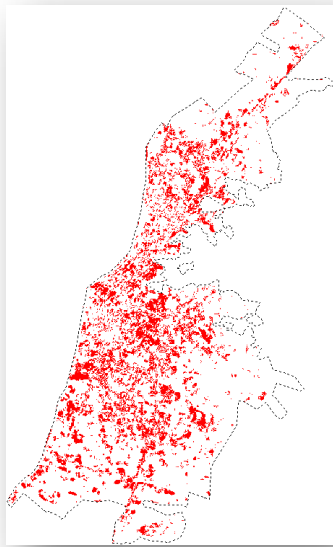


Figure 16. Class: Buildings



Figure 17. Class: Open spaces

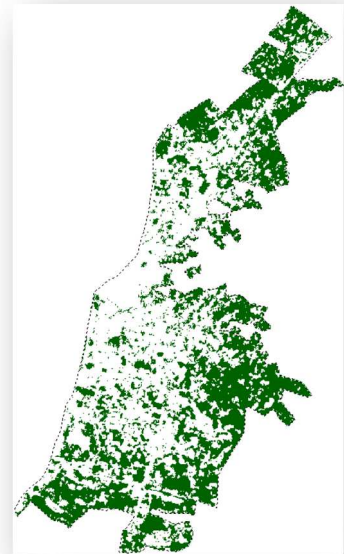


Figure 18. Class: Green spaces

1.1.3.4 Comparison of the results

Total urban area		25.06
	Rooftop area (km ²)	error (%)
GIS	4.79	0.0
IKONOS	4.76	-0.6
LANDSAT	4.50	-6.1

Therefore, the methodology proposed here can be applied in similar cases (i.e. city scale) in the urban region of interest without moving to more complicated, time consuming and costly methods.

Summing up, the general methodology used consists of three options as follows:

- **Option-1/2:** GIS or Cadastral building roof area data are available: in this case these data are directly used to calculate the aggregated available roof area of the city.
- **Option-3:** no GIS data are available: in this case we rely either on available aerial or high resolution satellite imagery, and alternatively at their absence on low resolution Landsat openly available data. Automatic unsupervised classification procedure is subsequently followed and finally the available aggregated roof area is calculated through GIS tools.

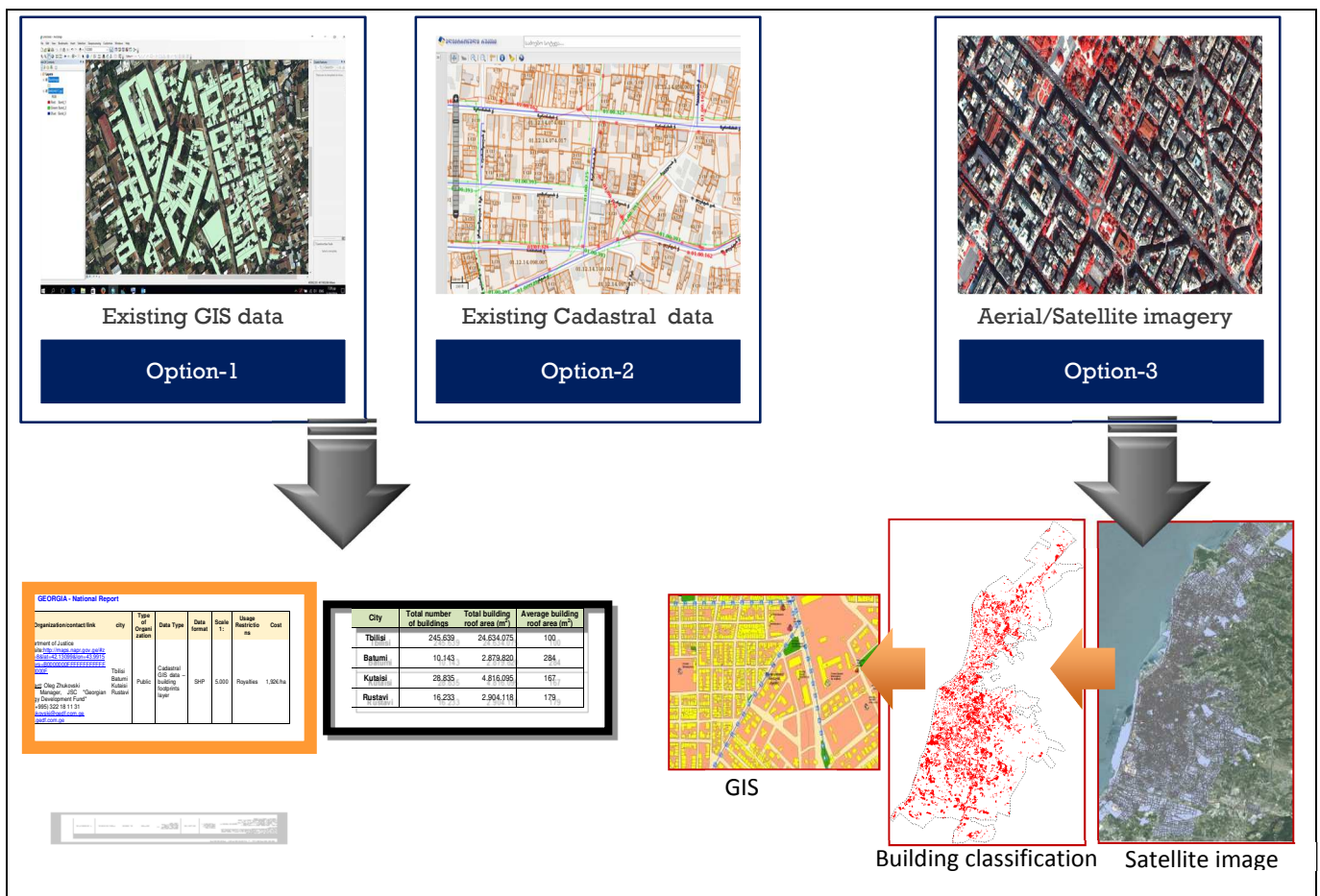


Figure 19. General methodology

1.2 Estimation of the rooftop solar potential

1.2.1 Methodological approach

The assessment of the solar potential to be utilised in the urban environment of the countries considered is based on the use of mainly Building Applied PhotoVoltaics (BAPVs), as Building Integrated PhotoVoltaics (BIPVs) are only suitable for new buildings and are a more cost-intensive and complicated technology.

The methodology to estimate the solar potential in urban environment, such as of the cities selected, comprises two main work phases:

- i) The first includes the use of available geographical data, such as GIS, aerial and satellite to calculate the total building rooftop areas per city. Taking into account available data about the total number of buildings, a mean building rooftop area can be also approximated.
- ii) The second includes a more detailed and complex elaboration of the above results of the building rooftop areas in order to deduce the actual building rooftop areas that are suitable for photovoltaic installations. Then, a series of solar simulation scenarios are examined to estimate the annual potential solar energy that can be generated on a city's level, with respect to technological, economic and policy parameters, as discussed in Component 2. Still, given the fact that PVs are still of negligible importance in electricity mix of the countries considered, it is reasonable to assume that technological parameters will be the key factor for the determination of the potential in the short- to medium termed future.

Regarding the second phase, since complex urban environments present various building block densities and miscellaneous building elevations as well as limited available rooftop construction data about most of the urban regions, the difficulties involved in the solar potential assessment are significant. In addition, the lack of available data about urban layouts, prevent an effective and valid reliable statistical approach of the actually suitable built areas for photovoltaics.

Therefore, in the present study a quantitative empirical methodology approach is proposed, which will compensate for the lack of available data, if any, in the selected cities. In particular, the proposed methodology comprises three separate tasks:

- i) The first task foresees the building roofs' classification according to their shape, i.e. flat and pitched roofs. This will allow assessing separately their solar suitability, which is for obvious technical reasons different.
- ii) The second task includes the estimation of the unavailable rooftop areas occupied by various roof obstacles.
- iii) The third and final task comprises the estimation of the potential PV capacities based on the PV technology utilised and the simulations to estimate the annual solar energy production and the potential electricity consumption savings.

1.2.2 First task - Classification of the examined roofs

The first task follows the gross rooftop area estimation within a city and concerns the classification of buildings according to their roof type, i.e. flat or sloped roof. The type of the roof can affect parameters, such as its capability (i.e. static load capability, etc.) to accept a photovoltaic installation, its area availability for solar panels and last but not least the annual solar yield of a photovoltaic system.

The area availability of a roof and the solar yield of the PV system are two interdependent factors, when evaluating rooftop PV potential. For example, in flat roofs there are no limitations regarding photovoltaics' orientation and inclination, thus both high solar yield and full rooftop area utilisation can be succeeded (Figure 20). The latter can reach 100%, unless there are major obstacles such as staircase wells and elevator shafts, major HVAC components, satellite antennas, water tanks, etc.

In contrast to the flat roofs, in the case of sloped ones, the orientation and inclination of the roofs is given and cannot be modified either to improve photovoltaics' efficiency or to increase the available area to install PV panels. Besides, when sloped roofs are discriminated between dual-pitched and hipped ones and high solar yield is set as a solar suitability criterion, then, by average, only the 50% of dual-pitched rooftop areas and the 62.5% of hipped rooftop areas will be ideal for solar utilisation in terms of good orientation, as it is illustrated in Figure 21.

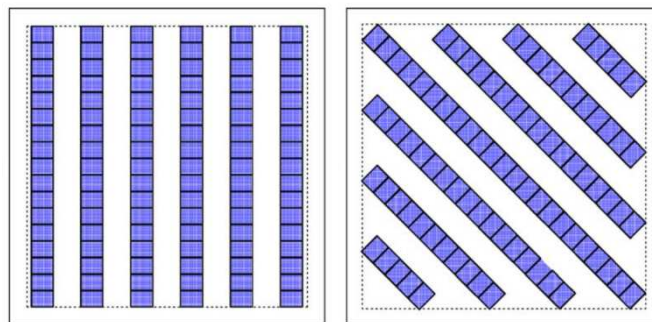


Figure 20. A flat roof can be totally utilised for photovoltaics

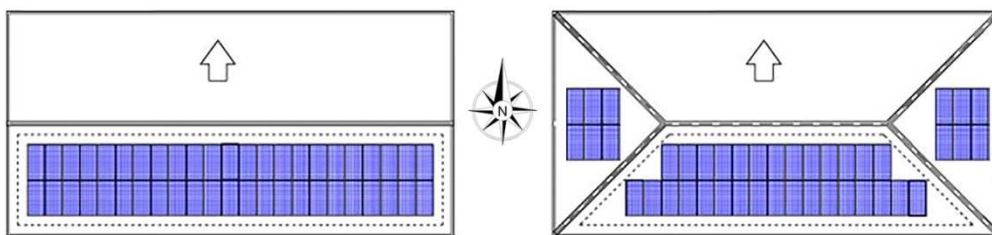


Figure 21. Dual-pitched (left) and hipped (right) roof solar suitability

1.2.3 Second task - Estimation of solar suitable rooftop areas

Within the second task, the suitable rooftop areas (S_a) for photovoltaic installations are obtained from the gross rooftop areas (estimated with the aerial/satellite/GIS analysis of the cities) by subtracting the unavailable rooftop areas and the areas with low solar yield using the following equation:

$$S_a = G_a \times RE_f \times Se_f \times Sh_f$$

where,

- G_a is the gross rooftop area.
- RE_f is the fraction of the rooftop area free from rooftop elements and obstacles, such as staircase wells and elevator shafts, major HVAC components, satellite antennas, water tanks, etc.

- Ser_f is the fraction of the rooftop area which is not needed for photovoltaic maintenance purposes. This zone can be extended along the outline of a flat or sloped roof or/and between PV series in a flat roof.
- Sh_f is the fraction of the rooftop area with high solar yield, in other words with optimal orientation or/and without significant shading issues for the PV system.

The RE_f and Ser_f factors can be approximated by gathering data from literature, building regulations and local authorities regarding common architectural and construction practices and constraints. The ultimate goal is to conclude to an average loss coefficient to obtain the suitable rooftop areas.

The Sh_f factor needs more thorough simulations requiring data that are usually collected with LiDAR (Light Detection and Ranging) technology, which is not available in the present study. Therefore, it was decided shading effects to be neglected, since on the one hand the present study concerns a city based assessment of solar potential and shading calculations are mostly vital in building unit level research and on the other hand it is anticipated that shading issues will be eliminated in future photovoltaics systems, given that the new generation of bypass diode enabled modules along with the rise of micro inverters allows photovoltaic arrays to produce energy from illuminated panels, although there are series-connected modules which are shaded. Still, the classification of the roofs into flat and sloped ones will ensure that only the rooftop areas with high solar yield characteristics are taken into account in present calculations.

1.2.4 Third task - Potential photovoltaic capacities within cities and solar energy simulations

1.2.4.1 Calculating potential photovoltaic capacities

To calculate the potential photovoltaic capacities within cities, certain scenarios were elaborated evaluating two different, most common though, types of photovoltaic technology (monocrystalline-Si and polycrystalline-Si). The crystalline solar panels have dominated over the last 30 years (Figure 22), thus represented the most typical technology to examine in the present study, since the latter concerns countries with currently undeveloped PV markets.

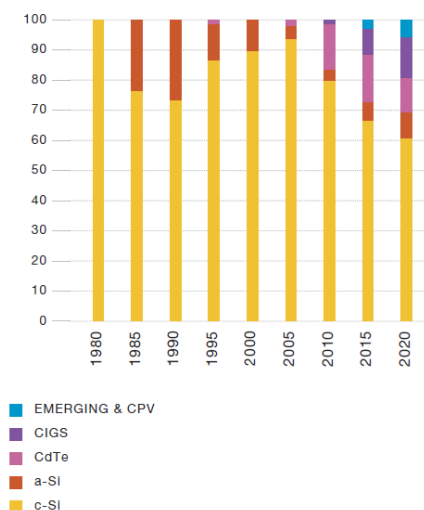


Figure 22. Historical evolution of technology market share and future trends¹

¹ EPIA. *Solar generation 6: Solar photovoltaic electricity empowering the world*. CBF, Brussels, Belgium : European Photovoltaic Industry Association, 2011. p. 100.

The main difference between the monocrystalline-Si and polycrystalline-Si panels is their solar cells' efficiency. That is why this parameter affects the overall performance ratio of the PV systems and eventually their required rooftop area and their potential size, which are the main subjects of the present section.

Solar cells made of mono-Si are quite easily recognisable by an external even colouring and uniform look, indicating high-purity silicon (Figure 23). The highest-grade silicon of monocrystalline solar panels leads to the highest efficiency rates among all the PV technologies, which means that they are space-efficient (or as it is also commonly referred to as they present greater energy intensity). Given that these solar panels yield the highest power outputs, they require the least amount of space compared to any other types. For example, monocrystalline solar panels produce up to four times the amount of electricity as thin-film solar panels. The efficiency rates of monocrystalline solar panels are typically 15-20%, in other words they can produce 150 up to 200Watt of electricity power per 1 m² of available area. Their major disadvantage is that they are more sensitive to shade, dirt and snow since their entire circuit can break down under these conditions.



Figure 23. Monocrystalline Silicon solar cell

As far as polycrystalline-Si panels are concerned (Figure 24), this technology is the first introduced in the market in 80s. As the required amount of waste silicon to manufacture them is smaller compared to monocrystalline Si, their production is simpler and more cost-effective. However, the efficiency of polycrystalline-based solar panels is typically lower (13-16%) than mono-Si, meaning they can produce only 130 up to 160Watt of electricity power per m² of available area and need more space to produce the same electrical capacity with mono-Si panels. In addition to their lower efficiency, they have also slightly lower heat tolerance than monocrystalline solar panels.

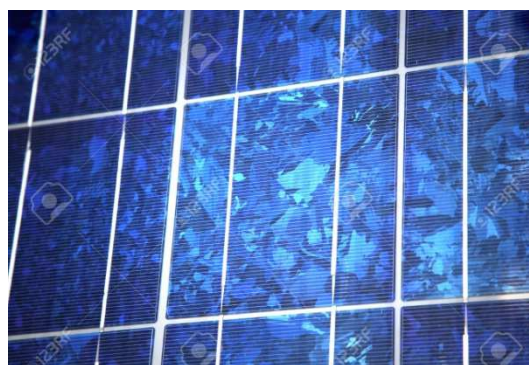


Figure 24. Polycrystalline Silicon solar cell

After the estimation of the potential PV capacities of the cities, the results can be classified accordingly to the kinds/scales of systems the existing national or local solar energy incentive

schemes, if any, promote in the building sector. A lower limit suitability criterion could also be applied on the potential photovoltaic capacity in each roof, but as there are no data on building unit level, this is not feasible for now.

1.2.4.2 Solar energy simulations

To approximate the solar energy supply from the estimated potential PVs in the examined cities, the RETScreen² software was used. RETScreen is a simple and useful Clean Energy Management Software system for energy efficiency, renewable energy and cogeneration project feasibility analysis as well as ongoing energy performance analysis. Its main advantage is that combines simplicity in the input data, accuracy in the results and vast climatic data for almost all countries, including these assessed in the present study.

Regarding the photovoltaic calculations, the RETScreen Photovoltaic Power Model can be used worldwide to evaluate the energy production and savings, costs, emission reductions, financial viability and risk for central-grid, isolated-grid and off-grid photovoltaic (solar electric) projects.

In order to validate the RETScreen's outcomes, the European Commission Joint Research Centre's Interactive Maps of Photovoltaic Geographical Information System³ were also used, carrying out solar simulations exclusively for the capital cities of each examined country.

As far as the present analysis is concerned, detailed calculations were performed based on monthly climate data and photovoltaic equipment data. Furthermore, specific orientation-inclination scenarios were evaluated both for flat and sloped roofs in order to cover all potential rooftop PV applications (Table 1).

In particular, one scenario was evaluated for flat roofs with the PV system set fixed with south orientation and the optimal inclination of solar panels accordingly to the geographical latitude of each examined city. Respectively three different simulations were conducted for the sloped roofs, which included all acceptable orientations for PV panels; south, southeast -southwest and east-west orientation, while regarding the inclination angle of PVs, in a business as usual scenario it was set at 12°, which is a common inclination angle of sloped roofs in the examined cities.

Table 1. Examined orientation - inclination scenarios

Proposed PV applications	Scenarios	Description
Flat roofs	Flat roof	PV modules installed on free-ventilated mounting devices in south orientation and optimal inclination according to the geographical latitude of each examined city
Sloped roofs (highly desirable scenario)	SE_12_S	PV modules installed on non-ventilated mounting devices in south orientation and 12° inclination angle, which corresponds to a typical inclination of the sloped roofs
Sloped roofs (mean desirable scenario)	SE_12_SE_SW	PV modules installed on non-ventilated mounting devices in southeast (or southwest) orientation and 12° inclination angle, which corresponds to a typical inclination of the sloped roofs
Sloped roofs (least desirable scenario)	SE_12_E_W	PV modules installed on non-ventilated mounting devices in east and west orientation and 12° inclination angle, which corresponds to a typical inclination of the sloped roofs

² Find at <http://www.nrcan.gc.ca/energy/software-tools/7465>

³ http://re.jrc.ec.europa.eu/pvg_tools/en/tools.html

Regarding the input data that are necessary to estimate the annual solar energy production in a specific location, typical technical parameters for a PV system with power capacity of 10kWp were assumed, as they are presented in detail in the following table.

Table 2. Input data for the solar energy simulations

Phase of analysis	Data	Description
Resource assessment	Solar tracking mode	The solar panels were assumed to be mounted on a fixed orientation and inclination
	Slope of PV panels	Flat roofs: Equal to the absolute value of the latitude of the site: This is the slope, which in general maximises the annual solar radiation in the plane of the PV panel. This is adequate for systems working year-round. Sloped roofs: 12°, which corresponds to a typical inclination of the sloped roofs within the examined cities.
	Azimuth	The preferred orientation should be facing the equator, in which case the azimuth angle is 0° (south) in the Northern Hemisphere. This is the orientation set for the flat roof scenario. In the case of a solar panel mounted directly on a sloped roof of a building, the azimuth is equal to that of the roof. Therefore, for the sloped roof scenarios, south, southeast - southwest and east - west orientation was applied.
	Climatic data	The climatic data were selected from a list with available cities per country in RETScreen's database. For the cities with lack of climatic data, the nearest climate data location was selected instead. The climatic data concern the following parameters: <ul style="list-style-type: none"> • Daily solar radiation - horizontal • Daily solar radiation - tilted • Annual solar radiation - horizontal • Annual solar radiation - tilted • Monthly air temperature • Monthly air humidity
	Electricity export rate	The model calculates the monthly electricity exported from the PV system to the grid and then multiplies it with the agreed feed-in tariff, if any, paid by the electric utility or another customer.
Photovoltaic system's evaluation	Type	The type of PV modules considered for the application includes all common PV technologies. In the present study, the option of crystalline Si was selected, which represents both monocrystalline and polycrystalline solar cells.
	Power capacity	A small-scale system of 10kWp was examined for all applications
	PV efficiency	14.5% was assumed as an average solar panel efficiency for PV panels

Phase of analysis	Data	Description
	Nominal Operating Cell Temperature (NOCT)	The model calculates the NOCT, in °C. NOCT is defined as the module temperature that is reached when the PV module is exposed to a solar radiation level of 800W/m ² , a wind speed of 1m/s, an ambient temperature of 20°C, and no load. 45°C was assumed as an average NOCT for the PV panels.
	Temperature coefficient	The model calculates the PV temperature coefficient for overall module efficiency. An efficiency decrease of 0.40%/°C was assumed.
	Solar collector area	The model calculates the area that will be covered by the PV array. This is simply the PV array power capacity divided by the nominal module efficiency.
	Inverter efficiency	In concerns the efficiency, expressed in %, of the electronic devices (e.g. inverter) used to transform the DC output to AC. Values between 80 and 95% are typical. A value of 94% was assumed as an average starting point.
	Miscellaneous losses	They refer to array losses (%) from miscellaneous sources (such as cables, batteries, etc.) not taken into account elsewhere in the model. 7% was assumed in the present calculations.
Solar energy production results	Capacity factor	The model calculates the capacity factor, which represents the ratio of the average power produced by the power system over a year to its rated power capacity. Typical values for photovoltaic system capacity factor range from 5 to 20%.
	Electricity exported to grid	The model calculates the electricity exported to the grid both on an annual and monthly basis.

1.3 PV technology overview

PVs are installed and produce electricity both on fields and on buildings. There are two main segments; the off-grid or stand-alone and on-grid systems. The former are not connected to the distribution network but are usually designed to cover private electricity demands of isolated facilities, such as monasteries, weather stations and rural buildings. There are also stand-alone applications for road signs, public lighting and phone booths. Last but not least, consumer applications, such as calculators or solar watches, also consist of off-grid PV cells.

However, the prevailing category until 2011 referred to the grid-connected PVs as they benefit from the profits obtained by selling the produced energy at a fixed high tariff for a specific time period, regardless of the electricity consumptions and the respective retail electricity rates. The grid-connected systems are classified to specific segments based on their installed capacity (Table 3).

Table 3. Typical types and sizes of PV systems

Type of application	Residential	Commercial	Utility
	<10kWp	10kWp-100kWp	>100kWp
Ground-mounted	-	X	x
BIPVs or BAPVs	x	X	x

When it comes to the PV technologies and applications, as already mentioned, the PV applications in the building sector are categorised among building integrated and building applied systems. Their difference depends on the level of integration and on the functionalities, they can perform. BAPVs are mounted on the existing building's structure, thus do not add any value in terms of replacement of an ordinary construction material, but only by producing electricity and affecting energy efficiency of buildings. On the contrary, BIPVs fit into the building structure and become an integrated part of the architectural design, avoiding the use of other more expensive conventional cladding or roofing materials. The avoided cost of these materials is subtracted from the installation cost of BIPV improving their economics. However, in order to be effective, BIPV products should match the dimensions, structural properties, qualities, and life expectancy of the materials they displace and obviously should be harmonised with the architecture of the buildings, especially the existing ones. Still, BIPVs are designed to play a multifunctional role, which, apart from the energy supply, includes also the aesthetic enhancement of the building's architectural design as well as its envelope's weather protection and thermal insulation, and the control of daylighting and outdoors noise.

In general, the BAPVs can be classified to two main categories:

- flat or pitched roof mounted and
- façade mounted systems

The mounted PVs on flat roofs are independent of the building skin (Figure 25). The available area is not completely utilised due to reciprocal shading effects between PV arrays. However, the system operates at maximum efficiency as the optimal inclination and orientation can be achieved. It can also be installed in new constructions or as a retrofit. Energy savings include reduced cooling loads, apart from the produced electricity.



Figure 25. Perspective of existing state of the art flat roof mounted PV systems⁴

The mounted PVs on pitched roofs (Figure 26) perform according to the orientation and inclination that is constrained by the roof structure, but the suitable surfaces can be fully exploited. The PV modules are mounted as a retrofit above the existing shingles, tiles or metal roofing.

⁴ PV database - Urban Scale Photovoltaic Systems. *PV Upscale program*. [Online] <http://www.pvdatabase.org/projects.php>.



Figure 26. Perspective of existing state of the art PV installations mounted on pitched roofs

The façade mounted PVs, similarly to the mounted pitched roof applications, are installed above the existing construction materials, which comprise the building's façade (Figure 27). The main drawback is the 90° inclination of the PVs, which drastically decreases the efficiency during the summer period. Obviously, the optimal façade orientations are near south ones.

On the other hand, the BIPV applications are designed to serve more than one function, so they are separated into the following categories:

- Roofing systems which include
 - i solar laminates and exterior insulation systems for flat and flexible roofs,
 - ii “standard in-roof” systems and solar shingles or tiles for pitched roofs,
 - iii atrium skylights with semi-transparent (glass to glass modules) or opaque PVs
- Façade systems which include
 - i curtain wall glazing systems with semi-transparent modules,
 - ii cladding systems (flexible or not) for external building walls
 - iii shading systems with PV awnings or louvers



Figure 27. Perspective of existing state of the art façade mounted PV systems

The solar flexible laminates and exterior insulation systems for flat and curved roofs operate as a building skin with reduced efficiency due to the horizontal or multiple inclinations of PVs (Figure 28). The replacement of conventional materials is beneficial while they are suitable only for new constructions. The added weight of the PVs, snow accumulation and probable uplifting forces by winds that could occur must be considered as well. Attention must be paid during the installation of the arrays to avoid water proofing or thermal bridge issues. The available areas are fully utilised and there is also a potential of existing thermal insulation's enhancement. Especially flexible BIPV systems require well designed and light-weight installation. Moreover, they are designed to be

attached onto existing building materials such as metal roofing. New and innovative material platforms are used for products from this specific group, such as thin-film and organic PVs, whereas crystalline Si modules are excluded due their rigidity.



Figure 28. Perspective of existing state of the art flat and curved roof BIPV systems

“Standard in-roof” systems and solar shingles or tiles refer to pitched roof applications (Figure 29). They are combined with rooftop structural system as panelised units with insulation and are fastened directly to the roof structure. Weatherproofing, weight and structural issues must be carefully resolved. As in previously mentioned flat and curved roof applications, the available areas are fully utilised but within the inclination and orientation limitations of the existing roofs. In detail “standard in-roof” systems refer to the thinner crystalline panels which are smoothly integrated on top of existing roof materials. The crystalline option creates great prospects for these systems’ diffusion. Additionally, the solar tiles and shingles are designed to fit with conventional pitched roofing materials. Thus, the design of a PV tile or shingle has to incorporate regional architectural roofing practices. The positive point of this technology is that the most common PV tiles/shingles are manufactured by multi- or mono-Si solar cells.



Figure 29. Perspective of existing state of the art “standard in-roof” systems (left image) and solar shingles or tiles

The remaining BIPV roofing system is associated with atrium skylights usually manufactured from semi-transparent PVs made of glass to glass modules (Figure 30). There are also installations with opaque modules. In these systems, PVs function as individual roof openings or semi-transparent materials. The latter can be optionally manufactured either from crystalline or thin-film cells. The replacement of conventional glazing is proved to be beneficial in terms daylighting control. More specifically, PV modules can provide both electricity and diffused light to the internal environment of the buildings. Therefore, their significant advantage is definitely related to further stimulation of the architectural design of the building.



Figure 30. Perspective of existing state of the art semi-transparent BIPV skylight systems

As far as BIPV façade systems are concerned, their most common application stands for curtain wall glazing systems with semi-transparent modules (Figure 31). This type of system can both consist of individual windows or whole glazing façades. This type of installation is proposed when some sunlight penetration is necessary, although it is usually foreseen for aesthetic and architectural purposes rather than operational. The desirable amount of light that goes through the modules can be determined by adjusting the number and spacing between the cells of the PV module, in the case of crystalline Si technology or by altering the production procedures in the case of thin-film cells. This also applies to the PV skylights, described in the previous paragraph. That kind of BIPVs can effectively contribute to thermal and acoustic comfort, when installed in double glazing layer façades. Last but not least, in this group there is another innovative technology that should be remarked; PV parapets, which can replace conventional glazing or metal material used on safety parapets on balconies and terraces (Figure 32).



Figure 31. Perspective of existing state of the art curtain wall glazing systems with semi-transparent modules



Figure 32. Perspective of existing state of the art PV parapets with semi-transparent PVs

The cladding BIPV systems seem alike with curtain wall glazing ones, but concern façades with opaque PV panels (Figure 33). In the majority of these applications, there is a ventilation gap between the building's envelope and the PVs, which provides the opportunity for creating a dynamic wall system for ventilation, by means of automatically driven ventilation louvers and by exhausting hot air in warmer months or alternatively directing it back into the building during the cooler months. Standards modules (frame or frameless) are usually applied although the use of customised modules is occasionally inevitable to harmonically match the architectural façade configurations.

The last but of great importance façade BIPV system refers to PV shading devices. The awnings and louvers of these installations are separated into two technologies; the uncontrolled fixed systems (Figure 34) and the controlled and one-way sun-tracking devices, which are of higher cost (Figure 35). As expected, both provide passive shading and daylight control and eventually achieve lighting energy savings and high levels of optical comfort in the indoor environment of the buildings. Controlled movable shading devices are the only building PV technology with a sun-tracking system and thus they maximise the electricity production during the day compared to other BIPV façade systems, even though, they are affected by the orientation constraints. Unfortunately, there are additional costs for the mounting structure that have to be considered. The PV panels can be either semi-transparent or opaque.



Figure 33. Perspective of existing state of the art cladding BIPV systems and opaque PV parapets (PV database - Urban Scale Photovoltaic Systems)



Figure 34. Perspective of existing state of the art fixed BIPV shading devices



Figure 35. Perspective of existing state of the art sun-tracking BIPV shading devices

2 Eastern Partner Countries situation review

2.1 Availability of GIS Data – Quantification of solar potential

In an effort to examine the availability of the relevant data in the various countries, a National Country Report template has been devised and distributed to the national experts in order to collect the information. As shown in Figure 36, the information sought is the availability of 3D or 3D GIS or alternatively Cadastral data from where the building roof areas could be calculated.

Organization/contact/link ¹	city ²	Type of Organization ³	Data Type ⁴	Data format ⁵	Scale 1: ⁶	Usage Restrictions ⁷	Cost ⁸
		Public/ Private	GIS data – building footprints/ Aerial photography/ Satellite imagery/	DXF/ SHP/ JPEG	Eg. 5.000	Free/ Reserved/Royalties	Free/ xxxxx€/ha

¹ Give contact name, email, website and any other useful link
² City to which the data refer to
³ Indicate whether the organization providing the data is either Public or Private. This may also connect to Restrictions/Cost/Royalties of data use
⁴ Indicate whether a GIS layer with building footprints is available that can be used for PV estimation. Alternative data sources can be either aerial images or satellite images
⁵ Indicate whether vector or raster data is available and the related format (Autocad DXF, ESRI SHP, raster etc)
⁶ Indicate the scale of GIS data or aerial imagery. In case of satellite imagery indicate the satellite name (eg. LANDSAT, SPOT, IKONOS, WORLDVIEW, etc)
⁷ Indicate whether the data are free to be used or there are of restricted use. Describe restrictions applied. Indicate whether Royalties are applied
⁸ Indicative cost per ha

Figure 36. Sample National Report

Besides, the available format of the data, their quality, up-to-date status, completeness and level of details/accuracy (i.e. scale) is sought. It is important to note also that as in many other countries, the sources of the data may have to be sought in various national agencies and very often restrictions on their use are imposed.

One should be aware of the fact, that there are significant differences in the level of analysis possible, based on the data available. As a result, summary results tables that include average roof area are available only for Georgia and Moldova, a fact that is related to the registered number of buildings, which will be discussed in the next chapter.

Within the line of this project, the ultimate goal is of course to collect the data necessary for the assessment of the solar potential. Still, there is a secondary aim, namely based on the assessment of currently available data, to identify gaps and shortcomings, which will have to be dealt with in the near future, in order to enable the successful implementation of an effective energy policy. It is therefore clear that more detailed and of higher quality data will be required. As regards to the estimation of building roof area, we can conclusively state that:

1. The calculations in GEORGIA and MOLDOVA have been based on the available GIS/Cadastral data, whereas in the rest of the EPCs, the calculations have been based on freely available satellite data.
2. Due to the low geometrical resolution of the imagery (pixel size), the expected accuracy of the calculations is limited, and although adequate for the purpose of this study, better data quality is necessary for more detailed future studies.
3. Due to low radiometric resolution (i.e. colour depth), the classified pixels as “buildings” also contain other “concrete/asphalt” features (like for instance: streets, sidewalks, etc.). From the contacted tests, the conclusion is that only approximately 40% of the total number are actually referring to building roofs and thus a rule-of-thumb final trimming has been applied for the purpose of this study. It is anticipated though that better data quality is necessary for more detailed future studies.

It is clear that the best option of such data is the existence of 3D GIS building data. However, such data requires extensive LIDAR aerial flights to cover nationwide area. Such data are, at the moment, extremely expensive, and it comes as no surprise that it is not available even to highly industrialised countries. Therefore, this is not really an option for the foreseen future, until at least such data are available from satellite sensors at appropriate resolution/accuracy.

The next better option is the existence of 2D GIS/Cadastral data, from where the building roof areas could be calculated, provided that the type of roof is also given. Such Cadastral data are actually expected to exist in all countries (including the EPCs) to one degree or another.

The development of a national cadastral system is of course time consuming and requires extensive resources, but its strength lies on its multi-purpose and multi-functionality purpose. In fact, the main reason the cadastral systems are been developed is related to taxation and public/private real estate ownership. Therefore, their use as “building roof calculator” is only a side-use and thus, if such GIS exist, their exploitation for our purposes is straight-forward; if they do not exist, they will never be developed for mere our purposes.

Supposing that 2D Cadastral/GIS data exist (which is the main and the most probable scenario), the following activities must be identified as crucial in leveraging more qualitative energy quantification:

Action 1 - Data coverage extent and update: 2D GIS/Cadastral data must cover all nationwide area and at least all major cities, providing that these can lead to qualitative conclusions for the whole country. The up-to-date status and completeness level of these data can never be underestimated, provided the extensive urbanisation and building construction activities in many countries.

Action 2 - Data resolution: 2D GIS/Cadastral data must be available at appropriate level of details/accuracy at city level, i.e. at a scale of 1: 5.000 or bigger, meaning that the building roof areas can be calculated at an accuracy of 5m² or better. It must be noted that a prerequisite is also that information about roof type is also provided.

Action 3 - Data interoperability: 2D GIS/Cadastral data must be provided in a form (i.e. vector form, operational/open data format) which is user friendly and available in widely used formats. To this end, it must be noted that adopting the EU INSPIRE Directive (embedded in all EU countries' national law system) is highly recommended, as it secures EU interoperability.

Action 4 - Data accessibility: 2D GIS/Cadastral data must be openly and publicly accessible, since in many countries, barriers and shortcomings have been identified: sources of the data may have to be sought in various national agencies and very often restrictions on their use are imposed. Hence, it is very important that: (i) a national one-stop-shop is developed, which is usually referred to as NSDI (National Spatial Data Infrastructure) portal or a National Cadastral portal, which aims at providing quick and officially updated 2D/3D GIS data; and (ii) a national open data policy is adopted, which will ensure the unrestricted and royal-free use of such multi-purpose data

In that sense, the simplified National Reports as well as the detailed calculations of the roof data in each city for each of the EPCs are presented next.

2.1.1 Armenia

Organisation/contact/link	city	Type of Organisation	Data Type	Data format	Scale 1:	Usage Restrictions	Cost
<u>Contact:</u> Armen Gharibyan LEED AP BD+C Renewable Resources and Energy Efficiency Fund (R2E2) Solar PV Project Manager	Yerevan Vanadzor Gyumri					Not available GIS or Cadastral data	

Regardless our efforts through the State Committee of Urban Planning, as well as the Foreign Relations Department of the Ministry of Energy Infrastructures and Natural Resources, it was not possible to find any useful GIS or Cadastral data.

The cities examined in Armenia are:

- Yerevan
- Vanadzor
- Gyumri

Since no Cadastral or GIS data were available for Armenia, we followed the alternative procedure.

Thirty six (36) classes have been used in automatic unsupervised classification and the information obtained (i.e. buildings, open space, green space) could be identified in each spectral class. Finally, the only general class which was of concern was that of the building rooftop area.

City : Yerevan

Data: Landsat 7 ETM+, 212-851, free downloaded from <http://glovis.usgs.gov>

Date: 13 August 2000

Resolution: 15m Panchromatic, 30m Multispectral

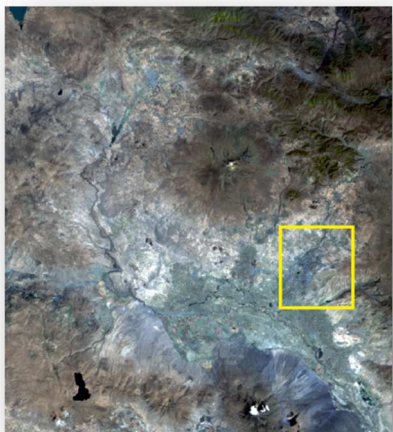


Figure 37. Yerevan: True colour, bands 1, 2, 3 the study area in yellow frame



Figure 38. Yerevan: Zoom in the study area

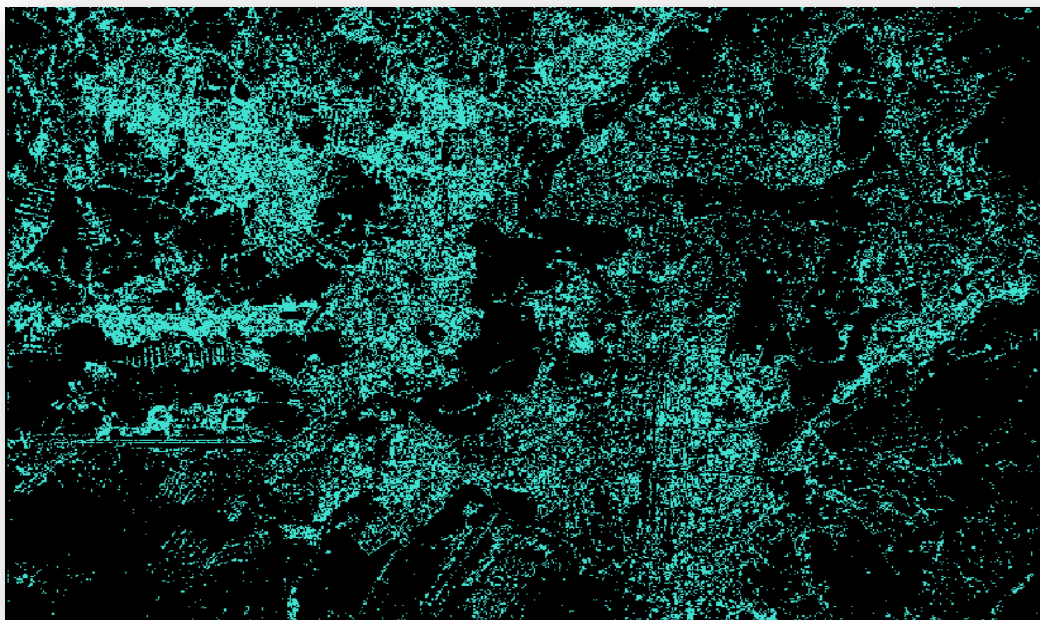


Figure 39. Yerevan: The results of the classification process

City : Vanadzor

Data: Landsat 7 ETM+, 219-433, free downloaded from <http://glcfapp.glc.f.umd.edu:8080/esdi/>

Date: 11 June 2006

Resolution: 15m Panchromatic, 30m Multispectral

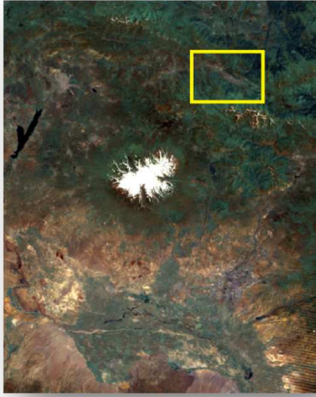


Figure 40. *Vanadzor: True colour, bands 1, 2, 3 the study area in yellow frame*



Figure 41. *Vanadzor: Zoom in the study area*

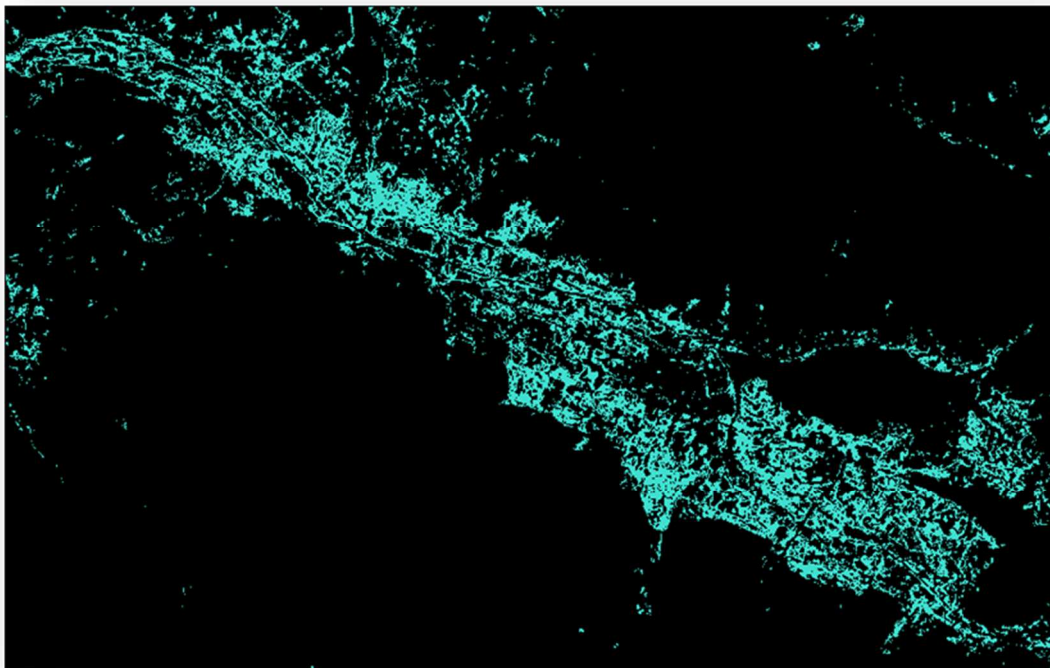


Figure 42. *Vanadzor: The results of the classification process*

City : Gyumri

Data: Landsat 7 ETM+, 219-433, free downloaded from <http://glofapp.glof.umd.edu:8080/esdi/>

Date: 11 June 2006

Resolution: 15m Panchromatic, 30m Multispectral



Figure 43. Gyumri: True colour, bands 1, 2, 3 the study area in yellow frame



Figure 44. Gyumri: Zoom in the study area

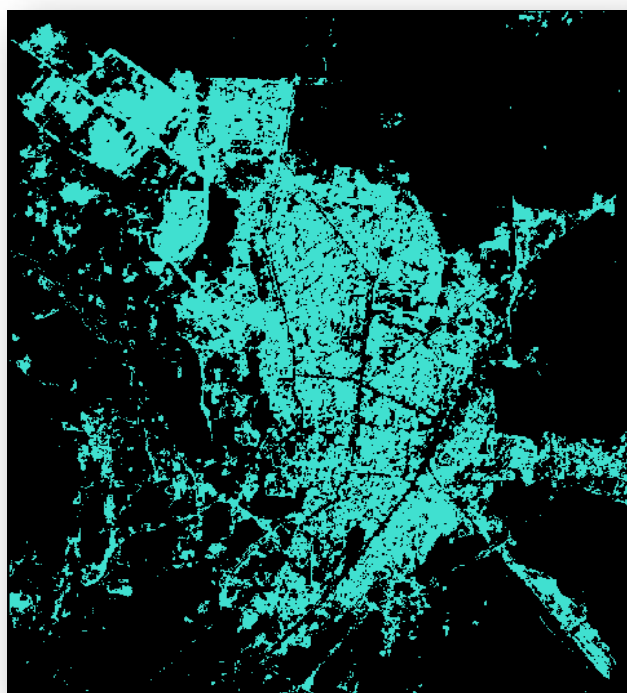


Figure 45. Gyumri: The results of the classification process

Calculation of built-up area in major cities in Armenia

City	Total building roof area (m ²)
------	--

Yerevan	23,494,972
Vanadzor	3,943,260
Gyumri	3,263,584

2.1.2 Azerbaijan

Organisation/contact/link	city	Type of Organisation	Data Type	Data format	Scale 1:	Usage Restrictions	Cost
<u>Contact</u> : Jahangir Efendiev	Baku Sumgait Ganja					Not available GIS or Cadastral data	

Regardless our efforts, through our local expert, it was not possible to find any useful GIS or Cadastral data.

The cities examined in Armenia are:

- Baku
- Sumgait
- Ganja

Since no Cadastral or GIS data were available for Azerbaijan, we followed the alternative procedure described in 2.3.4.

Thirty six (36) classes have been used in automatic unsupervised classification and the information obtained (i.e. buildings, open space, green space) could be identified in each spectral class. Finally, the only general class which was of concern was that of the building rooftop area.

City : Baku

Data: Landsat 7 ETM+, 212-559, free downloaded from <http://glcfapp.glcf.umd.edu:8080/esdi/>

Date: 15 August 1999

Resolution: 15m Panchromatic, 30m Multispectral



Figure 46. Baku: True colour, bands 1, 2, 3 the study area in yellow frame



Figure 47. Baku: Zoom in the study area

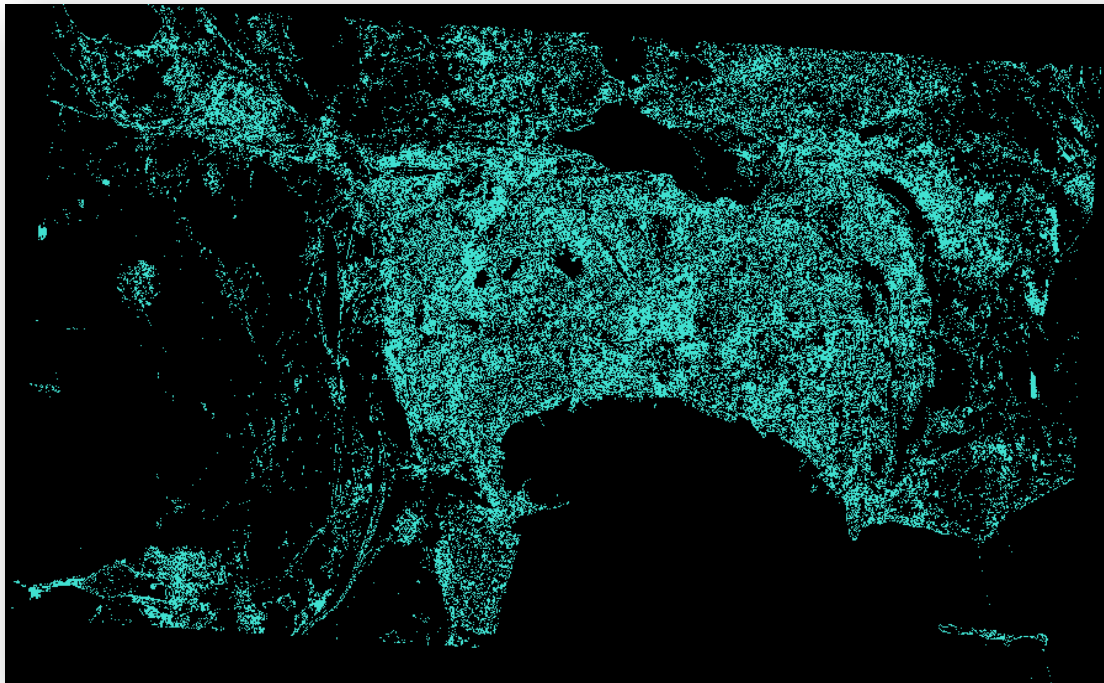


Figure 48. Baku: The results of the classification process

City : Sumgait

Data: Landsat 7 ETM+, 212-559, free downloaded from <http://glofapp.glof.umd.edu:8080/esdi/>

Date: 15 August 1999

Resolution: 15m Panchromatic, 30m Multispectral



Figure 49. Sumgait: True colour, bands 1, 2, 3 the study area in yellow frame



Figure 50. Sumgait: Zoom in the study area

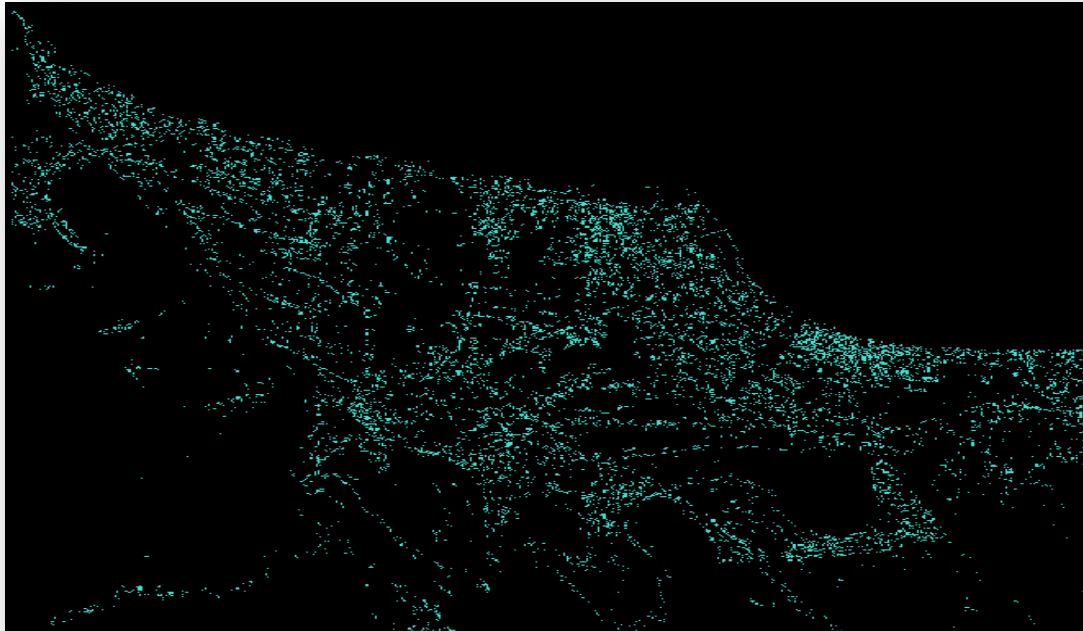


Figure 51. Sumgait: The results of the classification process

City : Ganja

Data: Landsat 7 ETM+, 212-700, free downloaded from <http://gclcfapp.glcf.umd.edu:8080/esdi/>

Date: 2 August 2001

Resolution: 15m Panchromatic, 30m Multispectral

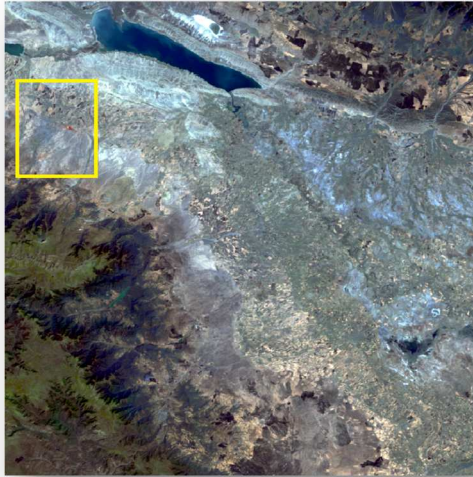


Figure 52. *Ganja: True colour, bands 1, 2, 3 the study area in yellow frame*



Figure 53. *Ganja: Zoom in the study area*

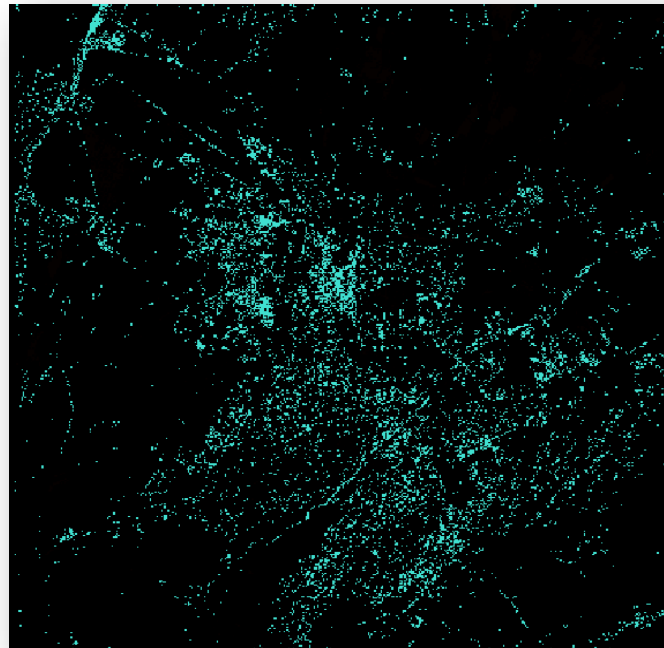


Figure 54. *Ganja: The results of the classification process*

Calculation of built-up area in major cities in Azerbaijan

City	Total building roof area (m ²)
Baku	43,260,600
Sumgait	4,428,452
Ganja	3,808,980

2.1.3 Belarus

Organisation/contact/link	city	Type of Organisation	Data Type	Data format	Scale 1:	Usage Restrictions	Cost
<u>Contact:</u> Andrew Malochka Head of energy department, BELTEI http://www.beltei.by	Minsk Mogilev Vitebsk		Not available			GIS or Cadastral data	

Regardless our efforts, through our local expert, it was not possible to find any useful GIS or Cadastral data.

The cities examined in Belarus are:

- Minsk
- Mogilev
- Vitebsk

Since no Cadastral or GIS data were available for Belarus, we followed the alternative procedure described in 2.3.4.

Thirty six (36) classes have been used in automatic unsupervised classification and the information obtained (i.e. buildings, open space, green space) could be identified in each spectral class. Finally, the only general class which was of concern was that of the building rooftop area.

City : Minsk

Data: Landsat 7 ETM+, 213-819, free downloaded from <http://glovis.usgs.gov>

Date: 27 May 2006

Resolution: 15m Panchromatic, 30m Multispectral

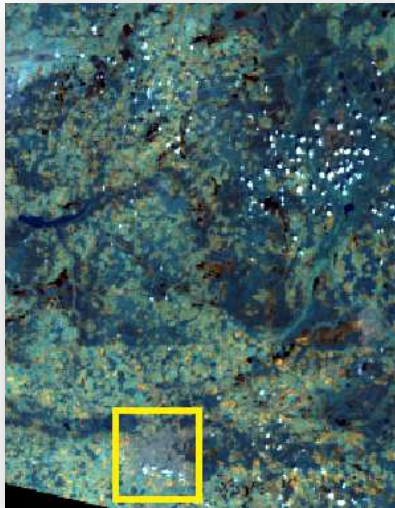


Figure 55. Minsk: True colour, bands 1, 2, 3 the study area in yellow frame

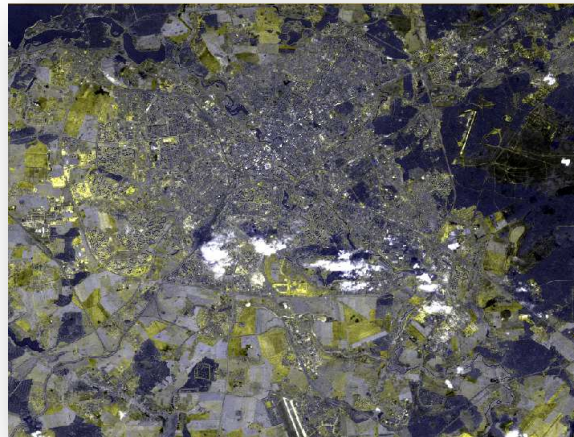


Figure 56. Minsk: Zoom in the study area

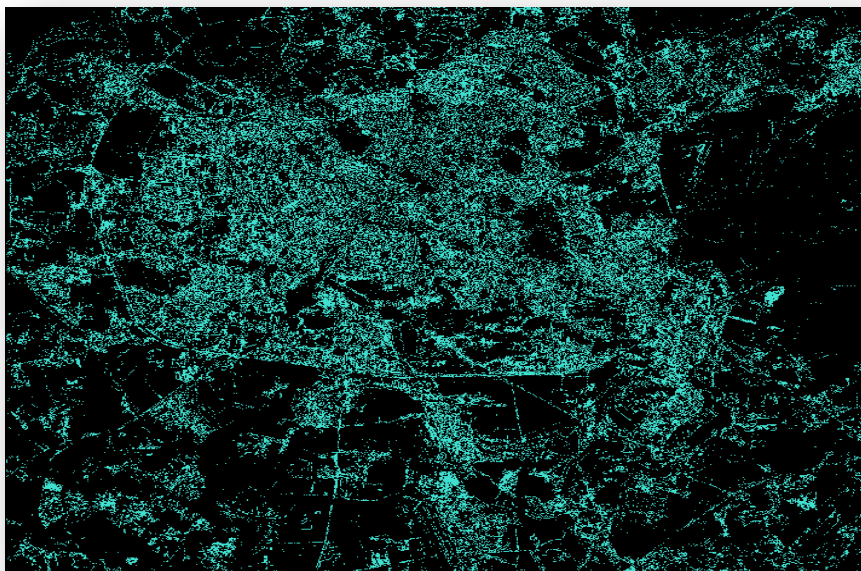


Figure 57. Minsk: The results of the classification process

City : **Mogilev**

Data: Landsat 7 ETM+, 213-703, free downloaded from <http://glofapp.glof.umd.edu:8080/esdi/>

Date: 2 October 1999

Resolution: 15m Panchromatic, 30m Multispectral

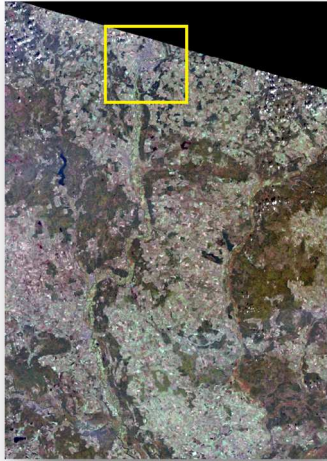


Figure 58. Mogilev: True colour, bands 1, 2, 3 the study area in yellow frame



Figure 59. Mogilev Zoom in the study area

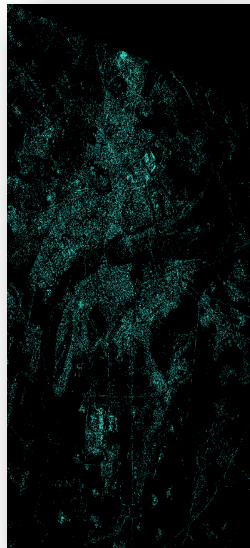


Figure 60. Mogilev The results of the classification process

City : Vitebsk

Data: Landsat 7 ETM+, 213-765, free downloaded from <http://glcfapp.glcf.umd.edu:8080/esdi/>

Date: 20 May 2000

Resolution: 15m Panchromatic, 30m Multispectral

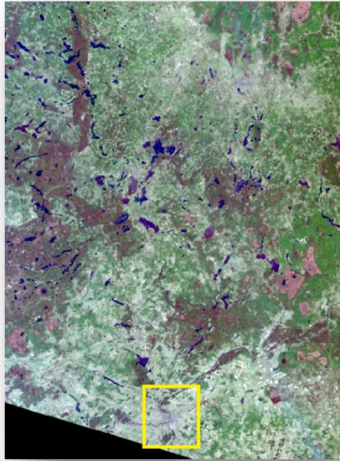


Figure 61. Vitebsk: True colour, bands 1, 2, 3 the study area in yellow frame

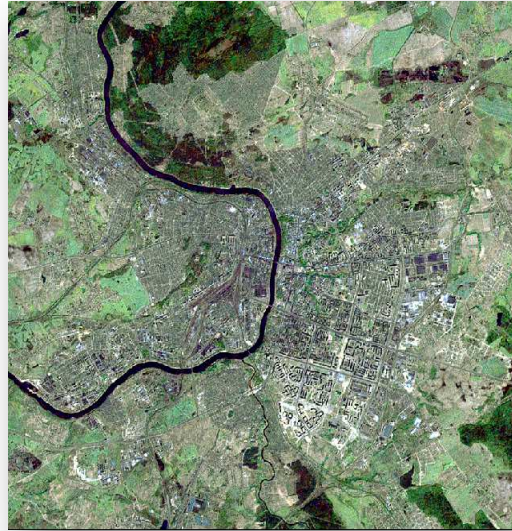


Figure 62. Vitebsk: Zoom in the study area

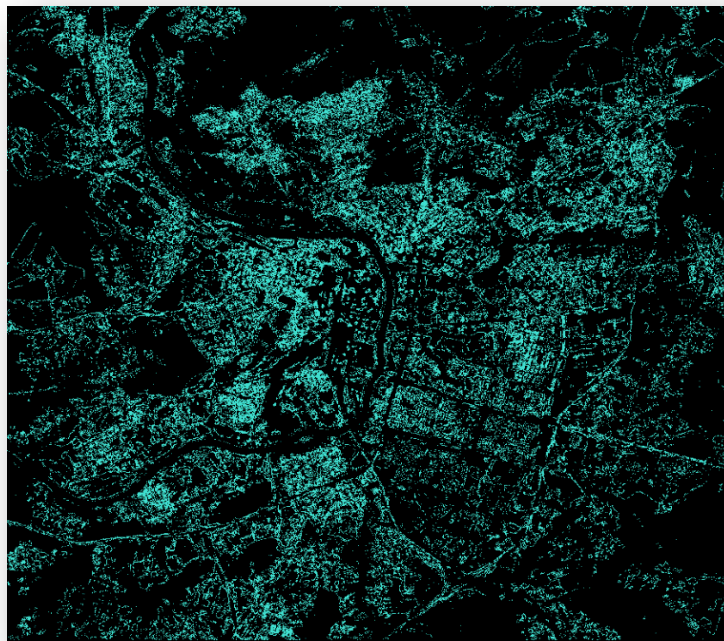


Figure 63. Vitebsk: The results of the classification process

Calculation of built-up area in major cities in Belarus

City	Total building roof area (m ²)
Minsk	41,663,680
Mogilev	8,822,708
Vitebsk	10,496,612

2.1.4 Georgia

Organisation/contact/link	city	Type of Organisation	Data Type	Data format	Scale 1:	Usage Restrictions	Cost
Department of Justice Website: http://maps.napr.gov.ge/#zoom=8&lat=42.13099&lon=43.9915&layers=B0000000FFFFFFFFFFFFFF0000F Contact: Oleg Zhukovski R&D Manager, JSC "Georgian Energy Development Fund" www.gedf.com.ge	Tbilisi Batumi Kutaisi Rustavi	Public	Cadastral GIS data – building footprints layer	SHP	5.000	Royalties	1,92€/ha

Georgia has developed a detailed Cadastral system, which covers the major cities of the country. These data have been used in this study.


The cities examined in Georgia are:

- Tbilisi
- Batumi
- Kutaisi
- Rustavi

Georgia has developed a detailed Cadastral system which covers the major cities of the country.

EuroGeographics Annual Review 2013

REPUBLIC OF GEORGIA ADDS 6 MORE CITIES TO ITS ADDRESSING PROJECT






Six major cities were included in the Republic of Georgia's Addressing Project during 2013 - Batumi, Kutaisi, Zugdidi, Gori, Bolnisi and Telavi.

The project is being delivered by the National Agency of Public Registry supported by the EC, US Agency for International Development (USAID) and the Swedish International Development Cooperation Agency (Sida). The goal is to create a complete, high quality address database based on unified standards and systems for a wide range of uses.

Activities include street descriptions such as names, directions, types of road; an inventory of immovable property units and identification of owners or users; preparation of road layer data; electronic drawings of buildings and their internal areas; and the creation of the correct address data. Inventory, verification, correction of data and GIS is carried out by field groups with registration units working on mapping and entering data in the address registry.

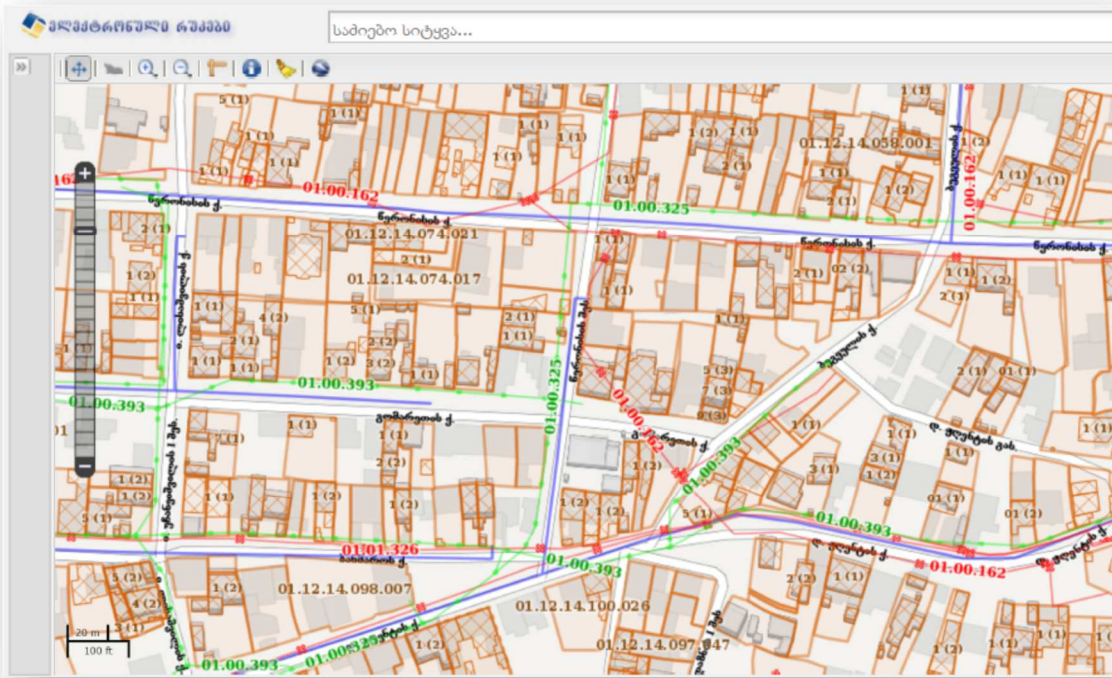
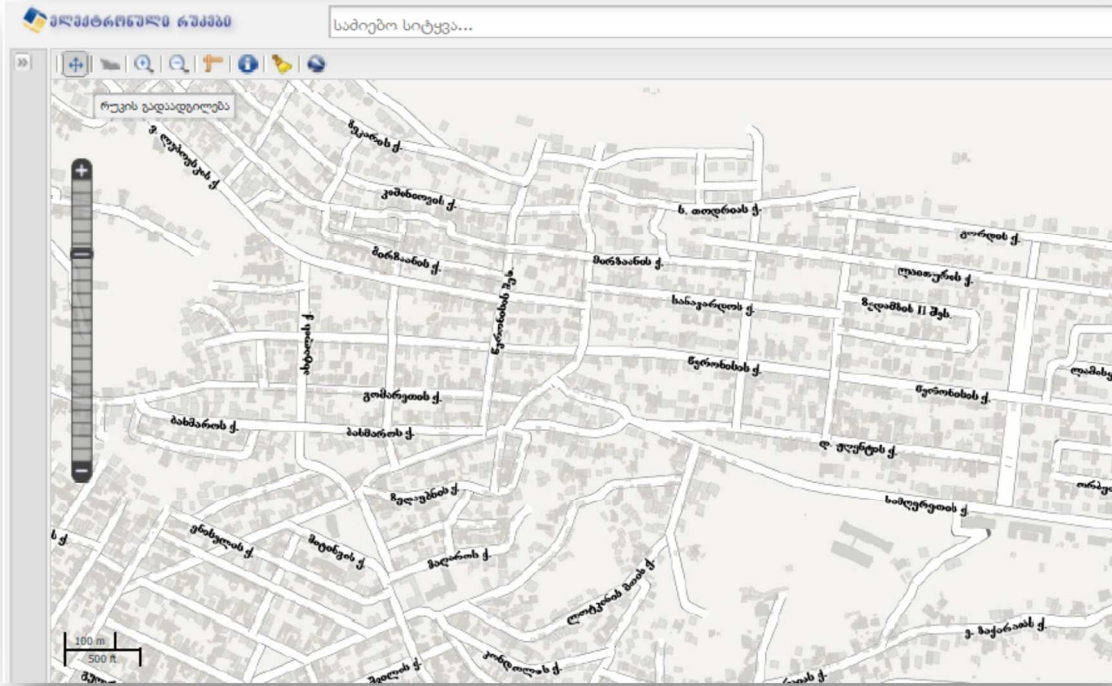
Tbilisi and Rustavi were added in 2011/12 with addressing for 11 more cities. All local districts (23 Sakrebulo) will be addressed in Mtskheta in 2014.

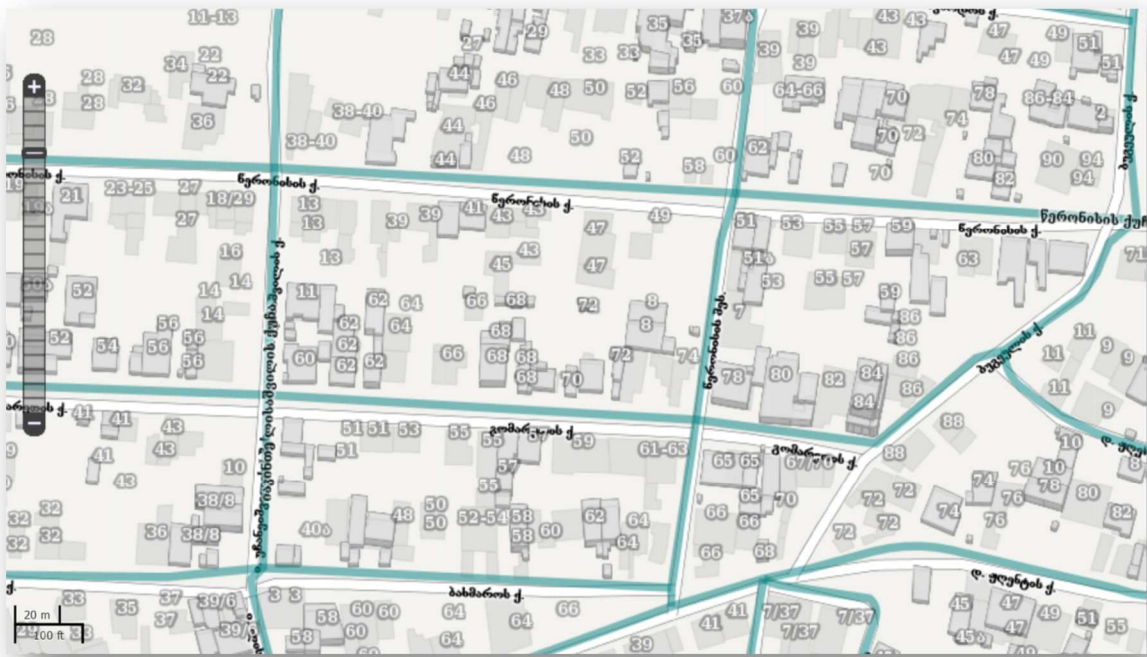




Sources: <http://eulis.eu/service/countries-profile/georgia/>
<http://www.eurogeographics.org/country/georgia>,
<http://www.kartverket.no/en/about-the-norwegian-mapping-authority/centre-for-property-rights-and-development/Georgia/>

Figure 64. *The Cadastral System of Georgia*

Cadastral data are available on-line regarding the Tbilisi area, through: www.napr.gov.ge.

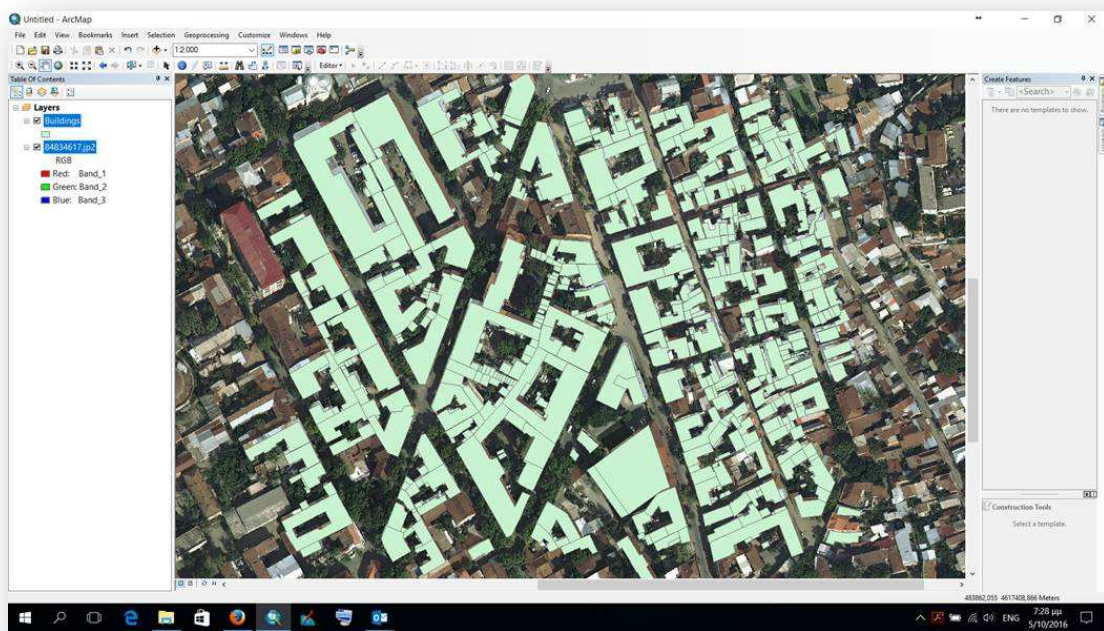
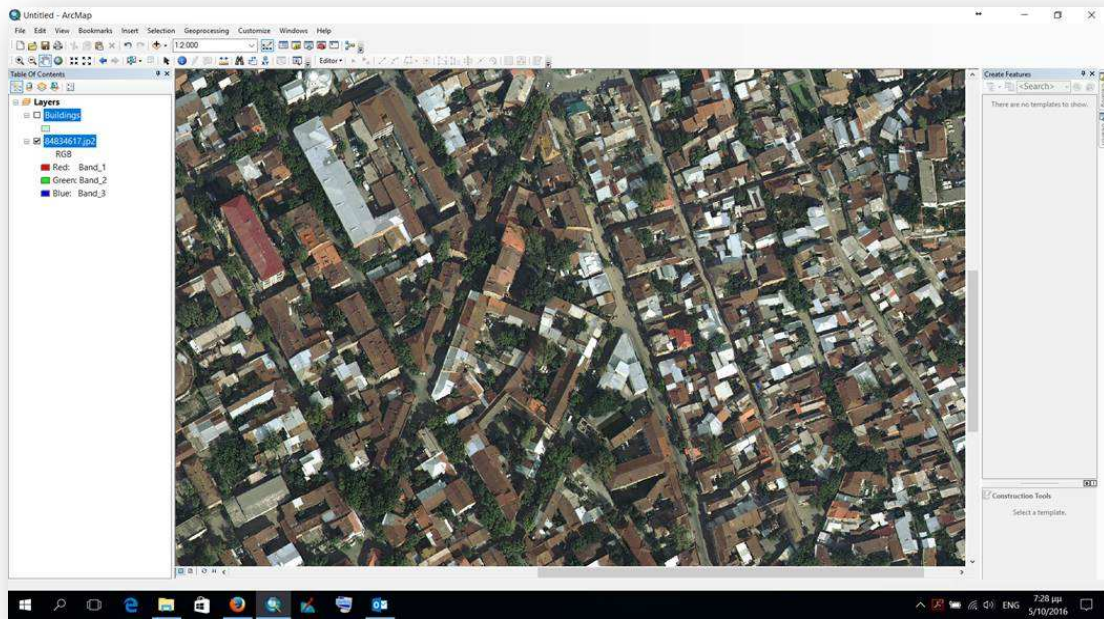


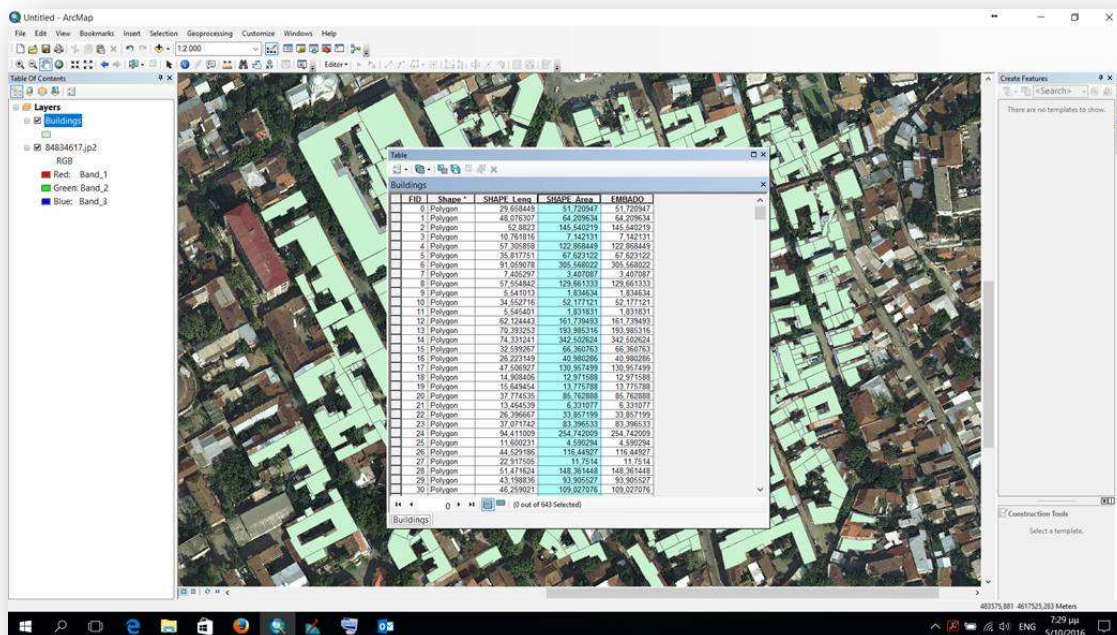


Source:
<http://maps.napr.gov.ge/#zoom=7&lat=42.13099&lon=43.9915&layers=B000000FFFFFFFFFFFFF0000F>

Figure 65. Extracts from Cadastral System of Georgia

A sample of these data has been checked for its accuracy and completeness and it was found that the area calculation is very accurate (as shown in figures below). Therefore, these data constitute a perfect source for calculation of the available PV area.





Source: www.napr.gov.ge

Figure 66. Evaluation of the quality of the Cadastral System of Georgia

Given the quality of the available Cadastral/GIS data, it has been decided to use this source for our calculations. The available building rooftop areas calculated in these cities are given at the table below:

City	Total number of buildings	Total building roof area (m ²)	Average building roof area (m ²)
Tbilisi	245.639	24.634.075	100
Batumi	10.143	2.879.820	284
Kutaisi	28.835	4.816.095	167
Rustavi	16.233	2.904.118	179

2.1.5 Moldova

Organisation/contact/link	city	Type of Organisation	Data Type	Data format	Scale 1:	Usage Restrictions	Cost
Agency Land Relations and Cadastre (ALRC) www.arfc.gov.md https://www.cadastru.md/ecadastru/webinfo/f?p=100:1:562019015817423 http://geoportal.md/ro/default/menu/browse/id/10 Contact: Andrei Sula	Chisinau Balti Cahul	Public	Cadastral GIS data – building footprints layer	SHP	10.000	The free data are to be used for informational purposes without juridical consequences	on request

For the calculation of the roofs surfaces of the residential buildings, various sources of data have been used:

- for the city of Chisinau, the data provided by the UNDP study⁵ has been used;
- for the city of Balti, the data provided by the Bureau of Statistics⁶ has been used;
- for the city of Cahul, the data provided by the USAID Report on city development⁷ has been used.

The cities examined in Moldova are:

- Chisinau
- Balti
- Cahul

Moldova has developed a detailed Cadastral system through ALRC:

⁵ ESCO Moldova Project – Moldova Green City/Promoting Low Carbon Growth in the City of Chisinau, p. 65, http://www.md.undp.org/content/dam/moldova/docs/Project%20Documents/ESCO%20Moldova%20Project%20Document_EN.pdf?download

⁶ The data are based on the area of the apartments located in residential buildings, connected to the district heating system, as provided by the Bureau of Statistics http://statbank.statistica.md/pxweb/pxweb/ro/30%20Statistica%20sociala/30%20Statistica%20sociala__06%20LOC__LOC010/LOC010100reg.px/?rxid=b2ff27d7-0b96-43c9-934b-42e1a2a9a774

⁷ The data are based on the area of residential buildings according to Cahul city development report (page 20): STRATEGIA LOCALĂ DE DEZVOLTARE SOCIO-ECONOMICĂ INTEGRATĂ A ORAȘULUI CAHUL (in Romanian) <http://www.primariacahul.md/images/strategiedezvoltare.pdf>

Agency Land Relations and Cadastre (ALRC) www.arfc.gov.md

Address: str. Pushkin, 47, Chisinau, Moldova, MD-2005

ALRC was founded in July 27, 1994 by Presidential Decree no. 230, aimed at development and promotion of state policy and strategy in the field of land administration and regulation of land relations, soil protection, and evaluation of real estate cadastre, geodesy, cartography and geoinformatics. The Agency is subordinated to the Government.

The work of the ALRC is guided by the Constitution, the Law on Government, Laws related to the scope, decrees of the President of Moldova, orders and decisions of the Government and international agreements to which Moldova is a party, other laws and its own rules.

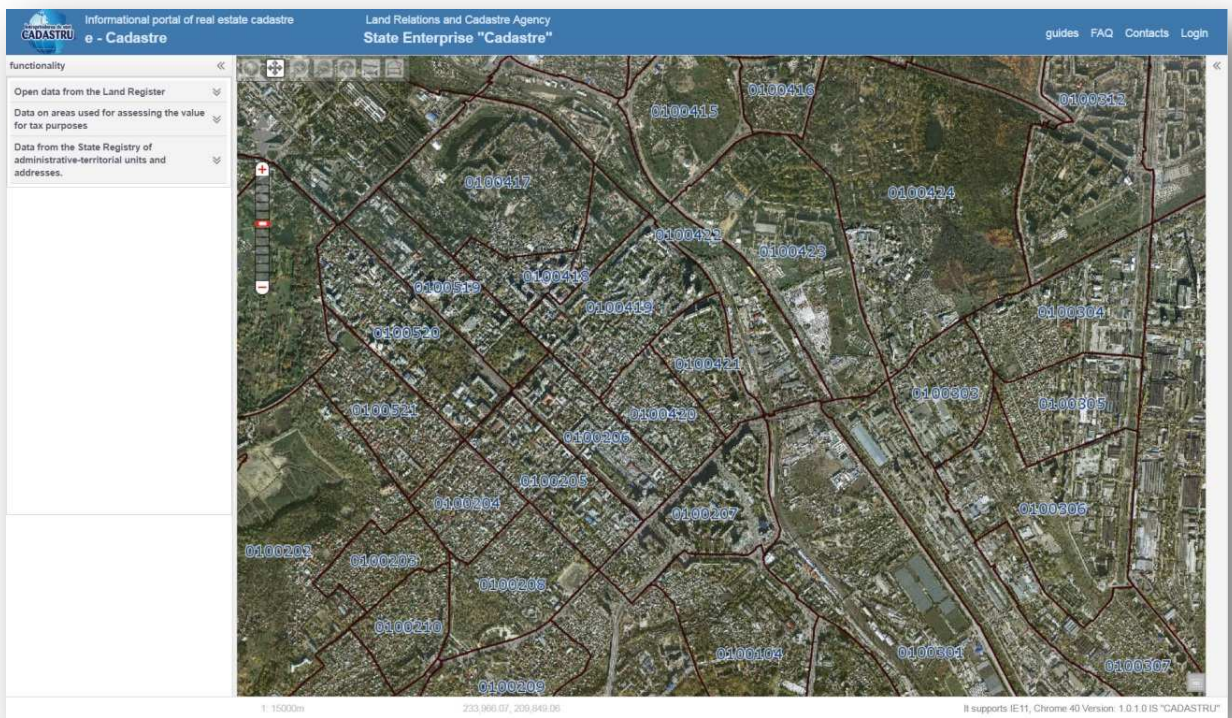
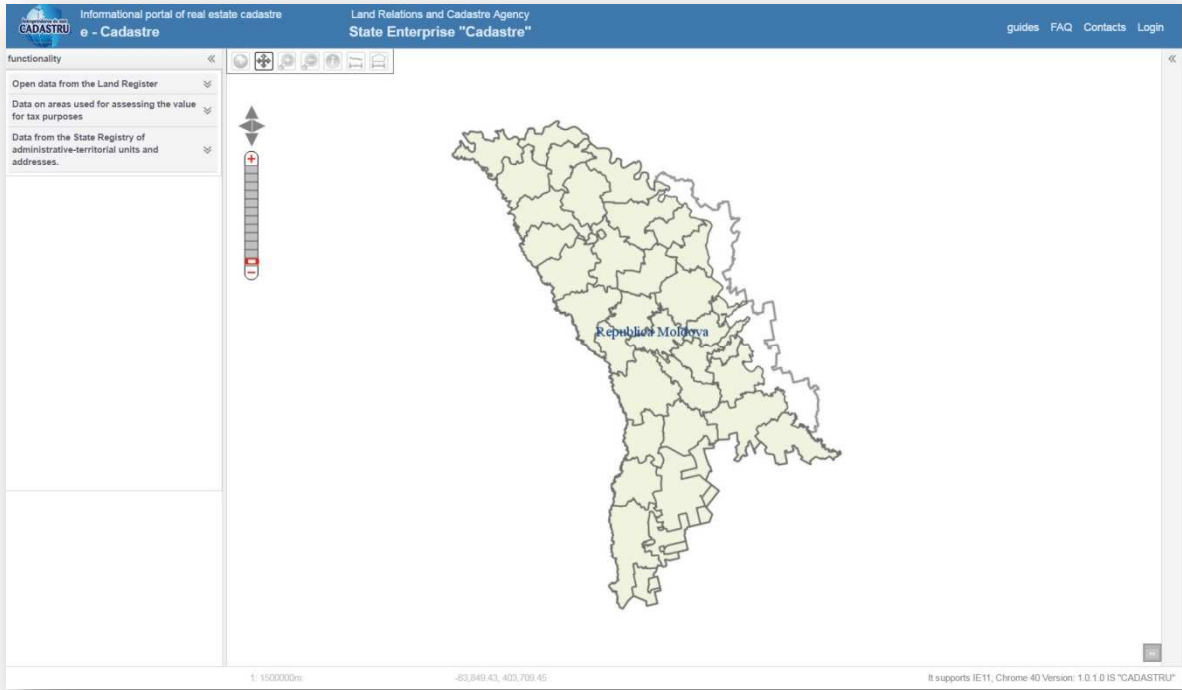
ALRC participate in socio-economic development forecasts on the country, coordinate central specialised bodies, public administration and local government in terms of developing and promoting programmes and national plans branch. However, ALRC promotes organisational reform - economic in its areas, harmonise laws and regulations in the scope of the powers entrusted to the European standards and norms, and promote the implementation of new technologies in its areas of activity.

ALRC manages assets of state enterprises subordinated to, capital of which is wholly or partly state responsible for the operation of state enterprises in the sector as well as the results of financial-economic activity of their founding state companies in its areas of activity, it organises and they liquidated in accordance with law force. However, the ALRC coordinates preparedness, training, recycling and certification of professionals within the field.

Subordinated ALRC four SOEs are as follows:

- State Enterprise "CADASTRU"
- State Enterprise Institute of Geodesy Technical Research and Cadastre "INGEOCAD"
- State Enterprise Project Institute for Land Management "assumptions";
- The State Association for Soil Protection.

Sources: <http://geoportal.md/ro/default/menu/browse/id/10>





Source: <https://www.cadastru.md/ecadastru/webinfo/f?p=100:1:562019015817423>

<http://geoportal.md/ro/default/menu/browse/id/10>

Figure 67. The Cadastral System of Moldova

Calculation of built-up area in major cities in Moldova

For the calculation of the roofs surfaces of the residential buildings, various sources of data have been used: (1) for the city of **Chisinau**, the data provided by the UNDP study⁸ has been used; (2) for the city of **Balti**, the data provided by the Bureau of Statistics⁹ has been used; (3) for the city of **Cahul**, the data provided by the USAID Report on city development¹⁰ has been used. All data has been updated by 2016 data received by the by the Bureau of Statistics:

⁸ ESCO Moldova Project – Moldova Green City/Promoting Low Carbon Growth in the City of Chisinau, p. 65, http://www.md.undp.org/content/dam/moldova/docs/Project%20Documents/ESCO%20Moldova%20Project%20Document_EN.pdf?download

⁹ The data are based on the area of the apartments located in residential buildings, connected to the district heating system, as provided by the Bureau of Statistics http://statbank.statistica.md/pxweb/pxweb/ro/30%20Statistica%20sociala/30%20Statistica%20sociala_06%20LOC_LOC010/LOC010100reg.px/?rxid=b2ff27d7-0b96-43c9-934b-42e1a2a9a774

¹⁰ The data are based on the area of residential buildings according to Cahul city development report (page 20): STRATEGIA LOCALĂ DE DEZVOLTARE SOCIO-ECONOMICĂ INTEGRATĂ A ORAȘULUI CAHUL (in Romanian) <http://www.primariacahul.md/images/strategiedezvoltare.pdf>

City	Total number of buildings	Total building roof area (m ²)	Average building roof area (m ²)
Chisinau	6.150	2.339.686	380
Balti	993	286.000	288
Cahul	204	73.000	359

2.1.6 Ukraine

Organisation/contact/link	city	Type of Organisation	Data Type	Data format	Scale 1:	Usage Restrictions	Cost
<p><u>Contact:</u> Kostiantyn Gura Acting Director State Company Subdivision "Green Investment Development Centre" State Agency on Energy Efficiency and Energy Saving of Ukraine www.sae.gov.ua www.gidc.in.ua</p>	Kyiv Odesa Lviv		Not available GIS or Cadastral data				

Regardless our efforts through the State Statics Service, City Councils of Kyiv, Lviv, Odesa, Zaporizhia and Ivano-Frankivsk, it was not possible to find any useful GIS or Cadastral data. Only general plans have been provided by relevant Municipal services.

The cities examined in Ukraine are:

- Kyiv
- Odesa
- Lviv

The general plans of the cities is an open source information that was received from official web-cites of municipal authorities.

Kyiv

The detailed information concerning the general plan of Kyiv city is provided by following reference (in Ukrainian):

<https://drive.google.com/drive/folders/0BxbGBoNdb1j6fmdGWVdtNzJSaWgyTXIWaW5WX1FxV3dSVIVEd1VwYm1UcF8wOVbhUUtmSnM>

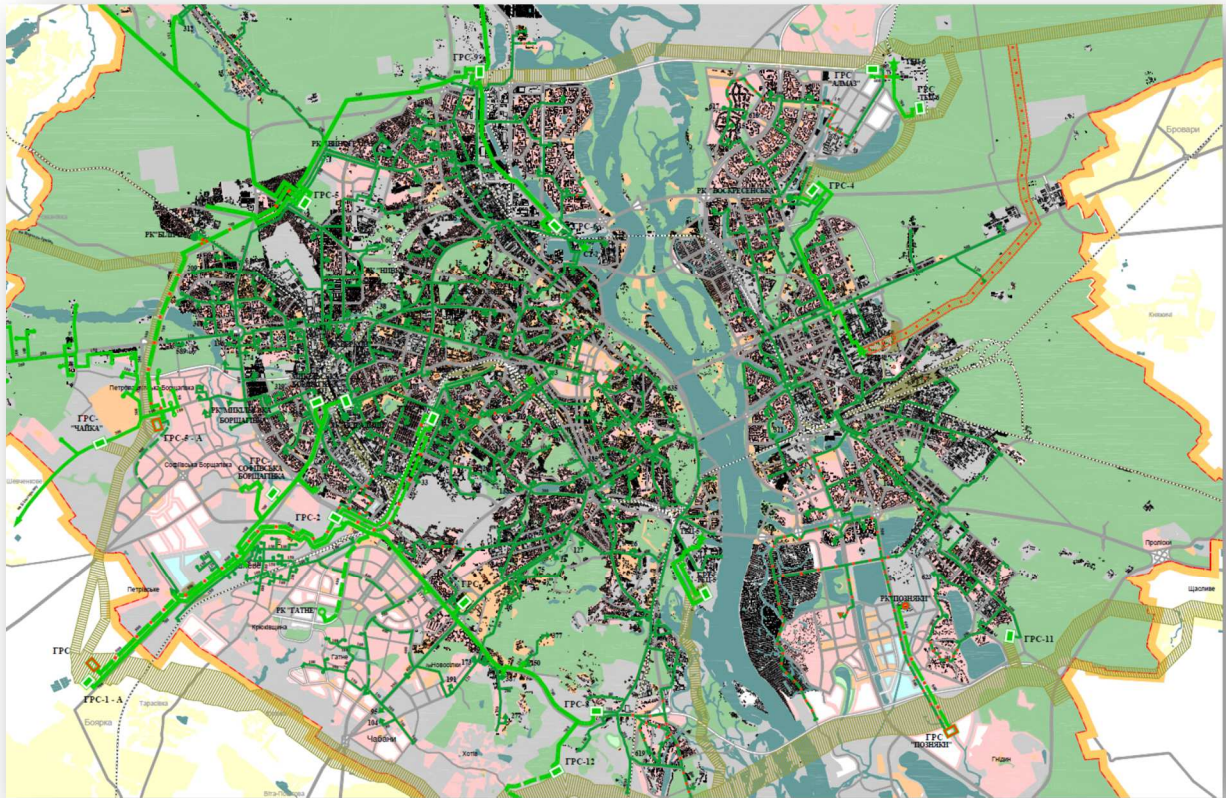


Figure 68. General city plan of Kyiv

Lviv

The detailed information concerning the general plan of Lviv is provided by following reference (in Ukrainian):

http://city-adm.lviv.ua/lmr/images/stories/arhitect/123/01_genplan.pdf

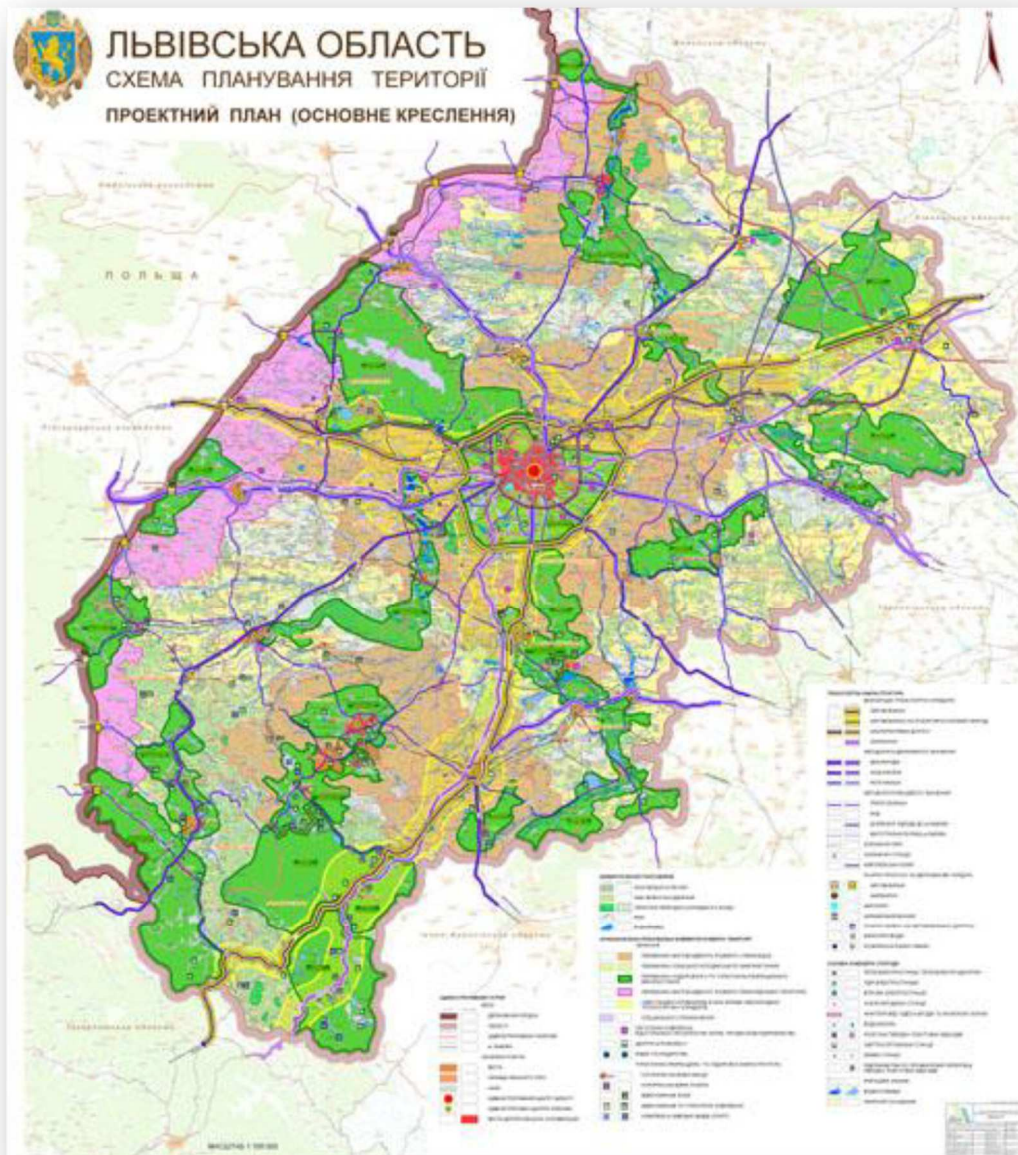


Figure 69. General city plan of Lviv

Odesa

The detailed information concerning the general plan of Odesa is provided by following reference (in Ukrainian): <http://www.citymap.Odesa.ua/?29>

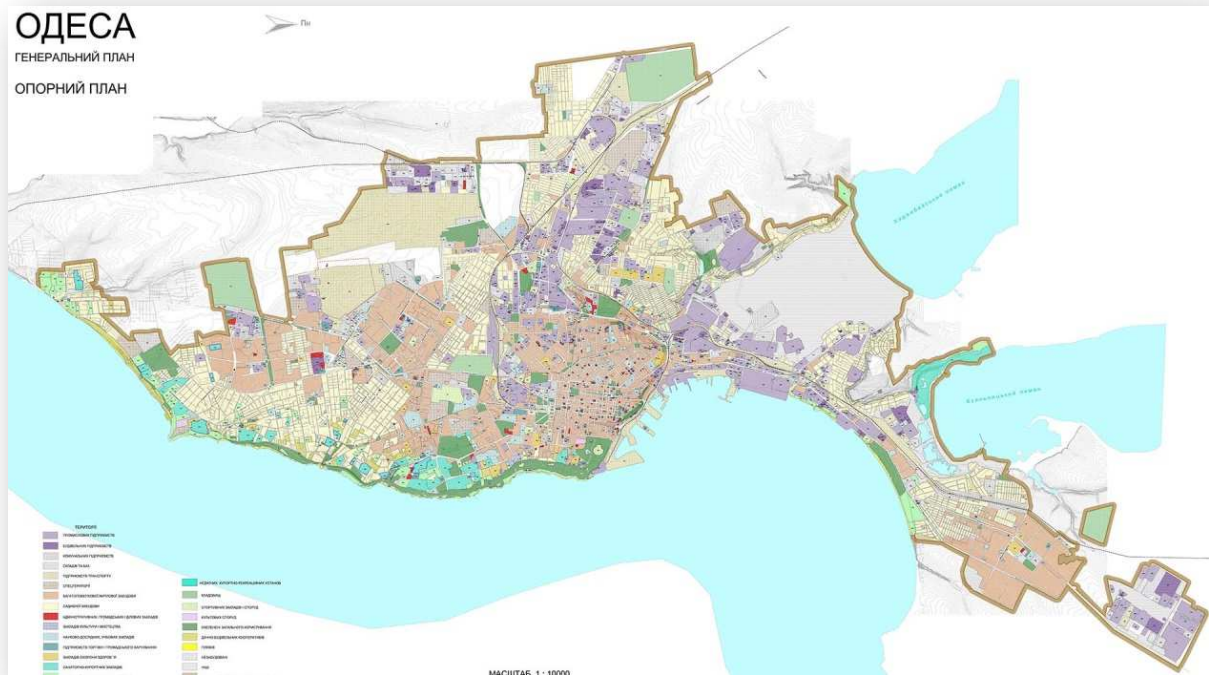


Figure 70. General city plan of Odesa

Since no Cadastral or GIS data were available for Ukraine, we followed the alternative procedure described in 2.3.4.

Thirty six (36) classes have been used in automatic unsupervised classification and the information obtained (i.e. buildings, open space, green space) could be identified in each spectral class. Finally, the only general class which was of concern was that of the building rooftop area.

City : Kyiv

Data: Landsat 7 ETM+, 220-154, free downloaded from <http://glovis.usgs.gov>

Date: 24 June 2006

Resolution: 15m Panchromatic, 30m Multispectral



Figure 71. Kyiv: True colour, bands 1, 2, 3 the study area in yellow frame



Figure 72. Kyiv: Zoom in the study area

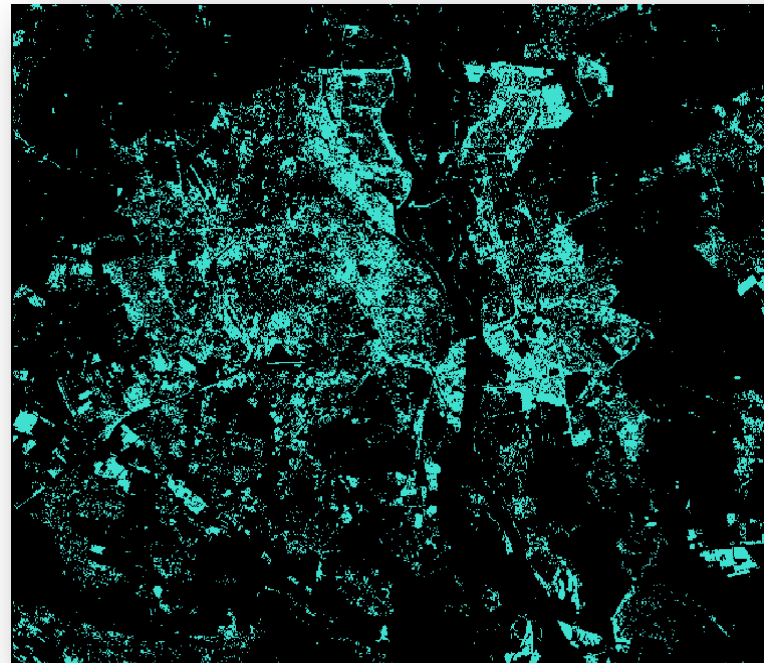


Figure 73. Kyiv: The results of the classification process

City : Odesa

Data: Landsat 7 ETM+, 220-099, free downloaded from <http://glovis.usgs.gov/data/landsat/landsat7/220-099/>

Date: 19 July 2006

Resolution: 15m Panchromatic, 30m Multispectral



Figure 74. Odesa: True colour, bands 1, 2, 3 the study area in yellow frame



Figure 75. Odesa: Zoom in the study area

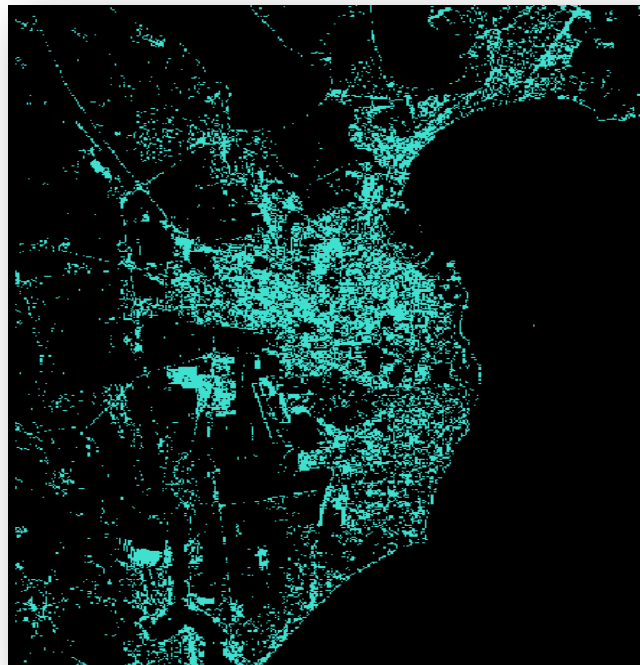


Figure 76. Odesa: The results of the classification process

City : Lviv

Data: Landsat 7 ETM+, 220-387, free downloaded from <http://glovis.usgs.gov>

Date: 21 September 2005

Resolution: 15m Panchromatic, 30m Multispectral

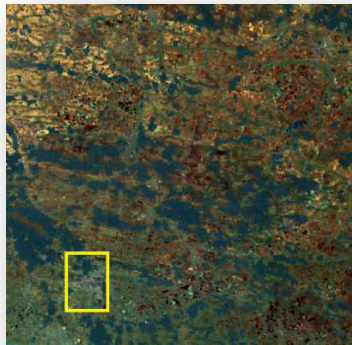


Figure 77. Lviv: True colour, bands 1, 2, 3 the study area in yellow frame



Figure 78. Lviv: Zoom in the study area

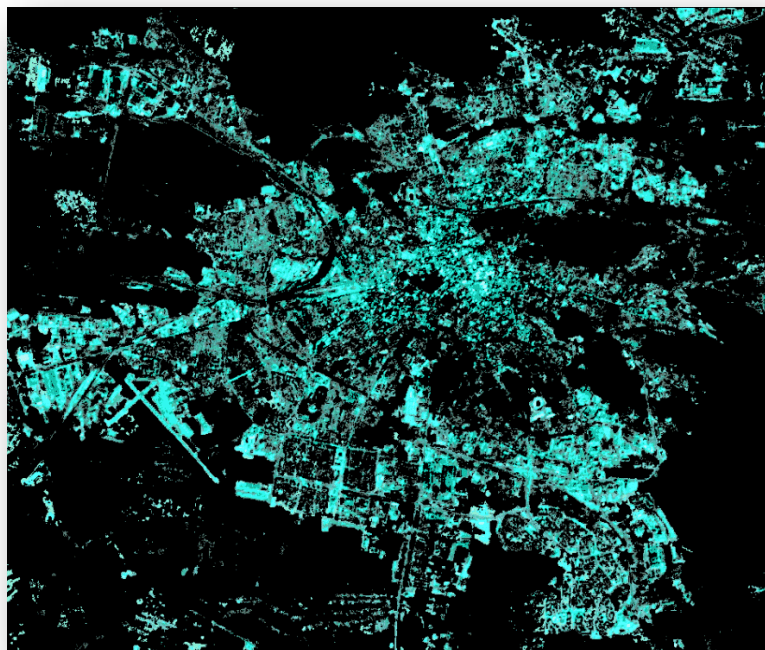


Figure 79. Lviv: The results of the classification process

Calculation of built-up area in major cities in Ukraine

City	Total building roof area (m ²)
Kyiv	59,075,200
Odesa	30,700,548
Lviv	17,659,260

3 Rooftop solar potential

3.1 Assumptions

The assessment of the solar potential in the examined cities, as mentioned above, was a complicated and demanding exercise. Albeit the gross roof areas were successfully estimated utilizing the capabilities of the GIS and satellite tools, there are – as it was anticipated - rather limited data available regarding the inclination (flat or sloped) and the orientation of the available roofs within the cities. Still, useful data have been obtained through a fact-finding mission via experts' (mostly at Municipality Architectural Department Head level) testimonies. These involved in particular the uses of the existing buildings and their basic roof characteristics with a view to clarify to a greater extent the main layouts of the roofs.

Regarding the building roofs' classification according to their inclination and shape (flat, pitched and hipped roofs) an extensive research was carried out, in cooperation with local experts in order to

- identify what kind of the existing buildings are most suitable for PV installations and which is their most common type of roofs and
- estimate eventually the fraction of the building stock they represent.

This analysis was conducted for each country separately and the outcomes are presented in the next paragraphs.

The second task of the estimation of the solar potential included the approximation of the suitable rooftop areas by applying the following equation (see also section 1.2.3):

$$S_a = G_a \times RE_f \times Ser_f \times Sh_f$$

RE_f and Ser_f parameters represent the rooftop areas that are free from roof elements and obstacles as well as not needed for PV maintenance work (please also refer to section 1.2.3 above). These parameters were defined in a common way for all the buildings regardless the country, based both on local experts' information and the international literature (Table 4).

As expected, the roof suitability coefficient of sloped roofs is over 90%, corresponding to fully exploitable rooftop areas, given that chimneys, antennas and satellite plates (which are movable) are usually only installed. On the contrary, flat roofs have large parts of their areas mostly covered by elevator-stairwell shafts or various HVAC components, water tanks and other similar equipment. So, their net suitable area for PVs is reasonably lower than 60%.

Table 4. Common roof suitability coefficients for all the examined rooftop areas

Type of roof	RE_f	Ser_f	Total roof suitability coefficient
Flat	55%	5%	60%
Sloped	80%	10%	90%

When it comes to the fraction of the available rooftop areas, in which the PV system can reach maximum efficiency and produce the highest amount of energy, flat roofs prevail against sloped roofs, as the PV system can be designed to operate in optimal orientation and inclination.

In order to calculate the Sh_f parameter, meaning the suitable rooftop areas from the solar yield point of view, in the case of the flat roofs one should consider that the PV arrays must be positioned with the appropriate distance between them, in order to eliminate mutual shadings especially during the winter when the sun's altitude position is lower (Figure 80). As it can be seen in Figure 81, the distance D is a variable dependent on the sunlight's angle, which differs according to the geographical latitude of the PV system's location. Therefore, the necessary distance between PV arrays was estimated for all the examined cities separately in order to determine the unavailable roof space for the PV panels (Table 5). The higher the latitude of the city, the longer the distance between the PVs that should be foreseen. The calculation was carried out considering the sunlight's angle during winter solstice (21st of December), since this is the worst-case scenario.



Figure 80. Example of PV arrays positioned on a flat roof with the appropriate distance between them, in order to eliminate mutual shadings

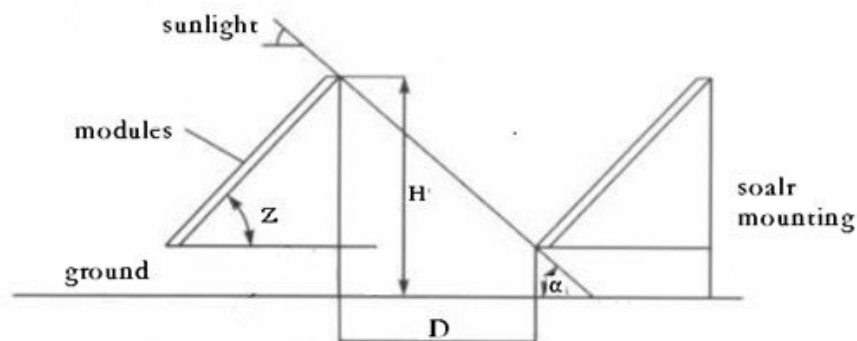


Figure 81. Calculating PV array spacing

Table 5. Solar suitability coefficient for flat roofs

Country	City	Latitude (°)	Sh_f
Georgia	Tbilisi	41.5	51%
	Batumi	41	50%

	Kutaisi	42	48%
	Rustavi	41	50%
Moldova	Chisinau	47	40%
	Balti	48	38%
	Cahul	46	42%
Armenia	Yerevan	40	52%
	Vanadzor	41	50%
	Gyumri	41	50%
Azerbaijan	Baku	40	52%
	Sumgait	40	52%
	Ganja	40.5	51%
Belarus	Minsk	54	26%
	Mogilev	54	26%
	Vitebsk	55	24%
Ukraine	Kyiv	50.5	33%
	Odesa	47	40%
	Lviv	50	34%
	Zaporizhia	48	38%

In the case of the sloped roofs, the Sh_r parameter is fixed and dependent on the shape of the roof, i.e. dual-pitched or hipped.

When high solar yield is the solar suitability criterion, then, by average, only the 50% of dual-pitched rooftop areas and the 62.5% of hipped rooftop areas will be ideal for solar utilisation in terms of optimal orientation, as it is illustrated in the following figure.

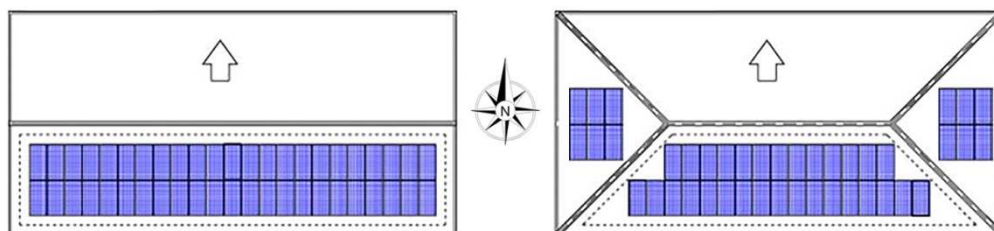


Figure 82. Dual-pitched (left) and hipped (right) roof solar suitability

Still, discussions with the local experts, with local stakeholders and also a thorough study of the, rather limited, literature available, has led to some basic considerations on the suitability of the roofs, especially in older, smaller single- or double family residential buildings.

Namely, for most building typologies met in all six countries, there are significant restrictions due to the limited bearing capacity of the roofs, the difficulty in providing adequate structural support and in ensuring effective water tightness.

On the other hand, one cannot oversee the success of the residential PV programme in the Ukraine. More than 1,300 PV systems have been installed under the net metering scheme in residential buildings, mainly in single-family houses, by April 2017, with expectations being high for the coming years. Still, one has to bear in mind that the Ukraine is different in some aspects to Georgia and the other countries considered: retail electricity prices are 2 to 3 times higher, so is available income and hence the chance to invest. Furthermore, there is an interesting construction rate in the residential sector, which means that new single-family houses will be available for PV installation.

In that sense, it is the bigger buildings with their flat roofs that are the ideal platform for BAPVs, from the old Khrushchyovkas to modern 15-storey blocks of flats, which include office spaces apart from the residential areas, not unlike condominiums in the Americas ^{11,12,13,14,15,16}

We have therefore chosen to use the flat roofs of the bigger buildings as the main platform for fostering the installation of PVs, allowing a small percentage of sloped-roof, smaller residences to be considered as a realistic potential.

3.2 Armenia

3.2.1 Yerevan

Regarding the city of Yerevan, there is generally lack of useful information about the amount of the buildings and the kind of their uses/ownerships but mostly about the type of their roofs. Therefore, a fair 30% was assumed to represent flat roofs suitable for PV applications and the rest 70% was considered to be sloped roofs (50% dual-pitched and 20% hipped ones) (Table 6) in order to estimate the city's potential from the gross rooftop areas.

Table 6. Types of roofs and the gross available rooftop areas within the city of Yerevan

Type of buildings	Total building roof area/ca	Flat roofs	Sloped roofs		Total number of registered buildings	Average rooftop area per building	G _a - Gross rooftop areas
			Dual pitched	Hipped			
	m ² /ca	%	%	%	m ²	m ²	
All	21.4	30	50	20	n/a	n/a	23,494,972

Taking into consideration the assumptions described in Section 3.1, Table 7 presents the estimated solar suitable areas and the potential PV capacities for the city of Yerevan. It seems that there is a great PV potential, over 1.4GWp that can, in theory, be implemented in the city.

¹¹ Pomonis A., The Spitak (Armenia, USSR) Earthquake: Residential Building Typology and Seismic Behaviour, Disasters, 14, 2, 1990, p. 89–114.

¹² NAMA Project, Energy efficient public housing and residences in Armenia, 2014

¹³ Durmanov V., Housing development in Ukraine and in Russia in past and in future, ARCHITECTURAE et ARTIBUS - 2/2010, p.12-18

¹⁴ Energy Efficiency in Buildings in the Contracting Parties of the Energy Community: Final Report, Energy Saving International SA, 2012

¹⁵ Jahanbakhsh S., The evaluation of using solar energy for heating buildings and residential areas in Azerbaijan, Geographical Research, 2009, 4(91), p.49-76

¹⁶ Vatin N., Gamayunova O., Energy Efficiency and Energy Audit: The Experience of the Russian Federation and the Republic of Belarus, Advanced Materials Research, 1065-1069, p. 2159-2162, 2015

Due to the lack of registered data about the amounts of the buildings, the scale of the potential PV systems for each available flat roof cannot currently be evaluated.

Table 7. Solar suitable rooftop areas and the potential PV capacities in the city of Yerevan

Type of buildings	S _a - Solar suitable roof areas (m ²)		Total potential PV capacity (MWp)				Potential PV capacities per building (kWp/building)	
	Flat roofs	Sloped roofs	Flat roofs		Sloped roofs		Mono-Si panels	Poly-Si panels
			Mono-Si	Poly-Si	Mono-Si	Poly-Si		
All	2,199,129	7,929,553	384.85	318.87	1,387	1,149	n/a	n/a

3.2.2 Vanazdor

Regarding the city of Vanazdor, due to the lack of useful information about the amount of the buildings and the kind of their uses/ownerships but mostly about the type of their roofs, the same fair 30% and 70%, considering also for the city of Yerevan, was assumed to represent flat and sloped roofs suitable for PV applications respectively (Table 26). This was used to approximate the city's PV potential from the gross rooftop areas.

Table 8. Types of roofs and the gross available rooftop areas within the city of Vanazdor

Type of buildings	Total building roof area/ca	Flat roofs	Sloped roofs		Total number of registered buildings	Average rooftop area per building	G _a - Gross rooftop areas
			Dual pitched	Hipped			
	m ² /ca	%	%	%	m ²	m ²	
All	45.3	30	50	20	n/a	n/a	3,943,260

Taking into consideration the assumptions described in Section 3.1, Table 27 presents the estimated solar suitable areas and the potential PV capacities for the city of Vanazdor.. It seems that there is a medium PV potential, over 240MWp that can be implemented in the city.

Due to the lack of registered data about the amounts of the buildings, the scale of the potential PV systems for each available flat roof cannot currently be evaluated.

Table 9. Solar suitable rooftop areas and the potential PV capacities in the city of Vanazdor

Type of buildings	S _a - Solar suitable roof areas (m ²)		Total potential PV capacity (MWp)				Potential PV capacities per building (kWp/building)	
	Flat roofs	Sloped roofs	Flat roofs		Sloped roofs		Mono-Si panels	Poly-Si panels
			Mono-Si	Poly-Si	Mono-Si	Poly-Si		
All	354,893	1,330,850	62.11	51.46	232.90	192.97	n/a	n/a

3.2.3 Gyumri

Regarding the city of Gyumri, due to the lack of useful information about the amount of the buildings and the kind of their uses/ownerships but mostly about the type of their roofs, the same fair 30% and 70%, considering also for the cities of Yerevan and Vanazdor, was assumed to represent flat and sloped roofs suitable for PV applications respectively (Table 10). This was used to approximate the city's PV potential from the gross rooftop areas.

Table 10. Types of roofs and the gross available rooftop areas within the city of Gyumri

Type of buildings	Total building roof area/ca	Flat roofs	Sloped roofs		Total number of registered buildings	Average rooftop area per building	G _a - Gross rooftop areas
	m ² /ca		Dual pitched	Hipped			
			%	%		%	m ²
All	26.8	30	50	20	n/a	n/a	3,263,584

Taking into consideration the assumptions described in Section 3.1, Table 11 presents the estimated solar suitable areas and the potential PV capacities for the city of Gyumri. It seems that there is a medium PV potential, over 200MWp that can be implemented in the city. Due to the lack of registered data about the amounts of the buildings, the scale of the potential PV systems for each available flat roof cannot currently be evaluated.

Table 11. Solar suitable rooftop areas and the potential PV capacities in the city of Gyumri

Type of buildings	S _a - Solar suitable roof areas (m ²)		Total potential PV capacity (MWp)				Potential PV capacities per building (kWp/building)	
	Flat roofs	Sloped roofs	Flat roofs		Sloped roofs		Mono-Si panels	Poly-Si panels
			Mono-Si	Poly-Si	Mono-Si	Poly-Si		
All	293,723	1,101,460	51.40	42.59	192.76	159.71	n/a	n/a

3.3 Azerbaijan

3.3.1 Baku

Regarding the city of Baku, there is generally lack of useful information about the amount of the buildings and the kind of their uses/ownerships but mostly about the type of their roofs. Therefore, a fair 50% was assumed to represent flat roofs suitable for PV applications and the rest 50% was considered to be sloped roofs (30% dual-pitched and 20% hipped ones) (Table 12) in order to estimate the city's potential from the gross rooftop areas.

Table 12. Types of roofs and the gross available rooftop areas within the city of Baku

Type of buildings	Total building roof area/ca	Flat roofs	Sloped roofs		Total number of registered buildings	Average rooftop area per building	G _a - Gross rooftop areas
	m ² /ca		Dual pitched	Hipped			
			%	%		%	m ²
All	20.4	50	30	20	n/a	n/a	43,260,600

Taking into consideration the assumptions described in Section 3.1, Table 13 presents the estimated solar suitable areas and the potential PV capacities for the city of Baku. It seems that there is a remarkable PV potential, over 2.5GWp that can be implemented in the city.

Due to the lack of registered data about the amounts of the buildings, the scale of the potential PV systems for each available flat roof cannot currently be evaluated.

Table 13. Solar suitable rooftop areas and the potential PV capacities in the city of Baku

Type of buildings	S _a - Solar suitable roof areas (m ²)		Total potential PV capacity (MWp)				Potential PV capacities per building (kWp/building)	
	Flat roofs	Sloped roofs	Flat roofs		Sloped roofs		Mono-Si panels	Poly-Si panels
			Mono-Si	Poly-Si	Mono-Si	Poly-Si		
All	6,748,654	10,706,999	1,181	978.55	1,873	1,552	n/a	n/a

3.3.2 Sumgait

Regarding the city of Sumgait, due to the lack of useful information about the amount of the buildings and the kind of their uses/ownerships but mostly about the type of their roofs, a fair 30% was assumed to represent flat roofs suitable for PV applications and the rest 70% was considered to be sloped roofs (40% dual-pitched and 30% hipped ones) (Table 14). This was used to approximate the city's PV potential from the gross rooftop areas.

Table 14. Types of roofs and the gross available rooftop areas within the city of Sumgait

Type of buildings	Total building roof area/ca	Flat roofs	Sloped roofs		Total number of registered buildings	Average rooftop area per building	G _a - Gross rooftop areas
			Dual pitched	Hipped			
	m ² /ca	%	%	%	m ²	m ²	
All	14.8	30	40	30	n/a	n/a	4,428,452

Taking into consideration the assumptions described in Section 3.1, Table 15 presents the estimated solar suitable areas and the potential PV capacities for the city of Sumgait.. It seems that there is a medium PV potential, over 280MWp that can be implemented in the city.

Due to the lack of registered data about the amounts of the buildings, the scale of the potential PV systems for each available flat roof cannot currently be evaluated.

Table 15. Solar suitable rooftop areas and the potential PV capacities in the city of Sumgait

Type of buildings	S _a - Solar suitable roof areas (m ²)		Total potential PV capacity (MWp)				Potential PV capacities per building (kWp/building)	
	Flat roofs	Sloped roofs	Flat roofs		Sloped roofs		Mono-Si panels	Poly-Si panels
			Mono-Si	Poly-Si	Mono-Si	Poly-Si		
All	414,503	1,544,423	72.54	60.10	270.27	223.94	n/a	n/a

3.3.3 Ganja

Regarding the city of Ganja, due to the lack of useful information about the amount of the buildings and the kind of their uses/ownerships but mostly about the type of their roofs, the same fair 30% and 70%, considering also for the city of Sumgait, was assumed to represent flat and sloped roofs suitable for PV applications respectively (Table 16). This was used to approximate the city's PV potential from the gross rooftop areas.

Table 16. Types of roofs and the gross available rooftop areas within the city of Ganja

Type of buildings	Total building roof area/ca	Flat roofs	Sloped roofs		Total number of registered buildings	Average rooftop area per building	G _a - Gross rooftop areas
	m ² /ca		Dual pitched	Hipped			
			%	%		%	m ²
All	11.7	30	40	30	n/a	n/a	3,808,980

Taking into consideration the assumptions described in Section 3.1, Table 17 presents the estimated solar suitable areas and the potential PV capacities for the city of Ganja. It seems that there is a medium PV potential, over 240MWp that can be implemented in the city.

Due to the lack of registered data about the amounts of the buildings, the scale of the potential PV systems for each available flat roof cannot currently be evaluated.

Table 17. Solar suitable rooftop areas and the potential PV capacities in the city of Ganja

Type of buildings	S _a - Solar suitable roof areas (m ²)		Total potential PV capacity (MWp)				Potential PV capacities per building (kWp/building)	
	Flat roofs	Sloped roofs	Flat roofs		Sloped roofs		Mono-Si panels	Poly-Si panels
			Mono-Si	Poly-Si	Mono-Si	Poly-Si		
All	349,664	1,328,382	61.19	50.70	232.47	192.62	n/a	n/a

3.4 Belarus

3.4.1 Minsk

Regarding the city of Minsk, there is generally lack of useful information about the amount of the buildings and the kind of their uses/ownerships but mostly about the type of their roofs. Therefore, a fair 50% was assumed to represent flat roofs suitable for PV applications and the rest 50% was considered to be sloped roofs (30% dual-pitched and 20% hipped ones) (Table 18) in order to estimate the city's potential from the gross rooftop areas.

Table 18. Types of roofs and the gross available rooftop areas within the city of Minsk

Type of buildings	Total building roof area/ca	Flat roofs	Sloped roofs		Total number of registered buildings	Average rooftop area per building	G _a - Gross rooftop areas
	m ² /ca		Dual pitched	Hipped			
			%	%*-		%	m ²
All	20.8	50	30	20	n/a	n/a	41,663,680

Taking into consideration the assumptions described in Section 3.1, Table 19 presents the estimated solar suitable areas and the potential PV capacities for the city of Minsk. It seems that there is a remarkable PV potential, over 1.9GWp that can be implemented in the city.

Due to the lack of registered data about the amounts of the buildings, the scale of the potential PV systems for each available flat roof cannot currently be evaluated.

Table 19. Solar suitable rooftop areas and the potential PV capacities in the city of Minsk

Type of buildings	S _a - Solar suitable roof areas (m ²)		Total potential PV capacity (MWp)				Potential PV capacities per building (kWp/building)	
	Flat roofs	Sloped roofs	Flat roofs		Sloped roofs		Mono-Si panels	Poly-Si panels
			Mono-Si	Poly-Si	Mono-Si	Poly-Si		
All	3,249,767	10,311,761	568.71	471.22	1,804	1,495	n/a	n/a

3.4.2 Mogilev

Regarding the city of Mogilev, due to the lack of useful information about the amount of the buildings and the kind of their uses/ownerships but mostly about the type of their roofs, a fair 30% was assumed to represent flat roofs suitable for PV applications and the rest 70% was considered to be sloped roofs (40% dual-pitched and 30% hipped ones) (Table 44). This was used to approximate the city's PV potential from the gross rooftop areas.

Table 20. Types of roofs and the gross available rooftop areas within the city of Mogilev

Type of buildings	Total building roof area/ca	Flat roofs	Sloped roofs		Total number of registered buildings	Average rooftop area per building	G _a - Gross rooftop areas
			Dual pitched	Hipped			
	m ² /ca	%	%	%	m ²	m ²	
All	23.5	30	40	30	n/a	n/a	8,822,708

Taking into consideration the assumptions described in Section 3.1, Table 45 presents the estimated solar suitable areas and the potential PV capacities for the city of Mogilev. It seems that there is a great PV potential, over 500MWp that can be implemented in the city.

Due to the lack of registered data about the amounts of the buildings, the scale of the potential PV systems for each available flat roof cannot currently be evaluated.

Table 21. Solar suitable rooftop areas and the potential PV capacities in the city of Mogilev

Type of buildings	S _a - Solar suitable roof areas (m ²)		Total potential PV capacity (MWp)				Potential PV capacities per building (kWp/building)	
	Flat roofs	Sloped roofs	Flat roofs		Sloped roofs		Mono-Si panels	Poly-Si panels
			Mono-Si	Poly-Si	Mono-Si	Poly-Si		
All	412,903	3,076,919	72.26	59.87	538.46	446.15	n/a	n/a

3.4.3 Vitebsk

Regarding the city of Vitebsk, due to the lack of useful information about the amount of the buildings and the kind of their uses/ownerships but mostly about the type of their roofs, the same fair 30% and 70%, considering also for the city Mogilev, was assumed to represent flat and sloped roofs suitable for PV applications respectively (Table 22). This was used to approximate the city's PV potential from the gross rooftop areas.

Table 22. Types of roofs and the gross available rooftop areas within the city of Vitebsk

			Sloped roofs			
--	--	--	---------------------	--	--	--

Type of buildings	Total building roof area/ca	Flat roofs	Dual pitched	Hipped	Total number of registered buildings	Average rooftop area per building	G _a - Gross rooftop areas
	m ² /ca	%	%	%		m ²	m ²
All	28.4	30	40	30	n/a	n/a	10,496,612

Taking into consideration the assumptions described in Section 3.1, Table 23 presents the estimated solar suitable areas and the potential PV capacities for the city of Vitebsk. It seems that there is a great PV potential, over 590MWp that can be implemented in the city.

Due to the lack of registered data about the amounts of the buildings, the scale of the potential PV systems for each available flat roof cannot currently be evaluated.

Table 23. Solar suitable rooftop areas and the potential PV capacities in the city of Vitebsk

Type of buildings	S _a - Solar suitable roof areas (m ²)		Total potential PV capacity (MWp)				Potential PV capacities per building (kWp/building)	
	Flat roofs	Sloped roofs	Flat roofs		Sloped roofs		Mono-Si panels	Poly-Si panels
			Mono-Si	Poly-Si	Mono-Si	Poly-Si		
All	453,454	3,660,693	79.35	65.75	640.62	530.80	n/a	n/a

3.5 Georgia

3.5.1 Tbilisi

New buildings in Tbilisi do not have to satisfy a specific regulation with respect to their roof. Depending on the style, aesthetics and visibility of the building the roof can be flat or sloped. The municipality has put in place an incentive scheme for green roofs, which is based on a deduction of municipal taxes based on the green roof coverage ratio. There are also restrictions on chimneys, antennas, etc., which are imposed and enforced mainly on central streets of the city.

Approximately 25% of the city is occupied by older buildings, which have between 2-3 and up to 8 floors (Table 24). Approximately 60% of the city comprises newer buildings built from the 1980s and onwards and 90% of them are high-rise as well. The high-rise buildings feature flat roofs, whilst the older buildings as a rule hipped and pitched roofs.

Table 24. Types of roofs and the gross available rooftop areas within the city of Tbilisi

Type of buildings	Total building roof area/ca	Flat roofs	Sloped roofs		Total number of registered buildings	Average rooftop area per building	G _a - Gross rooftop areas
			Dual pitched	Hipped			
	m ² /ca	%	%	%	m ²	m ²	
All	22.2	n/a	n/a	n/a	245639	100	24,634,075
High rise new buildings		90%	10%	0%	132645		14,780,445
Older buildings (2-8 storeys)		80%	20%	0%	61410		6,158,519

Taking into consideration the assumptions described in Section 3.1, Table 25 presents the estimated solar suitable areas and the potential PV capacities for the city of Tbilisi.

It seems that there is a great PV potential over 980MWp that can be implemented in the city. However, based on the estimated amount of the buildings, small-scale PV potential of 4 to 5kWp by average is estimated per building.

Table 25. Solar suitable rooftop areas and the potential PV capacities in the city of Tbilisi

Type of buildings	S _a - Solar suitable roof areas (m ²)		Total potential PV capacity (MWp)				Potential PV capacities per building (kWp/building)	
	Flat roofs	Sloped roofs	Flat roofs		Sloped roofs		Mono-Si panels	Poly-Si panels
			Mono-Si	Poly-Si	Mono-Si	Poly-Si		
High rise new buildings	4,070,535	665,120	712.34	590.23	116.40	96.44	6.2	5.2
Older buildings (2-8 storeys)	1,507,605	554,267	263.83	218.60	97.00	80.37	5.9	4.9

A special note should be made to a possible case for the application of PVs on a community's level: In the outskirts of Tbilisi, but also of other cities, there are recently built settlements for the refugees from the regions of Abkhazia and Ossetia, which consist of small, uniform single-family houses with pitched and hipped roofs. These roofs are able to accommodate a 3-4 kW PV system. Equipping those settlements with PVs would be of obvious benefit for the residents and would be a useful demonstration project for the whole policy.

3.5.2 Batumi

Considering the Batumi city, there are poor information about the types of roofs and the uses of the buildings within the city. Therefore, taking into account the classification of buildings in the other three examined cities of Georgia, a modest 50% of all buildings in Batumi was assumed to have flat roofs suitable for PV applications and the rest of 50% represent sloped roofs (30% dual pitched and 20% hipped ones) (Table 26).

Table 26. Types of roofs and the gross available rooftop areas within the city of Batumi

Type of buildings	Total building roof area/ca	Flat roofs	Sloped roofs		Total number of registered buildings	Average rooftop area per building	G _a - Gross rooftop areas
			Dual pitched	Hipped			
	m ² /ca	%	%	%	m ²	m ²	
All	18.8	50	30	20	10143	284	2,879,820

Taking into consideration the assumptions described in Section 3.1, Table 27 presents the estimated solar suitable areas and the potential PV capacities for the city of Batumi.

It seems that there is a medium PV potential over 160MWp that can be implemented in the city. Based on the estimated amount of the buildings, medium scale PV potential of over 30kWp by average is estimated per building.

Table 27. Solar suitable rooftop areas and the potential PV capacities in the city of Batumi

Type of buildings	S _a - Solar suitable roof areas (m ²)		Total potential PV capacity (MWp)				Potential PV capacities per building (kWp/building)	
	Flat roofs	Sloped roofs	Flat roofs		Sloped roofs		Mono-Si panels	Poly-Si panels
			Mono-Si	Poly-Si	Mono-Si	Poly-Si		
All	431,973	712,755	75.60	62.64	124.73	103.35	39.5	32.7

3.5.3 Kutaisi

In Kutaisi the major area of possible deployment of building PV are multi apartment blocks, (blocks of flats). They represent around the 60% of the building stock in the city and have only flat roofs (Table 28). The rest of the buildings have by 50% flat roofs and by 50% sloped roofs (30% dual pitched and 20% hipped ones). The pitched roofs are made of zinc, while the flat roofs are covered by 12-16mm thick of concrete. The supporting structures of PVs could be either of galvanised steel or aluminium, while due care has to be taken in order to avoid leakages due to the installation of the systems. The major obstructions on the roofs refer to elevator and staircase wells, but also to water tanks, since the city water network is old and prone to frequent supply interruptions.

In Kutaisi there are 37 kindergartens of an average floor area between 140 and 600m², which could potentially be a good-scale pilot project for the city.

Table 28. Types of roofs and the gross available rooftop areas within the city of Kutaisi

Type of buildings	Total building roof area/ca m ² /ca	Flat roofs %	Sloped roofs		Total number of registered buildings	Average rooftop area per building m ²	G _a - Gross rooftop areas m ²
			Dual pitched %	Hipped %			
All	24	n/a	n/a	n/a	28835	167	4,816,095
Multi apartment blocks		100%	0%	0%	17301		2,889,657
Other buildings		50%	30%	20%	11534		1,926,438
Kindergartens		100%	0%	0%	37		13,690

Taking into consideration the assumptions described in Section 3.1,

Table 29 presents the estimated solar suitable areas and the potential PV capacities for the city of Kutaisi. It seems that over 120MWp of PVs can be implemented in the multi apartment blocks and 109MWp in the rest of the buildings, while in the kindergartens, which are managed by the Municipality, 15 up to 18kWp per building could be also installed.

Table 29. Solar suitable rooftop areas and the potential PV capacities in the city of Kutaisi

Type of buildings	S _a - Solar suitable roof areas (m ²)		Total potential PV capacity (MWp)				Potential PV capacities per building (kWp/building)	
	Flat roofs	Sloped roofs	Flat roofs		Sloped roofs		Mono-Si panels	Poly-Si panels
			Mono-Si	Poly-Si	Mono-Si	Poly-Si		
All	431,973	712,755	75.60	62.64	124.73	103.35	39.5	32.7

Multi apartment blocks	832,221	0	145.64	120.67	0	0	8.4	7.0
Other buildings	277,407	476,793	48.55	40.22	83.44	69.14	11.4	9.5
Kindergartens	3,943	0	0.69	0.57	0	0	18.6	15.5

3.5.4 Rustavi

Rustavi is an industrial city close to Tbilisi and its population became, after the de-industrialisation of the 1990s' economically vulnerable. In terms of the shape of roofs in the buildings of Rustavi around 30% are blocks of flats with flat roofs (Table 30). The remaining buildings are 2 to 5 storey ones with 50% flat and 50% sloped roofs. There is currently not a big construction activity and there are 3 new 11-13 floor buildings (high rise). Almost all commercial buildings have a flat roof.

Table 30. Types of roofs and the gross available rooftop areas within the city of Rustavi

Type of buildings	Total building roof area/ca m ² /ca	Flat roofs %	Sloped roofs		Total number of registered buildings	Average rooftop area per building m ²	G _a - Gross rooftop areas m ²
			Dual pitched %	Hipped %			
All		n/a	n/a	n/a	16233		2,904,118
Blocks with flat apartments	23.2	100%	0%	0%	4870	179	871,235
2-5 storey buildings		50%	30%	20%	5682		2,032,883

Taking into consideration the assumptions described in Section 3.1, Table 31 presents the estimated solar suitable areas and the potential PV capacities for the city of Rustavi.

It seems that there is a medium PV potential, over 150MWp that can be implemented in the city with the higher potential capacity calculated for the 2-5 storey buildings., Based on the estimated amount of the buildings, small to medium-scale PV potential of 8 to 25kWp by average is estimated per building.

Table 31. Solar suitable rooftop areas and the potential PV capacities in the city of Rustavi

Type of buildings	S _a - Solar suitable roof areas (m ²)		Total potential PV capacity (MWp)				Potential PV capacities per building (kWp/building)	
	Flat roofs	Sloped roofs	Flat roofs		Sloped roofs		Mono-Si panels	Poly-Si panels
			Mono-Si	Poly-Si	Mono-Si	Poly-Si		
Blocks with flat apartments	261,371	0	45.74	37.90	0	0	9.4	7.8
2-5 storey buildings	304,932	503,138	53.36	44.22	88.05	72.96	24.9	20.6

3.6 Moldova

3.6.1 Chisinau

Regarding the city of Chisinau, there is useful information about the amount of the buildings but not about the kind of their uses/ownerships and mostly about the type of their roofs. Therefore, a fair 30% was assumed to represent flat roofs suitable for PV applications and the rest 70% was considered to be sloped roofs (40% dual-pitched and 30% hipped ones) (Table 32) in order to estimate the city's potential from the gross rooftop areas.

Table 32. Types of roofs and the gross available rooftop areas within the city of Chisinau

Type of buildings	Total building roof area/ca	Flat roofs	Sloped roofs		Total number of registered buildings	Average rooftop area per building	G _a - Gross rooftop areas
	m ² /ca		Dual pitched	Hipped			
		%	%	%	m ²	m ²	
All	4.7	30	40	30	1845	380	2,339,686

Taking into consideration the assumptions described in Section 3.1, Table 33 presents the estimated solar suitable areas and the potential PV capacities for the city of Chisinau. It seems that there is a great PV potential, over 140MWp that can be implemented in the city. Besides, based on the registered data of the amount of the buildings, it seems that a large-scale PV potential of over70kW is estimated per building.

Table 33. Solar suitable rooftop areas and the potential PV capacities in the city of Chisinau

Type of buildings	S _a - Solar suitable roof areas (m ²)		Total potential PV capacity (MWp)				Potential PV capacities per building (kWp/building)	
	Flat roofs	Sloped roofs	Flat roofs		Sloped roofs		Mono-Si panels	Poly-Si panels
			Mono-Si	Poly-Si	Mono-Si	Poly-Si		
All	168,457	815,965	29.48	24.43	142.79	118.31	93.4	77.4

3.6.2 Balti

Regarding the small city of Balti, there are available registered data for buildings but due to the lack of useful information about the kind of their uses/ownerships but mostly about the type of their roofs, the same fair 30% and 70%, considering also for the city of Chisinau, was assumed to represent flat and sloped roofs suitable for PV applications respectively (Table 34). This was used to approximate the city's PV potential from the gross rooftop areas.

Table 34. Types of roofs and the gross available rooftop areas within the city of Balti

Type of buildings	Total building roof area/ca	Flat roofs	Sloped roofs		Total number of registered buildings	Average rooftop area per building	G _a - Gross rooftop areas
	m ² /ca		Dual pitched	Hipped			
		%	%	%	m ²	m ²	
All	3.7	30	40	30	298	288	286,000

Taking into consideration the assumptions described in Section 3.1, Table 35 presents the estimated solar suitable areas and the potential PV capacities for the city of Balti. It seems that there is a very poor PV potential, only up to 17MWp that can be implemented in the city. However,

based on the registered data of the amount of the buildings, it seems that a large-scale PV potential of over 65kW is estimated per building.

Table 35. Solar suitable rooftop areas and the potential PV capacities in the city of Balti

Type of buildings	S _a - Solar suitable roof areas (m ²)		Total potential PV capacity (MWp)				Potential PV capacities per building (kWp/building)	
	Flat roofs	Sloped roofs	Flat roofs		Sloped roofs		Mono-Si panels	Poly-Si panels
			Mono-Si	Poly-Si	Mono-Si	Poly-Si		
All	19,562	99,743	3.42	2.84	17.45	14.46	70.1	58.1

3.6.3 Cahul

Regarding the very small city of Cahul, there are available registered data for buildings but due to the lack of useful information about the kind of their uses/ownerships but mostly about the type of their roofs, the same fair 30% and 70%, considering also for the cities of Chisinau and Balti, was assumed to represent flat and sloped roofs suitable for PV applications respectively (Table 36). This was used to approximate the city's PV potential from the gross rooftop areas.

Table 36. Types of roofs and the gross available rooftop areas within the city of Cahul

Type of buildings	Total building roof area/ca	Flat roofs	Sloped roofs		Total number of registered buildings	Average rooftop area per building	G _a - Gross rooftop areas
			Dual pitched	Hipped			
	m ² /ca	%	%	%	m ²	m ²	
All	1.8	30	40	30	61	358	73,000

Taking into consideration the assumptions described in Section 3.1, Table 37 presents the estimated solar suitable areas and the potential PV capacities for the city of Cahul. It seems that there is a very poor PV potential, only up to 4.5MWp that can be implemented in the city. However, based on the registered data of the amount of the buildings, it seems that a large-scale PV potential of over 70kW is estimated per building.

Table 37. Solar suitable rooftop areas and the potential PV capacities in the city of Cahul

Type of buildings	S _a - Solar suitable roof areas (m ²)		Total potential PV capacity (MWp)				Potential PV capacities per building (kWp/building)	
	Flat roofs	Sloped roofs	Flat roofs		Sloped roofs		Mono-Si panels	Poly-Si panels
			Mono-Si	Poly-Si	Mono-Si	Poly-Si		
All	5,519	25,459	0.97	0.80	4.46	3.69	88.6	73.4

3.7 Ukraine

In Ukraine, the building stock comprises 6.5 million detached houses, 8 million multi-apartment buildings (on average of 15 floors) in addition to the public and commercial buildings. The building

stock is of an older age, i.e. a percentage of 50-60% was built before 1970, whereas 40% of the buildings were built in the decade between 1975 to 1985.

Detached houses are already eligible for up to 30kWp PV rooftop systems (whereas the average size of each installation is at the order of 5-10kWp).

3.7.1 Kyiv

Regarding the city of Kyiv, there is useful information about the types of roofs according to the uses/ownership of the buildings within the city (Table 38) that helped to estimate the solar potential..

Table 38. Types of roofs and the gross available rooftop areas within the city of Kyiv

Type of buildings	Total building roof area/ca m ² /ca	Flat roofs %	Sloped roofs		Total number of registered buildings	Average rooftop area per building m ²	G _a - Gross rooftop areas m ²
			Dual pitched %	Hipped %			
All	20.6	n/a	n/a	n/a	11405	n/a	59,075,200
Private households		0%	50%	50%	n/a	n/a	44,706,400
Communal property		100%	0%	0%	8419	1183	9,962,600
Housing cooperatives		100%	0%	0%	907	1126	1,021,000
Condominium associations		100%	0%	0%	491	1143	561,400
Departmental houses		50%	50%	0%	438	692	303,300
Departmental dormitories		50%	50%	0%	379	710	269,000
Investment apartment buildings		100%	0%	0%	771	2920	2,251,500

Taking into consideration the assumptions described in Section 3.1, Table 39 presents the estimated solar suitable areas and the potential PV capacities for the city of Kyiv.

It seems that there is a great PV potential of 3.7GWp that can be implemented in the city. Based on the registered amount of the buildings, a medium-scale PV potential of over 30kWp is estimated per building. In the investment apartment buildings, the capacities can reach 100kWp, which corresponds more to commercial scale systems.

Table 39. Solar suitable rooftop areas and the potential PV capacities in the city of Kyiv

Type of buildings	S _a - Solar suitable roof areas (m ²)		Total potential PV capacity (MWp)				Potential PV capacities per building (kWp/building)	
	Flat roofs	Sloped roofs	Flat roofs		Sloped roofs		Mono-Si panels	Poly-Si panels
			Mono-Si	Poly-Si	Mono-Si	Poly-Si		
Private households	0	22,632,615	0.00	0.00	3,960	3,281	n/a	n/a
Communal property	1,972,595	0	345.20	286.03	0	0	41.0	34.0
Housing cooperatives	202,158	0	35.38	29.31	0	0	39.0	32.3

Condominium associations	111,157	0	19.45	16.12	0	0	39.6	32.8
Departmental houses	30,027	68,243	5.25	4.35	11.94	9.90	39.3	32.5
Departmental dormitories	26,631	60,525	4.66	3.86	10.59	8.78	40.2	33.3
Investment apartment buildings	445,797	0	78.01	64.64	0	0	101.2	83.8

3.7.2 Odesa

Regarding the city of Odesa, there is useful information only about the uses/ownership of the buildings within the city (Table 40), but not enough data for the respective types of the roofs. Therefore, it was assumed, in correspondence with the assumptions for Kyiv, that the private households have only sloped roofs and the rest of the building stock represents the flat roofs of the city.

Table 40. Types of roofs and the gross available rooftop areas within the city of Odesa

Type of buildings	Total building roof area/ca m ² /ca	Flat roofs %	Sloped roofs		Total number of registered buildings	Average rooftop area per building m ²	G _a - Gross rooftop areas m ²
			Dual pitched %	Hipped %			
All		n/a	n/a	n/a	n/a	n/a	30,700,548
Private households	30.1	0.0%	50.0%	50.0%	36997	n/a	23,025,411
Housing cooperatives, Condominium associations, Departmental houses		100.0%	0.0%	0.0%	1403	n/a	921,016
State and communal property		100.0%	0.0%	0.0%	5273	751	3,958,153
Other legal entities and individuals		100.0%	0.0%	0.0%	34	n/a	2,795,968

Taking into consideration the assumptions described in Section 3.1, Table 41 presents the estimated solar suitable areas and the potential PV capacities for the city of Odesa.

It seems that there is a great PV potential, over 1.9 GWp that can be implemented in the city. Still, one has to be aware of the fact, that this is the maximum theoretical potential. Based on the registered number of the buildings, a medium-scale PV potential of over 20kWp is estimated per building, which is considered to be reasonable. However, with respect to the utilisation of the potential one should consider the legal, administrative and financial obstacles that exist. As the experience in Southern or in Western Europe showed, one could consider a utilisation factor of

30% a very good one¹⁷. In that sense, the goal of 750 MW set by the SEAP for Odesa is possible if boundary conditions are met.

Table 41. Solar suitable rooftop areas and the potential PV capacities in the city of Odesa

Type of buildings	S _a - Solar suitable roof areas (m ²)		Total potential PV capacity (MWp)				Potential PV capacities per building (kWp/building)	
	Flat roofs	Sloped roofs	Flat roofs		Sloped roofs		Mono-Si panels	Poly-Si panels
			Mono-Si	Poly-Si	Mono-Si	Poly-Si		
Private households	0	11,656,614	0.00	0.00	2,039	1,960	55.1	45.7
Housing cooperatives, Condominium associations, Departmental houses	221,044	0	38.68	32.05	0	0	27.6	22.8
State and communal property	949,957	0	166.24	137.74	0	0	31.5	26.1
Other legal entities and individuals	671,032	0	117.43	97.30	0	0	n/a	n/a

3.7.3 Lviv

Regarding the city of Lviv, there is useful information about the uses/ownership of the buildings within the city (Table 42) but less data for the respective types of roofs. Particularly, only the multi-apartment buildings were considered suitable for PV applications and have only flat roofs.

Table 42. Types of roofs and the gross available rooftop areas within the city of Lviv

Type of buildings	Total building roof area/ca	Flat roofs	Sloped roofs	Total number of registered buildings	Average rooftop area per building	G _a - Gross rooftop areas
	m ² /ca	%	%		m ²	m ²
All	24.2	n/a	n/a	n/a	n/a	17,659,260
Other buildings		n/a	n/a	n/a	n/a	6,373,334
Private households		n/a	n/a	9485	149	1,411,534
Multi-apartment buildings		100.0%	0.0%	8735	565	4,937,196
State and communal property		n/a	n/a	7904	440	3,476,733
Other legal entities and individuals		n/a	n/a	831	1757	1,460,463

¹⁷ Karteris M. and Papadopoulos A.M. (2012), Residential photovoltaic systems in Greece and in other European countries: a comparison and an overview, *Advances in Building Energy Research*, 141-158

Taking into consideration the assumptions described in Section 3.1, Table 43 presents the estimated solar suitable areas and the potential PV capacities for the city of Lviv, focusing on the flat roofs. It seems that there is a great PV potential, over 140MWp that can be implemented in the city. Based on the registered amount of the buildings, a medium-scale PV potential of over 15kWp is estimated per building.

Table 43. Solar suitable rooftop areas and the potential PV capacities in the city of Lviv

Type of buildings	S _a - Solar suitable roof areas (m ²)		Total potential PV capacity (MWp)		Potential PV capacities per building (kWp/building)	
	Flat roofs	Sloped roofs	Mono-Si panels	Poly-Si panels	Mono-Si panels	Poly-Si panels
Multi-apartment buildings	1,007,188	0	176.26	146.04	20.2	16.7

3.7.4 Zaporizhia

Regarding the city of Zaporizhia, there is useful information about the types of roofs according to the uses/ownership of the buildings within the city (Table 44) that helped to estimate the solar potential. Particularly, only the private households were considered to have sloped roofs. The rest of the building stock have flat roofs. In addition, valuable data were obtained for specific communal buildings that have suitable flat roofs for PV implementation.

Table 44. Types of roofs and the gross available rooftop areas within the city of Zaporizhia

Type of buildings	Total building roof area/ca m ² /ca	Flat roofs %	Sloped roofs		Total number of registered buildings	Average rooftop area per building m ²	G _a - Gross rooftop areas m ²
			Dual pitched %	Hipped %			
All	n/a	n/a	n/a	n/a	n/a	n/a	11,831,880
Private households		0.0%	50%	50%	n/a	n/a	5,915,940
Multi-apartment buildings		100.0%	0.0%	0.0%	3609	984	3,549,919
State and communal property		100.0%	0.0%	0.0%	2215	694	1,537,402
Other legal entities and individuals		100.0%	0.0%	0.0%	n/a		828,232
Recreation Centre Titan		100.0%	0.0%	0.0%	1	896	896
Recreation Centre Orbita		100.0%	0.0%	0.0%	1	1,584	1,584
Recreation Centre Zavodskiy		100.0%	0.0%	0.0%	1	2,883	2,883
District State Administration Voznesenskiy District		100.0%	0.0%	0.0%	1	1,338	1,338
District State Administration		100.0%	0.0%	0.0%	1	909	909

Dniprovskiy District							
District State Administration Kommunariskiy District	100.0%	0.0%	0.0%	1	889	889	
District State Administration Olexandrivskiy District	100.0%	0.0%	0.0%	1	1,070	1,070	
Sport Complex "Motor Sich"	100.0%	0.0%	0.0%	1	240	240	
Sport Complex Lokomotiv	100.0%	0.0%	0.0%	1	197	197	
Sport Complex Lokomotiv-2	100.0%	0.0%	0.0%	1	161	161	
Central Stadium Slavutich Arena	100.0%	0.0%	0.0%	1	800	800	
District Centre for Social Protection	100.0%	0.0%	0.0%	1	692	692	
District Centre for Social Protection	100.0%	0.0%	0.0%	1	1,305	1,305	

Taking into consideration the assumptions described in Section 3.1, Table 45 presents the estimated solar suitable areas and the potential PV capacities for the city of Zaporizhia.

It seems that there is a great PV potential, over 600MWp that can be implemented in the city. Based on the registered amount of the buildings, a medium-scale PV potential of over 30kWp is estimated per building.

In the communal buildings that were examined separately, medium to large scale PV systems are estimated from 30 to 120kWp.

Table 45. Solar suitable rooftop areas and the potential PV capacities in the city of Zaporizhia

Type of buildings	S _a - Solar suitable roof areas (m ²)		Total potential PV capacity (MWp)				Potential PV capacities per building (kWp/building)	
	Flat roofs	Sloped roofs	Flat roofs		Sloped roofs		Mono-Si panels	Poly-Si panels
			Mon o-Si	Poly-Si	Mon o-Si	Poly-Si		
Private households	0	2,994,945	0	0	542.1	434.3	n/a	n/a
Multi-apartment buildings	809,382	0	141.6	117.4	0	0	39.2	32.5
State and communal property	350,528	0	61.34	50.83	0	0	27.7	22.9

Other legal entities and individuals	188,837	0	33.05	27.38	0	0	n/a	n/a
Recreation Centre Titan	204	0	0.04	0.04	0	0	35.8	29.6
Recreation Centre Orbita	361	0	0.06	0.05	0	0	63.2	52.4
Recreation Centre Zavodskiy	657	0	0.12	0.10	0	0	115.0	95.3
District State Administration Voznesenskiy District	305	0	0.05	0.04	0	0	53.4	44.2
District State Administration Dniprovskiy District	207	0	0.04	0.03	0	0	36.3	30.1
District State Administration KommunarSKIY District	203	0	0.04	0.03	0	0	35.5	29.4
District State Administration Olexandrivskiy District	244	0	0.04	0.04	0	0	42.7	35.4
Central Stadium Slavutich Arena	182	0	0.03	0.03	0	0	31.9	26.4
District Centre for Social Protection	298	0	0.05	0.05	0	0	52.1	43.1

4 PV energy supply

4.1 Assumptions

As already described in section 1.2.4.2, to estimate the solar energy supply from the estimated potential PVs in the examined cities, the RETScreen¹⁸ software was used. Detailed calculations were performed based on available monthly climate data for each city and typical photovoltaic equipment data setting for a small-scale PV system of 10kWp. In order to validate the results, the PVGIS tool of the European Commission JRC was also used, running simulations for the capital cities of the examined countries.

4.1.1 Orientation and inclination

Furthermore, specific orientation-inclination scenarios were evaluated both for flat and sloped roofs in order to cover all potential rooftop PV applications (Table 46). One only scenario was evaluated for flat roofs with the PV system set fixed with south orientation and the optimal inclination of solar panels according to the geographical latitude of each examined city. Respectively, three different simulations were conducted for the sloped roofs, which included all acceptable orientations for PV panels; south, southeast -southwest and east-west orientation,

¹⁸ Find at <http://www.nrcan.gc.ca/energy/software-tools/7465>

while regarding the inclination angle of PVs, in a business as usual scenario it was set at 12°, which is a common inclination angle of sloped roofs in the examined cities.

Table 46. Examined orientation - inclination scenarios

Proposed PV applications	Scenarios	Orientation	Inclination
Flat roofs	Flat roof	South	Optimal on a yearly basis
Sloped roofs (highly desirable scenario)	SE_12_S	South	12°
Sloped roofs (mean desirable scenario)	SE_12_SE_SW	Southeast - Southwest	
Sloped roofs (least desirable scenario)	SE_12_E_W	East – West	

Regarding the input data for the PV system’s efficiency and miscellaneous losses that are necessary to estimate the annual solar energy production, typical values for a PV system with power capacity of 10kWp were assumed, as they are already presented in detail in section 1.2.4.2.

4.1.2 Assessment of the temperature impact

Though solar global radiation should be considered a main factor when estimating the final yield of a PV-power plant (Šúri, Huld, Dunlop, & Ossenbrink, 2007), it is not the only one. The technical characteristics and operational conditions must also be taken into account to obtain a reasonably accurate result. Almost all city/municipality-wide potential estimations on a yearly basis use constant efficiency factors for PV-modules and inverters. In the best cases, yearly fixed efficiency losses are included to consider the effects of the ambient air temperature on the performance of the PV-modules.

The daily estimations delivered satisfactory results. However, the functions and coefficients fit only the punctual local conditions and require further testing to confirm similar performance in other locations. Jakubiec and Reinhart (2013) increased the temporal resolution to hours and calculated the reduction in the PV-power production due to changes in the ambient air temperature (T_{amb}) for every time step. This approach can be used in other locations because only two additional parameters are necessary: a temperature correction factor (α_{PMPP}), which is normally provided by the module manufacturer, and a reduction factor (kT) expressing the changes in module performance due to differences in the module’s actual and nominal operating temperatures (T_0). kT can be calculated if the irradiance on the cell surface and the air temperature used to determine T_0 are known. The values assumed by Jakubiec and Reinhart (2013) are 800 W/m² and 20 °C, which are compatible with the $kT = 0.035$ °C/(W/m²) used in the PV-GIS and the RETScreen tools for free-standing PV-systems.

This is however different building integrated systems because the module temperature is increased by the heat absorbed by the roofs and therefore kT values have to be taken into account by calculating the “urban ambient temperature” to estimate the module temperature. Calculating the urban ambient temperature requires detailed knowledge about the materials of the roofs, which is not always available, and certainly not for the cities considered in this study. One can however approach this higher temperature, by using use $kT = 0.05$ °C/(W/m²), as suggested in the PV-GIS web service for building integrated systems (DG Joint Research Centre, 2005).

4.2 Armenia

The climate in Armenia is markedly continental, which means that Armenia is subject to hot summers and cold winters. Summers are dry and sunny, lasting from June to mid-September, whereas winters are quite cold with plenty of snow, with temperatures ranging between -10 and -5°C .

Table 47 presents the climatic data of Armenia that were used for the solar energy simulations.

Table 47. Climatic data of the examined cities of Armenia

City: Yerevan				
	Unit	Climate data location	Project location	
Latitude	$^{\circ}\text{N}$	40.1	40.1	
Longitude	$^{\circ}\text{E}$	44.5	44.5	
Elevation	m	1,140	1,140	
Heating design temperature	$^{\circ}\text{C}$	-11.1		
Cooling design temperature	$^{\circ}\text{C}$	34.6		
Earth temperature amplitude	$^{\circ}\text{C}$	22.4		
Optimal inclination of solar panels for the maximum annual efficiency	$^{\circ}$	32		
Month		Air temperature	Relative humidity	Daily solar radiation - horizontal
		$^{\circ}\text{C}$	%	$\text{kWh/m}^2/\text{d}$
January		-2.8	76.8%	2.04
February		-0.1	70.7%	2.91
March		5.9	60.7%	3.85
April		13.3	57.9%	4.69
May		17.5	56.6%	5.68
June		22.5	50.8%	6.76
July		26.5	47.5%	6.75
August		26.0	47.9%	6.04
September		20.9	51.3%	4.96
October		13.3	64.7%	3.53
November		6.3	71.2%	2.31
December		-0.3	77.6%	1.71
Annual		12.5	61.1%	4.28
City: Gyumri				
	Unit	Climate data location	Project location	
Latitude	$^{\circ}\text{N}$	40.8	40.8	
Longitude	$^{\circ}\text{E}$	43.8	43.8	
Elevation	m	1,866	1,866	
Heating design temperature	$^{\circ}\text{C}$	-18.0		
Cooling design temperature	$^{\circ}\text{C}$	27.2		
Earth temperature amplitude	$^{\circ}\text{C}$	22.8		
Optimal inclination of	$^{\circ}$	32		

solar panels for the maximum annual efficiency				
Month		Air temperature	Relative humidity	Daily solar radiation - horizontal
		°C	%	kWh/m ² /d
January		-8.3	84.4%	2.13
February		-7.4	83.5%	3.10
March		-2.2	76.9%	4.06
April		6.5	70.5%	4.83
May		10.8	73.3%	5.65
June		14.8	70.1%	6.84
July		18.9	66.0%	6.87
August		18.5	64.4%	6.17
September		14.4	66.1%	5.05
October		7.8	74.3%	3.53
November		0.7	80.9%	2.34
December		-6.1	82.5%	1.75
Annual		5.8	74.4%	4.37
City: Vanazdor				
	Unit	Climate data location	Project location	
Latitude	°N	40.6	40.6	
Longitude	°E	44.9	44.9	
Elevation	M	1,937	1,937	
Heating design temperature	°C	-15.3		
Cooling design temperature	°C	22.7		
Earth temperature amplitude	°C	22.4		
Optimal inclination of solar panels for the maximum annual efficiency	°	28		
Month		Air temperature	Relative humidity	Daily solar radiation - horizontal
		°C	%	kWh/m ² /d
January		-6.9	75.6%	2.04
February		-7.1	78.5%	2.91
March		-2.8	73.3%	3.85
April		4.8	69.6%	4.69
May		8.6	70.9%	5.68
June		12.9	71.5%	6.76
July		16.3	71.4%	6.75
August		15.5	70.3%	6.04
September		12.8	65.9%	4.96
October		6.3	70.6%	3.53
November		1.0	73.7%	2.31
December		-4.9	77.8%	1.71
Annual		4.8	72.4%	4.28

The results of the solar energy simulations for Armenia are summed up in

Table 48, referring particularly to the best-case scenario of installing a PV system in south orientation and optimal inclination on a flat roof.

The PV system's capacity factor represents the ratio of the average power produced by the power system over a year to its rated power capacity. Typical values for this parameter usually range from 5 to 20%, meaning that the capacity factor in Armenia can reach the maximum possible value. Similarly, the high annual electricity produced in all examined cities seems very promising for utilizing photovoltaic technology, while the best city for that application proves to be Gyumri. In addition, one can also verify that the difference in total annual solar electricity in Yerevan between RETScreen and PVGIS results is negligible.

Table 48. Solar energy production of a PV system in south orientation and optimal inclination in the examined cities of Armenia

City: Yerevan			
Summary	Capacity factor	Total annual electricity produced	Total annual electricity calculated with PVGIS
	%	kWh/kWp	kWh/kWp
	16.9	1,477	1490
Monthly results	Daily solar radiation - tilted	Daily solar radiation - horizontal	
	kWh/m ² /d	kWh/kWp	
January	3.30	932	
February	4.04	1,014	
March	4.56	1,235	
April	4.91	1,248	
May	5.47	1,410	
June	6.25	1,517	
July	6.35	1,562	
August	6.15	1,513	
September	5.71	1,391	
October	4.68	1,223	
November	3.58	942	
December	2.80	786	
Annual	4.82	1,477	
City: Vanadzor			
Summary	Capacity factor	Total annual electricity produced	
	%	kWh/kWp	
	17.5	1,537	
Monthly results	Daily solar radiation - tilted	Daily solar radiation - horizontal	
	kWh/m ² /d	kWh/kWp	
January	3.25	933	
February	4.07	1,049	
March	4.61	1,292	
April	4.95	1,303	
May	5.57	1,487	
June	6.40	1,615	
July	6.49	1,665	
August	6.22	1,602	
September	5.71	1,440	
October	4.62	1,245	

November	3.51	943
December	2.78	797
Annual	4.85	1,537
City: Gyumri		
Summary	Capacity factor	Total annual electricity produced
	%	kWh/kWp
	18.0	1,580
Monthly results	Daily solar radiation - tilted	Daily solar radiation - horizontal
	kWh/m ² /d	kWh/kWp
January	3.62	1.041
February	4.56	1.171
March	4.96	1.382
April	5.09	1.328
May	5.46	1.447
June	6.35	1.590
July	6.49	1.647
August	6.31	1.602
September	5.87	1.467
October	4.73	1.265
November	3.72	0.998
December	3.03	0.869
Annual	5.02	1,580

Finally, the sloped roofs, as expected, present worse energy production results, as one can see in Figure 83. Lower inclination angle of the PVs can decrease the efficiency by 4 to 5% depending on the geographical latitude of the city, while when combined with east or west orientation, the production decreases even more by 12% to 14% respectively. Still, the good solar radiation conditions in Armenia turn photovoltaics into a profitable investment even in the worst-case orientation-inclination scenario. Taking into account the potential capacities estimated in the previous paragraphs for the solar suitable flat roofs in the examined cities, a full exploitation of PVs could contribute to the Armenia's national electricity mix by 2,708GWh on a yearly basis.

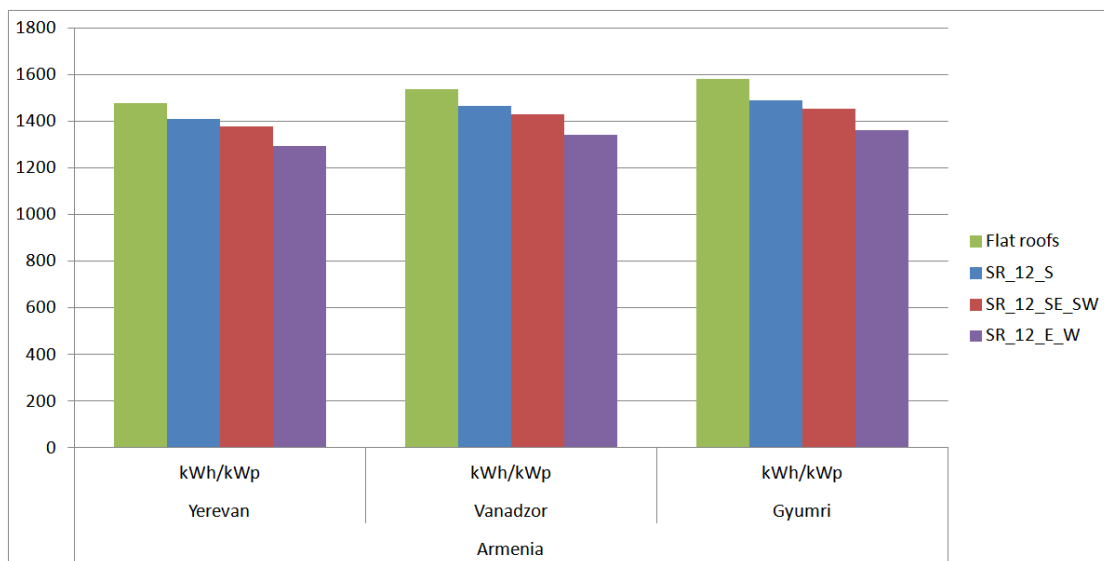


Figure 83. Solar energy production for all simulation scenarios in Armenia

4.3 Azerbaijan

The climate in Azerbaijan varies considerably from east to west. In the western mountains, the weather is drier and more extreme. The eastern part of Azerbaijan, near the Caspian Sea, has a more moderate climate.

Table 49 presents the climatic data of Azerbaijan that were used in the solar energy simulations. For Baku and Sumgait, the same data were used since they are near distant cities.

Table 49. Climatic data of the examined cities of Azerbaijan

City: Baku and Sumgait				
	Unit	Climate data location	Project location	
Latitude	°N	40.4	40.4	
Longitude	°E	49.9	49.9	
Elevation	m	151	151	
Heating design temperature	°C	0.5		
Cooling design temperature	°C	27.4		
Earth temperature amplitude	°C	13.9		
Optimal inclination of solar panels for the maximum annual efficiency	°	31		
Month		Air temperature	Relative humidity	Daily solar radiation - horizontal
		°C	%	kWh/m ² /d
January		4.9	73.1%	1.91
February		4.5	71.6%	2.64
March		6.6	74.2%	3.59
April		11.4	71.6%	4.70
May		16.3	66.1%	5.58
June		21.6	60.8%	6.21
July		24.8	58.6%	5.99
August		24.9	58.5%	5.14
September		20.9	62.3%	4.04
October		15.6	69.8%	2.86
November		10.5	73.3%	1.95
December		6.5	72.8%	1.64
Annual		14.1	67.7%	3.86
City: Ganja				
	Unit	Climate data location	Project location	
Latitude	°N	40.7	40.7	
Longitude	°E	46.4	46.4	
Elevation	m	841	841	
Heating design temperature	°C	-6.5		
Cooling design temperature	°C	25.5		
Earth temperature amplitude	°C	22.3		
Optimal inclination of	°	32		

solar panels for the maximum annual efficiency				
Month		Air temperature	Relative humidity	Daily solar radiation - horizontal
		°C	%	kWh/m ² /d
January		-2.1	79.8%	1.98
February		-1.9	78.1%	2.75
March		2.4	75.9%	3.55
April		9.0	71.2%	4.45
May		13.5	63.9%	5.20
June		18.2	55.7%	5.80
July		21.2	51.6%	5.58
August		20.4	56.7%	4.95
September		15.7	65.1%	4.16
October		10.3	72.7%	3.09
November		4.2	78.3%	2.12
December		-0.8	80.3%	1.66
Annual		9.2	69.0%	3.78

The results of the solar energy simulations for Azerbaijan are summed up in Table 50, referring particularly to the best-case scenario of installing a PV system in south orientation and optimal inclination on a flat roof.

The PV system's capacity factor represents the ratio of the average power produced by the power system over a year to its rated power capacity. Typical values for this parameter usually range from 5 to 20%, meaning that the capacity factor in Azerbaijan is above average. Similarly, the high annual electricity produced in all examined cities seems very promising for utilizing photovoltaic technology, while the best city for that application proves to be Ganja.

In addition, one can also verify that the difference in total annual solar electricity in Baku between RETScreen and PVGIS results is negligible.

Table 50. Solar energy production of a PV system in south orientation and optimal inclination in the examined cities of Azerbaijan

City: Baku and Sumgait			
Summary	Capacity factor	Total annual electricity produced	Total annual electricity calculated with PVGIS
	%	kWh/kWp	kWh/kWp
	15.0	1,318	1380
Monthly results	Daily solar radiation - tilted	Daily solar radiation - horizontal	
	kWh/m ² /d	kWh/kWp	
January	2.98	819	
February	3.57	885	
March	4.21	1,140	
April	4.94	1,265	
May	5.40	1,400	
June	5.80	1,419	
July	5.68	1,418	
August	5.21	1,302	
September	4.53	1,117	
October	3.61	945	

November	2.86	744
December	2.64	723
Annual	4.29	1,318
City: Ganja		
Summary	Capacity factor	Total annual electricity produced
	%	kWh/kWp
	15.3	1,341
Monthly results	Daily solar radiation - tilted	Daily solar radiation - horizontal
	kWh/m ² /d	kWh/kWp
January	3.22	908
February	3.84	973
March	4.17	1,149
April	4.65	1,207
May	5.02	1,321
June	5.40	1,347
July	5.28	1,343
August	5.01	1,277
September	4.70	1,182
October	4.00	1,067
November	3.25	864
December	2.75	775
Annual	4.28	1,341

Finally, the sloped roofs, as expected, present worse energy production results, as one can see in Figure 84. Lower inclination angle of the PVs can decrease the efficiency by 4 to 5% depending on the geographical latitude of the city, while when combined with east or west orientation, the production decreases even more by 11% to 13% respectively. Still, the good solar radiation conditions in Azerbaijan can ensure that photovoltaics are a profitable investment even in the worst-case orientation-inclination scenario.

Taking also into account the potential capacities estimated in the previous paragraphs for the solar suitable flat roofs in the examined cities, a full exploitation of PVs could contribute to the Azerbaijan's national electricity mix by 3,883GWh on a yearly basis.

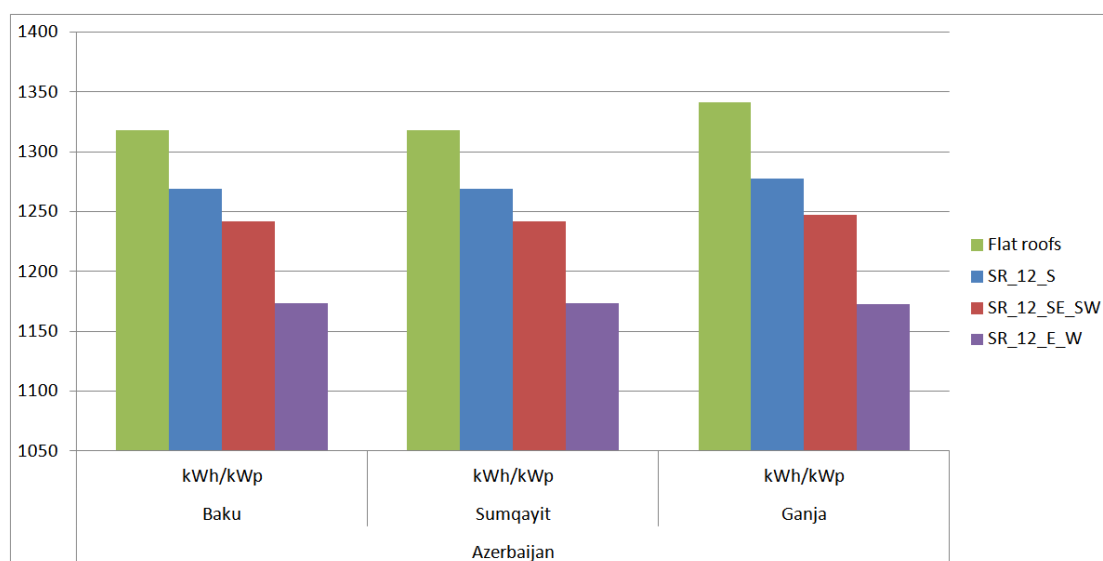


Figure 84. Solar energy production for all simulation scenarios in Azerbaijan

4.4 Belarus

Because of the proximity of the Baltic Sea, Belarus has a temperate continental climate. Winters last between 105 and 145 days, and summers last up to 150 days. Average annual precipitation ranges from 550 to 700mm and is sometimes excessive.

Table 51 presents the climatic data of Belarus that were used in the solar energy simulations.

Table 51. Climatic data of the examined cities of Belarus

City: Minsk				
	Unit	Climate data location	Project location	
Latitude	°N	53.9	53.9	
Longitude	°E	27.6	27.6	
Elevation	m	231	231	
Heating design temperature	°C	-17.2		
Cooling design temperature	°C	26.8		
Earth temperature amplitude	°C	21.5		
Optimal inclination of solar panels for the maximum annual efficiency	°	33		
Month		Air temperature	Relative humidity	Daily solar radiation - horizontal
		°C	%	kWh/m ² /d
January		-6.9	83.6%	0.58
February		-5.8	80.3%	0.94
March		-1.4	74.1%	2.59
April		6.0	66.0%	3.14
May		12.9	65.2%	4.98
June		16.1	70.3%	5.20
July		17.3	70.7%	5.08
August		16.5	72.0%	3.93
September		11.7	78.5%	2.41
October		6.3	81.7%	1.34
November		0.8	86.1%	0.52
December		-3.8	86.3%	0.33
Annual		5.9	76.2%	2.60
City: Vitebsk				
	Unit	Climate data location	Project location	
Latitude	°N	55.2	55.2	
Longitude	°E	30.2	30.2	
Elevation	m	176	176	
Heating design temperature	°C	-18.7		
Cooling design temperature	°C	25.8		
Earth temperature amplitude	°C	21.2		

Optimal inclination of solar panels for the maximum annual efficiency	°	34		
Month		Air temperature	Relative humidity	Daily solar radiation - horizontal
		°C	%	kWh/m ² /d
January		-5.3	83.4%	0.72
February		-5.6	79.4%	1.50
March		-0.9	73.1%	2.70
April		6.8	66.4%	3.87
May		13.0	64.6%	5.20
June		16.2	72.0%	5.24
July		18.2	73.3%	5.21
August		16.8	75.5%	4.24
September		11.5	79.9%	2.75
October		6.0	81.7%	1.52
November		-0.4	85.8%	0.80
December		-4.3	85.6%	0.51
Annual		6.1	76.7%	2.86
City: Mogilev				
	Unit	Climate data location	Project location	
Latitude	°N	54.0	54.0	
Longitude	°E	30.1	30.1	
Elevation	m	192	192	
Heating design temperature	°C	-19.1		
Cooling design temperature	°C	26.0		
Earth temperature amplitude	°C	22.2		
Optimal inclination of solar panels for the maximum annual efficiency	°	33		
Month		Air temperature	Relative humidity	Daily solar radiation - horizontal
		°C	%	kWh/m ² /d
January		-5.2	86.1%	0.86
February		-5.6	83.1%	1.69
March		-1.0	77.9%	2.85
April		6.8	71.3%	3.82
May		12.9	68.2%	5.01
June		15.9	73.6%	5.05
July		18.0	74.2%	4.99
August		16.8	74.7%	4.23
September		11.5	79.6%	2.84
October		5.9	83.3%	1.66
November		-0.4	87.9%	0.85
December		-4.3	88.1%	0.65
Annual		6.0	79.0%	2.88

The results of the solar energy simulations for Belarus are summed up in

Table 52, referring particularly to the best-case scenario of installing a PV system in south orientation and optimal inclination on a flat roof.

The PV system's capacity factor represents the ratio of the average power produced by the power system over a year to its rated power capacity. Typical values for this parameter usually range from 5 to 20%, meaning that the capacity factor in Belarus is below or close to the average depending on the city. Similarly, the annual electricity produced is relatively limited in all examined cities, so it seems not very promising for utilizing photovoltaic technology without the proper incentives, while the worst city for PVs proves to be Minsk.

In addition, one can also verify that the difference in total annual solar electricity in Minsk between RETScreen and PVGIS results is negligible.

Table 52. Solar energy production of a PV system in south orientation and optimal inclination in the examined cities of Belarus

City: Minsk			
Summary	Capacity factor	Total annual electricity produced	Total annual electricity calculated with PVGIS
	%	kWh/kWp	kWh/kWp
	10.7	941	930
Monthly results	Daily solar radiation - tilted	Daily solar radiation - horizontal	
	kWh/m ² /d	kWh/kWp	
January	1.08	317	
February	1.42	373	
March	3.50	984	
April	3.46	919	
May	5.10	1,344	
June	5.10	1,286	
July	5.07	1,315	
August	4.23	1,103	
September	2.86	743	
October	1.87	516	
November	0.97	270	
December	0.81	237	
Annual	2.97	941	
City: Vitebsk			
Summary	Capacity factor	Total annual electricity produced	
	%	kWh/kWp	
	12.7	1,109	
Monthly results	Daily solar radiation - tilted	Daily solar radiation - horizontal	
	kWh/m ² /d	kWh/kWp	
January	1.79	516	
February	2.82	731	
March	3.80	1,062	
April	4.45	1,166	
May	5.36	1,408	
June	5.15	1,297	
July	5.22	1,346	
August	4.63	1,203	
September	3.43	886	
October	2.35	646	

November	1.66	457
December	1.27	366
Annual	3.50	1,109
City: Mogilev		
Summary	Capacity factor	Total annual electricity produced
	%	kWh/kWp
	12.8	1,125
Monthly results	Daily solar radiation - tilted	Daily solar radiation - horizontal
	kWh/m ² /d	kWh/kWp
January	2.05	589
February	3.11	804
March	3.95	1,103
April	4.33	1,137
May	5.13	1,352
June	4.95	1,252
July	4.98	1,288
August	4.58	1,191
September	3.49	903
October	2.52	694
November	1.63	448
December	1.71	492
Annual	3.54	1,125

Finally, the sloped roofs, as expected, present even worse energy production results, as one can see in Figure 85. Lower inclination angle of the PVs can decrease the efficiency by 5 to 9% depending on the geographical latitude of the city, while when combined with east or west orientation, the production decreases even more by 13% to 19% respectively.

Taking also into account the potential capacities estimated in the previous paragraphs for the solar suitable flat roofs in the examined cities, a full exploitation of PVs could contribute to the Belarus's national electricity mix only by 2,844GWh on a yearly basis.

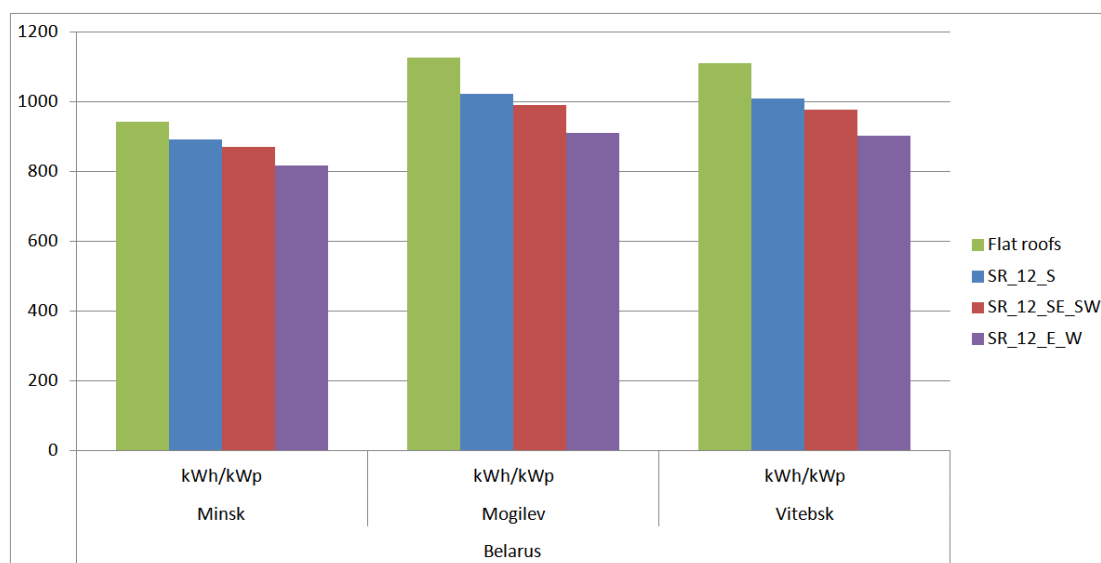


Figure 85. Solar energy production for all simulation scenarios in Belarus

4.5 Georgia

Georgia's climate is affected by subtropical influences from the west and continental influences from the east. Along the Black Sea coast, from Abkhazia to the Turkish border, and in the region known as the Kolkhida Lowlands inland from the coast, the dominant subtropical climate features high humidity and heavy precipitation. The plains of eastern Georgia are shielded from the influence of the Black Sea by mountains that provide a more continental climate. At higher elevations, precipitation is sometimes twice as heavy as in the eastern plains.

Table 53 presents the climatic data of Georgia that were used in the solar energy simulations.

Table 53. Climatic data of the examined cities of Georgia

City: Tbilisi				
	Unit	Climate data location	Project location	
Latitude	°N	41.7	41.7	
Longitude	°E	45.0	45.0	
Elevation	m	448	448	
Heating design temperature	°C	-4.2		
Cooling design temperature	°C	33.0		
Earth temperature amplitude	°C	21.1		
Optimal inclination of solar panels for the maximum annual efficiency	°	34		
Month		Air temperature	Relative humidity	Daily solar radiation - horizontal
		°C	%	kWh/m ² /d
January		1.7	73.7%	1.54
February		2.9	72.1%	2.17
March		6.9	68.6%	3.17
April		12.8	67.4%	4.51
May		17.4	66.9%	5.50
June		21.2	62.3%	6.28
July		24.4	59.5%	6.18
August		23.7	60.8%	5.33
September		19.6	65.1%	4.18
October		13.5	73.2%	2.70
November		8.1	77.0%	1.65
December		3.8	76.4%	1.26
Annual		13.1	68.6%	3.71
City: Rustavi				
	Unit	Climate data location	Project location	
Latitude	°N	41.7	41.7	
Longitude	°E	45.0	45.0	
Elevation	m	448	448	
Heating design temperature	°C	-4.2		
Cooling design temperature	°C	33.0		

Earth temperature amplitude	°C	21.1		
Optimal inclination of solar panels for the maximum annual efficiency	°	36		
Month		Air temperature	Relative humidity	Daily solar radiation - horizontal
		°C	%	kWh/m ² /d
January		1.7	73.7%	1.54
February		2.9	72.1%	2.17
March		6.9	68.6%	3.17
April		12.8	67.4%	4.51
May		17.4	66.9%	5.50
June		21.2	62.3%	6.28
July		24.4	59.5%	6.18
August		23.7	60.8%	5.33
September		19.6	65.1%	4.18
October		13.5	73.2%	2.70
November		8.1	77.0%	1.65
December		3.8	76.4%	1.26
Annual		13.1	68.6%	3.71
City: Batumi				
	Unit	Climate data location	Project location	
Latitude	°N	41.6	41.6	
Longitude	°E	41.6	41.6	
Elevation	m	32	32	
Heating design temperature	°C	-0.1		
Cooling design temperature	°C	27.2		
Earth temperature amplitude	°C	14.8		
Optimal inclination of solar panels for the maximum annual efficiency	°	33		
Month		Air temperature	Relative humidity	Daily solar radiation - horizontal
		°C	%	kWh/m ² /d
January		6.3	69.7%	1.58
February		6.2	69.8%	2.26
March		8.2	73.5%	3.20
April		12.5	75.3%	4.20
May		15.6	79.2%	5.32
June		20.0	77.7%	5.91
July		22.2	79.7%	5.54
August		22.8	79.8%	4.82
September		19.7	78.5%	4.14
October		15.7	78.3%	2.94
November		12.0	72.6%	1.92
December		8.1	68.4%	1.36
Annual		14.2	75.2%	3.61
City: Kutaisi				

	Unit	Climate data location	Project location	
Latitude	°N	42.3	42.3	
Longitude	°E	42.6	42.6	
Elevation	m	116	116	
Heating design temperature	°C	-1.1		
Cooling design temperature	°C	30.7		
Earth temperature amplitude	°C	20.4		
Optimal inclination of solar panels for the maximum annual efficiency	°	36		
Month		Air temperature	Relative humidity	Daily solar radiation - horizontal
		°C	%	kWh/m ² /d
January		5.2	74.0%	1.66
February		5.5	68.9%	2.41
March		8.5	70.6%	3.38
April		14.1	70.7%	4.34
May		17.5	72.5%	5.43
June		21.0	74.5%	5.73
July		22.7	81.0%	5.62
August		23.5	77.6%	5.00
September		20.3	75.7%	4.19
October		16.1	72.2%	3.03
November		11.1	72.0%	1.95
December		7.0	71.8%	1.41
Annual		14.4	73.5%	3.69

The results of the solar energy simulations for Georgia are summed up in Table 54, referring particularly to the best-case scenario of installing a PV system in south orientation and optimal inclination on a flat roof.

The PV system's capacity factor represents the ratio of the average power produced by the power system over a year to its rated power capacity. Typical values for this parameter usually range from 5 to 20%, meaning that the capacity factor in Georgia is above the average. Similarly, the noticeable annual electricity produced in all examined cities seems very promising for utilizing photovoltaic technology, while the best city for that application proves to be Kutaisi.

In addition, one can also verify that the difference in total annual solar electricity in Tbilisi between RETScreen and PVGIS results is negligible.

Table 54. Solar energy production of a PV system in south orientation and optimal inclination in the examined cities of Georgia

City: Tbilisi			
Summary	Capacity factor	Total annual electricity produced	Total annual electricity calculated with PVGIS
	%	kWh/kWp	kWh/kWp
	14.3	1,249	1,290
Monthly results	Daily solar radiation – tilted	Daily solar radiation - horizontal	
	kWh/m ² /d	kWh/kWp	
January	2.36	661	
February	2.89	724	
March	3.70	1,005	
April	4.73	1,208	
May	5.29	1,367	
June	5.80	1,423	
July	5.81	1,451	
August	5.41	1,355	
September	4.77	1,179	
October	3.54	935	
November	2.41	636	
December	1.94	541	
Annual	4.06	1,249	
City: Rustavi			
Summary	Capacity factor	Total annual electricity produced	
	%	kWh/kWp	
	14.2	1,246	
Monthly results	Daily solar radiation - tilted	Daily solar radiation - horizontal	
	kWh/m ² /d	kWh/kWp	
January	2.39	669	
February	2.91	729	
March	3.70	1,006	
April	4.71	1,202	
May	5.24	1,354	
June	5.73	1,407	
July	5.75	1,436	
August	5.37	1,346	
September	4.77	1,178	
October	3.56	940	
November	2.43	642	
December	1.97	548	
Annual	4.05	1,246	
City: Batumi			
Summary	Capacity factor	Total annual electricity produced	
	%	kWh/kWp	
	14.1	1,235	
Monthly results	Daily solar radiation - tilted	Daily solar radiation - horizontal	
	kWh/m ² /d	kWh/kWp	
January	2.43	667	

February	3.03	749
March	3.74	1,009
April	4.39	1,125
May	5.14	1,339
June	5.50	1,359
July	5.24	1,328
August	4.88	1,234
September	4.72	1,166
October	3.92	1,022
November	2.95	762
December	2.16	590
Annual	4.01	1,235
City: Kutaisi		
Summary	Capacity factor	Total annual electricity produced
	%	kWh/kWp
	14.6	1,278
Monthly results	Daily solar radiation - tilted	Daily solar radiation - horizontal
	kWh/m ² /d	kWh/kWp
January	2.73	751
February	3.39	836
March	4.03	1,084
April	4.54	1,154
May	5.19	1,342
June	5.26	1,298
July	5.25	1,328
August	5.04	1,269
September	4.81	1,185
October	4.17	1,082
November	3.15	814
December	2.32	636
Annual	4.16	1,278

Finally, the sloped roofs, as expected, present worse energy production results, as one can see in Figure 86. Lower inclination angle of the PVs can decrease the efficiency by 3 to 4% depending on the geographical latitude of the city, while when combined with east or west orientation, the production decreases even more by 9% to 12% respectively. Still, the good solar radiation conditions in Georgia can ensure that photovoltaics are a profitable investment even in the worst-case orientation-inclination scenario.

Taking also into account the potential capacities estimated in the previous paragraphs for the solar suitable flat roofs in the examined cities, a full exploitation of PVs could contribute to the Georgia's national electricity mix by 1.9TWh on a yearly basis.

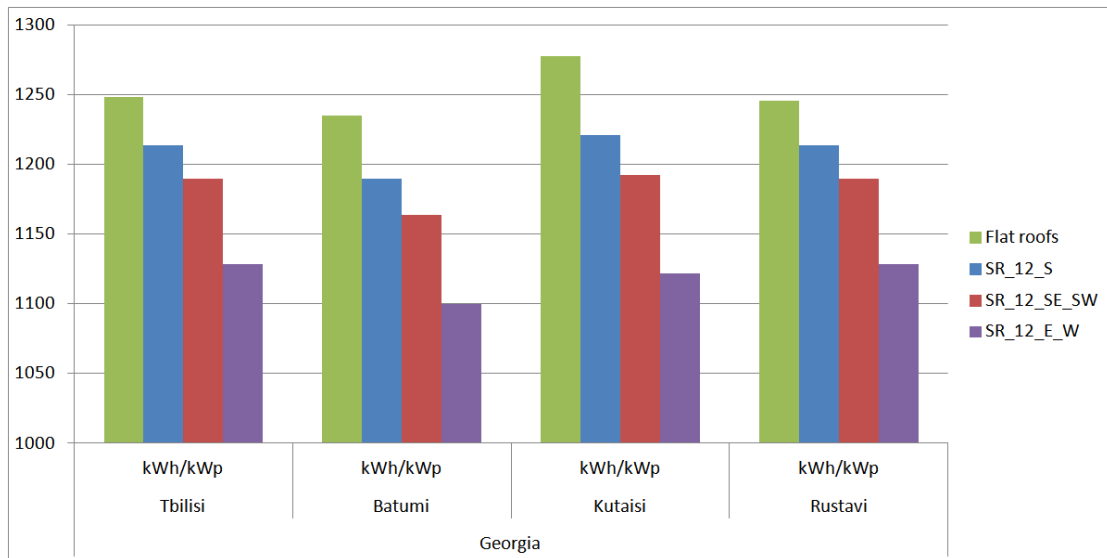


Figure 86. Solar energy production for all simulation scenarios in Georgia

4.6 Moldova

Moldova's proximity to the Black Sea gives it a mild and sunny climate. The country's climate is moderately continental, meaning the summers are warm and long, with temperatures averaging about 20°C, and the winters are relatively mild and dry, with January temperatures averaging at -4°C. Annual rainfall, which ranges from around 6cm in the north to 4cm in the south, can vary greatly. Besides, long dry spells are not unusual. Table 55 presents the climatic data of Moldova that were used for the solar energy simulations.

Table 55. Climatic data of the examined cities of Moldova

City: Chisinau				
	Unit	Climate data location	Project location	
Latitude	°N	47.0	47.0	
Longitude	°E	29.0	29.0	
Elevation	m	173	173	
Heating design temperature	°C	-11.9		
Cooling design temperature	°C	29.5		
Earth temperature amplitude	°C	22.6		
Optimal inclination of solar panels for the maximum annual efficiency	°	35		
Month		Air temperature	Relative humidity	Daily solar radiation – horizontal
		°C	%	kWh/m ² /d
January		-2.0	79.4%	1.24
February		-1.4	76.0%	2.07
March		3.3	69.9%	3.09
April		10.4	63.3%	4.13
May		16.4	59.6%	5.46

June		19.6	64.0%	5.62
July		21.9	62.5%	5.61
August		21.4	61.1%	5.00
September		16.3	66.2%	3.58
October		10.4	71.7%	2.33
November		3.8	80.0%	1.29
December		-0.7	81.0%	1.01
Annual		10.0	69.5%	3.38
City: Cahul				
	Unit	Climate data location	Project location	
Latitude	°N	45.5	45.5	
Longitude	°E	28.0	28.0	
Elevation	m	72	72	
Heating design temperature	°C	-10.6		
Cooling design temperature	°C	30.8		
Earth temperature amplitude	°C	21.8		
Optimal inclination of solar panels for the maximum annual efficiency	°	35		
Month		Air temperature	Relative humidity	Daily solar radiation - horizontal
		°C	%	kWh/m ² /d
January		-1.4	85.1%	1.46
February		0.0	79.8%	2.43
March		4.6	74.2%	3.53
April		11.1	71.1%	4.99
May		17.2	67.5%	6.17
June		20.6	70.1%	6.79
July		22.8	68.4%	6.58
August		22.2	69.4%	5.74
September		17.4	72.4%	4.36
October		11.5	77.2%	2.93
November		4.9	83.3%	1.60
December		-0.1	85.3%	1.22
Annual		11.0	75.3%	3.99
City: Balti				
	Unit	Climate data location	Project location	
Latitude	°N	48.2	48.2	
Longitude	°E	28.3	28.3	
Elevation	m	233	233	
Heating design temperature	°C	-8.6		
Cooling design temperature	°C	26.7		
Earth temperature amplitude	°C	22.1		
Optimal inclination of solar panels for the maximum annual efficiency	°	34		

Month	Air temperature	Relative humidity	Daily solar radiation - horizontal
	°C	%	kWh/m ² /d
January	-3.6	79.4%	1.16
February	-2.7	77.8%	1.97
March	2.2	71.9%	3.06
April	10.0	58.3%	4.03
May	16.3	51.5%	5.29
June	19.1	55.4%	5.45
July	21.4	54.9%	5.40
August	21.2	50.8%	4.83
September	16.3	55.4%	3.36
October	10.1	63.6%	2.12
November	2.5	76.0%	1.18
December	-2.6	78.9%	0.95
Annual	9.3	64.4%	3.24

The results of the solar energy simulations for Moldova are summed up in Table 56, referring particularly to the best-case scenario of installing a PV system in south orientation and optimal inclination on a flat roof.

The PV system's capacity factor represents the ratio of the average power produced by the power system over a year to its rated power capacity. Typical values for this parameter usually range from 5 to 20%, meaning that the capacity factor in Moldova is over the average. Similarly, the noticeable annual electricity produced in all examined cities seems very promising for utilizing photovoltaic technology, while the best city by far for that application proves to be Cahul.

In addition, one can also verify that the difference in total annual solar electricity in Chisinau between RETScreen and PVGIS results is negligible.

Table 56. Solar energy production of a PV system in south orientation and optimal inclination in the examined cities of Moldova

City: Chisinau			
Summary	Capacity factor	Total annual electricity produced	Total annual electricity calculated with PVGIS
	%	kWh/kWp	kWh/kWp
	13.8	1,207	1240
Monthly results	Daily solar radiation – tilted	Daily solar radiation - horizontal	
	kWh/m ² /d	kWh/kWp	
January	2.18	0,618	
February	3.16	0,803	
March	3.86	1,061	
April	4.46	1,152	
May	5.39	1,396	
June	5.31	1,316	
July	5.40	1,368	
August	5.22	1,323	
September	4.23	1,064	
October	3.29	0,882	
November	2.10	0,566	
December	1.83	0,519	
Annual	3.87	1,207	

City: Cahul		
Summary	Capacity factor	Total annual electricity produced
	%	kWh/kWp
	16.2	1,419
Monthly results	Daily solar radiation – tilted	Daily solar radiation – horizontal
	kWh/m ² /d	kWh/kWp
January	2.54	717
February	3.71	933
March	4.44	1,207
April	5.44	1,387
May	6.06	1,553
June	6.35	1,553
July	6.29	1,574
August	5.99	1,501
September	5.23	1,299
October	4.27	1,128
November	2.69	716
December	2.20	621
Annual	4.61	1,419
City: Balti		
Summary	Capacity factor	Total annual electricity produced
	%	kWh/kWp
	13.4	1,172
Monthly results	Daily solar radiation – tilted	Daily solar radiation – horizontal
	kWh/m ² /d	kWh/kWp
January	2.10	600
February	3.07	783
March	3.87	1,069
April	4.39	1,135
May	5.27	1,367
June	5.19	1,293
July	5.24	1,334
August	5.08	1,290
September	3.97	1,002
October	2.97	801
November	1.95	528
December	1.80	514
Annual	3.75	1,172

Finally, the sloped roofs, as expected, present worse energy production results, as one can see in Figure 87. Lower inclination angle of the PVs can decrease the efficiency by 6%, while when combined with east or west orientation, the production decreases even more by 6% to 14% depending on the geographical latitude of the city. Still, the moderately good solar radiation conditions in Moldova can ensure that photovoltaics are a profitable investment even in the worst-case scenario.

Taking into account the potential capacities estimated in the previous paragraphs for the solar suitable flat roofs in the examined cities, a full exploitation of PVs could contribute to the Moldova's national electricity mix only by 186GWh on a yearly basis. The latter not so promising outcome stems mostly from the limited PV potential found at the examined cities.

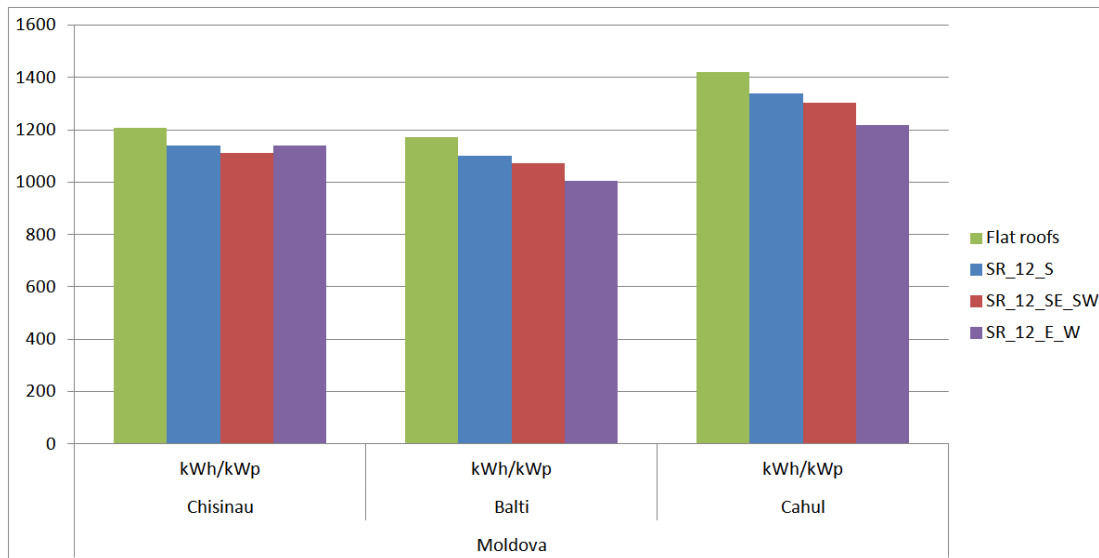


Figure 87. Solar energy production for all simulation scenarios in Moldova

4.7 Ukraine

Ukraine has a mostly temperate climate, with the exception of the southern coast of Crimea, which has a subtropical climate. The climate is influenced by moderately warm, humid air coming from the Atlantic Ocean. Precipitation is disproportionately distributed; it is highest in the west and north and lowest in the east and southeast. Table 57 presents the climatic data of Ukraine that were used in the solar energy simulations.

Table 57. Climatic data of the examined cities of Ukraine

City: Kyiv				
	Unit	Climate data location	Project location	
Latitude	°N	50.4	50.4	
Longitude	°E	30.6	30.6	
Elevation	m	167	167	
Heating design temperature	°C	-15.1		
Cooling design temperature	°C	27.8		
Earth temperature amplitude	°C	22.2		
Optimal inclination of solar panels for the maximum annual efficiency	°	34		
Month		Air temperature	Relative humidity	Daily solar radiation - horizontal
		°C	%	kWh/m ² /d
January		-5.6	82.3%	0.79
February		-4.2	78.9%	1.27
March		0.7	73.5%	2.56
April		8.7	66.1%	3.21
May		15.1	63.1%	4.98
June		18.2	69.5%	5.44
July		19.3	69.7%	5.70
August		18.6	69.3%	4.62

September		13.9	75.2%	3.04
October		8.1	78.3%	1.80
November		2.1	84.9%	0.73
December		-2.3	84.7%	0.58
Annual		7.8	74.6%	2.90
City: Lviv				
	Unit	Climate data location	Project location	
Latitude	°N	49.8	49.8	
Longitude	°E	24.0	24.0	
Elevation	m	323	323	
Heating design temperature	°C	-14.2		
Cooling design temperature	°C	26.6		
Earth temperature amplitude	°C	20.5		
Optimal inclination of solar panels for the maximum annual efficiency	°	35		
Month		Air temperature	Relative humidity	Daily solar radiation - horizontal
		°C	%	kWh/m ² /d
January		-3.1	81.5%	1.08
February		-2.4	79.4%	1.83
March		1.7	75.6%	2.82
April		8.3	69.3%	3.78
May		13.8	70.1%	4.67
June		16.3	73.7%	4.83
July		18.3	74.5%	4.83
August		17.6	75.6%	4.45
September		13.0	78.9%	3.00
October		8.2	79.7%	1.85
November		2.4	83.0%	1.06
December		-1.8	83.5%	0.83
Annual		7.7	77.1%	2.93
City: Odesa				
	Unit	Climate data location	Project location	
Latitude	°N	46.4	46.4	
Longitude	°E	30.8	30.8	
Elevation	m	42	42	
Heating design temperature	°C	-11.1		
Cooling design temperature	°C	29.8		
Earth temperature amplitude	°C	20.3		
Optimal inclination of solar panels for the maximum annual efficiency	°	35		
Month		Air temperature	Relative humidity	Daily solar radiation - horizontal

		°C	%	kWh/m ² /d
January		-1.7	82.9%	0.97
February		-1.0	80.2%	1.64
March		2.6	77.4%	2.68
April		9.0	73.8%	4.14
May		15.1	69.1%	5.62
June		19.4	69.2%	6.16
July		21.5	63.6%	6.15
August		21.2	64.2%	5.38
September		17.0	70.6%	3.99
October		11.2	76.3%	2.41
November		5.8	82.2%	1.09
December		1.4	83.1%	0.76
Annual		10.2	74.3%	3.43
City: Zaporizhia				
	Unit	Climate data location	Project location	
Latitude	°N	47.8	47.8	
Longitude	°E	35.0	35.0	
Elevation	m	112	112	
Heating design temperature	°C	-14.8		
Cooling design temperature	°C	30.5		
Earth temperature amplitude	°C	23.6		
Optimal inclination of solar panels for the maximum annual efficiency	°	34		
Month		Air temperature	Relative humidity	Daily solar radiation - horizontal
		°C	%	kWh/m ² /d
January		-3.2	85.3%	1.21
February		-3.3	82.2%	2.00
March		1.9	77.0%	2.91
April		10.1	66.2%	4.20
May		16.2	61.0%	5.62
June		19.7	65.8%	5.72
July		22.2	62.4%	5.88
August		21.5	60.6%	5.18
September		16.0	66.0%	3.87
October		9.2	74.0%	2.44
November		2.1	84.9%	1.25
December		-2.1	86.1%	0.95
Annual		9.3	72.6%	3.44

The results of the solar energy simulations for Ukraine are summed up in Table 58, referring particularly to the best-case scenario of installing a PV system in south orientation and optimal inclination on a flat roof.

The PV system's capacity factor represents the ratio of the average power produced by the power system over a year to its rated power capacity. Typical values for this parameter usually range from 5 to 20%, meaning that the capacity factor in Ukraine is round the average, with the lower fraction estimated for Kyiv and Lviv and the higher for Odesa and Zaporizhia. In the same pattern,

the annual electricity produced seems more promising in Odesa and Zaporizhia, while the least efficient location for PVs proves to be the city of Kyiv.

In addition, one can also verify that the difference in total annual solar electricity in Kyiv between RETScreen and PVGIS results is negligible.

Table 58. Solar energy production of a PV system in south orientation and optimal inclination in the examined cities of Ukraine

City: Kyiv			
Summary	Capacity factor	Total annual electricity produced	Total annual electricity calculated with PVGIS
	%	kWh/kWp	kWh/kWp
	11.7	1,022	1,110
Monthly results	Daily solar radiation – tilted	Daily solar radiation - horizontal	
	kWh/m ² /d	kWh/kWp	
January	1.35	393	
February	1.80	469	
March	3.22	899	
April	3.45	907	
May	5.00	1,307	
June	5.23	1,307	
July	5.60	1,431	
August	4.92	1,265	
September	3.62	926	
October	2.54	691	
November	1.17	322	
December	1.05	302	
Annual	3.26	1,022	
City: Lviv			
Summary	Capacity factor	Total annual electricity produced	
	%	kWh/kWp	
	12.4	1,083	
Monthly results	Daily solar radiation - tilted	Daily solar radiation - horizontal	
	kWh/m ² /d	kWh/kWp	
January	2.11	602	
February	2.95	754	
March	3.61	1,000	
April	4.13	1,079	
May	4.65	1,226	
June	4.61	1,168	
July	4.70	1,216	
August	4.69	1,215	
September	3.54	910	
October	2.60	709	
November	1.77	479	
December	1.67	476	
Annual	3.42	1,083	
City: Odesa			

Summary	Capacity factor	Total annual electricity produced
	%	kWh/kWp
	13.3	1,170
Monthly results	Daily solar radiation – tilted	Daily solar radiation - horizontal
	kWh/m ² /d	kWh/kWp
January	1.46	418
February	2.25	577
March	3.21	891
April	4.45	1,156
May	5.53	1,439
June	5.80	1,432
July	5.91	1,492
August	5.63	1,421
September	4.77	1,191
October	3.39	905
November	1.58	425
December	1.21	344
Annual	3.77	1,170
City: Zaporizhia		
Summary	Capacity factor	Total annual electricity produced
	%	kWh/kWp
	14.2	1,241
Monthly results	Daily solar radiation – tilted	Daily solar radiation - horizontal
	kWh/m ² /d	kWh/kWp
January	2.18	623
February	3.10	795
March	3.62	1,003
April	4.58	1,183
May	5.60	1,448
June	5.44	1,348
July	5.71	1,440
August	5.47	1,381
September	4.67	1,173
October	3.55	953
November	2.07	561
December	1.75	499
Annual	3.98	1,241

Finally, the sloped roofs, as expected, present even worse energy production results, as one can see in Figure 88. Lower inclination angle of the PVs can decrease the efficiency by 4 to 7% depending on the geographical latitude of the city, while when combined with east or west orientation, the production decreases more by 10 to 16% respectively. Eventually, the variable solar radiation conditions in the vast country of Ukraine are the key parameter to define what incentives are required for PV technology to be a profitable investment even in the worst-case inclination-orientation scenario.

Taking also into account the potential capacities estimated in the previous paragraphs for the solar suitable flat roofs in the examined cities, a full exploitation of PVs could contribute to the Ukraine's national electricity mix only by 6,654GWh on a yearly basis.

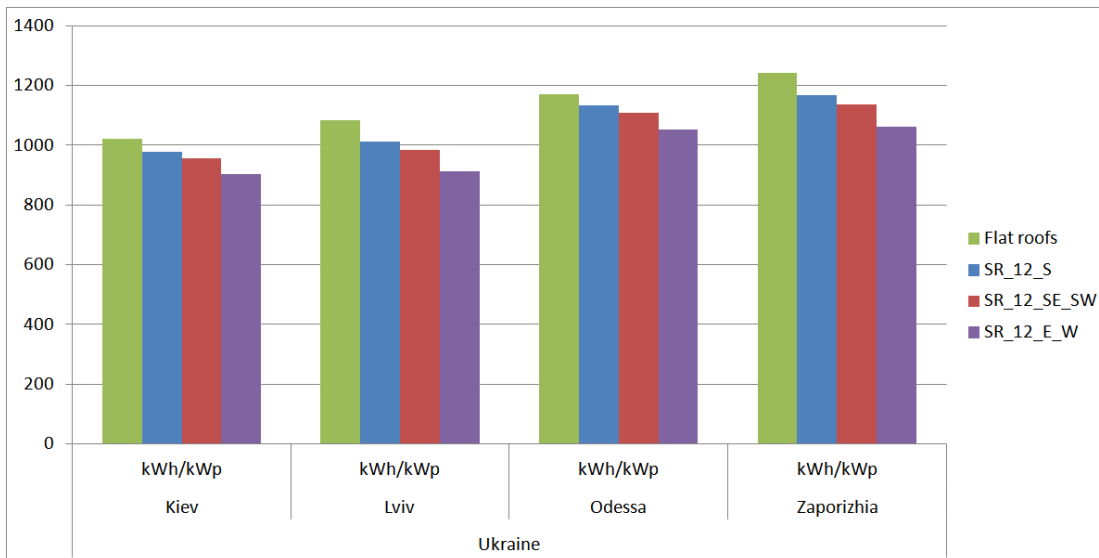


Figure 88. Solar energy production for all simulation scenarios in Ukraine

4.8 Aggregated results

The aggregated results for the solar energy production for all cities in the six countries and for flat and sloped roofs are depicted in the following Figure 89.

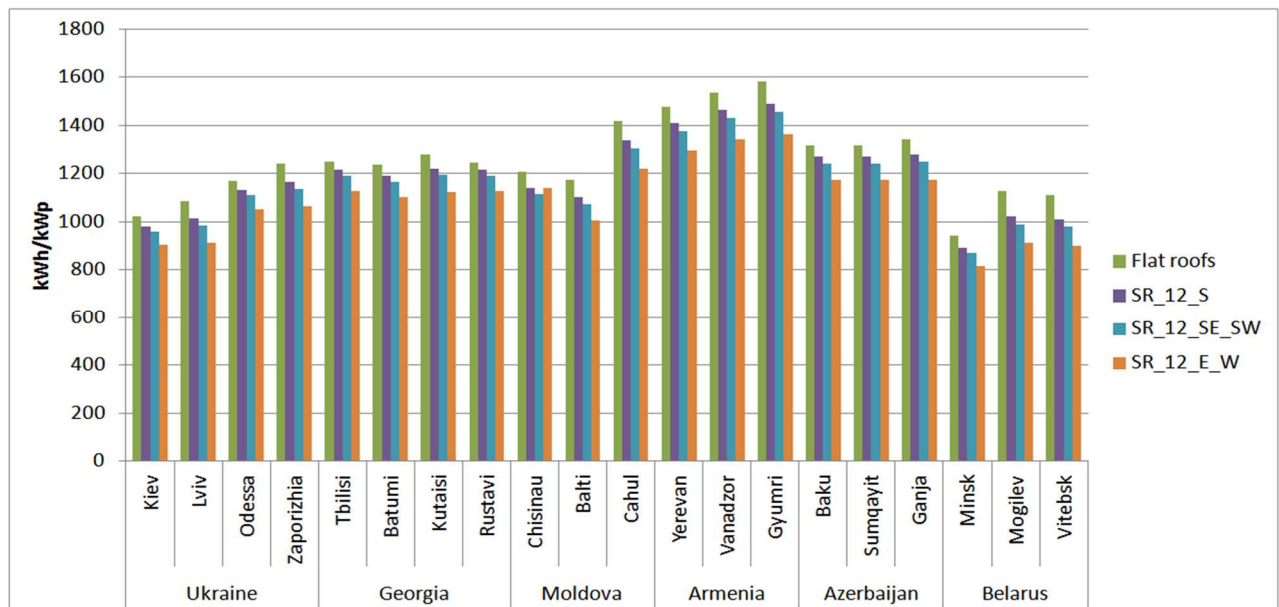


Figure 89. Solar energy production for all orientation-inclination scenarios in all examined cities

As it can be seen, Armenia has the highest solar yield and Belarus the lowest. When it comes to each country separately and having a threshold of 1.200 kWh/kWp as a good value:

- In the Ukraine, Zaporizhia is the most promising city, with a yield almost 20% higher than Kyiv, being in absolute terms good.

- In Georgia, the four cities' yield is quite similar and of a good level.
- In Moldova, Cahul is the best location by far, with Chisinau being also good.
- In Armenia, all four cities have a splendid yield.
- In Azerbaijan, all three cities have a very good yield.
- In Belarus, Mogilev and Vitebsk are on the limit and Minsk has a rather unsatisfactory yield.

Finally, in all cities, the performance of PVs on Eastern and Western inclined roofs is significantly reduced compared to all other options; it is a solution that should, if possibly, be avoided

5 Assessment of the electricity production and the grid supply

5.1 Assumptions

In this section is presented the potential for PV capacity and the respective electricity production, based on the assumptions that (a) state of the art Mono-Si panels are used, (b) that the whole solar potential of flat roofs is utilised (as described in section3) and (c) that the whole solar potential of the sloped roofs is utilised (under the constrains discussed in the previous sections).

Two different segment potentials have been considered, representing the two major market that can be detected, based on the buildings' typology and on technical, legal and practical differentiations:

Segment A:

It consists of the small domestic applications, which are as a rule the small single family houses, with a sloped roof. In those one can apply in up to 10 kWp, as a rule between 3 and 8, depending on the size of the houses, on the type of the roof (pitched or hipped) and on its orientation.

It is clear, that this is not the true total potential. The real one is a 'constrained' one, taking into consideration all the structural and practical problems mentioned earlier. This real potential varies, from city to city and from country to country, with generalisations not being safe as there are no descriptive statistics on those. Based on the information gathers on site, by the local experts and from the literature sources in section 3.1, the real, constrained potential can hardly exceed 15-20% the theoretical one.

Segment B

This segments consists of the bigger applications, namely of commercial/industrial buildings, of big multifamily blocks and of public buildings, all featuring flat roofs, which can support 50 to 200kWp PV systems.

For those buildings, there are figures available in most of the cities, making it possible to determine with a fair degree of accuracy the potential for capacities and assumptions, according to the calculations of sections 3 and 4.

The overall results for the two segments are presented for each city and country in the following sections.

5.2 Armenia

Table 59. Potential and solar energy production for Armenia

City	Segment A PV capacity (MWp)	Segment B PV capacity (MWp)	Total potential PV capacity (MWp)	Segment B Annual electricity production (GWh)	Segments A&B Maximum theoretical annual electricity (GWh)
Yerevan	1,387.7	384.9	1,772.5	471.1	2,617.9
Vanadzor	232.9	62.1	295.0	79.1	453.4
Gyumri	192.8	51.4	244.2	67.3	385.8
Total	1,813.3	498.4	2,311.7	617.5	3,457.1

5.3 Azerbaijan

Table 60. Total potential and solar energy production for Azerbaijan

City	Segment A PV capacity (MWp)	Segment B PV capacity (MWp)	Total potential PV capacity (MWp)	Segment B Annual electricity production (GWh)	Segments A&B Maximum theoretical annual electricity (GWh)
Baku	2,346.1	708.6	3,054.7	1,289.4	4,025.2
Sumgait	270.3	72.5	342.8	79.2	451.8
Ganja	232.5	61.2	293.7	68.0	393.8
Total	2,848.9	842.3	3,691.2	1,436.6	4,870.8

5.4 Belarus

Table 61. Total potential and solar energy production for Belarus

City	Segment A PV capacity (MWp)	Segment B PV capacity (MWp)	Total potential PV capacity (MWp)	Segment B Annual electricity production (GWh)	Segments A&B Maximum theoretical annual electricity (GWh)
Minsk	2,032.0	341.2	2,373.3	443.3	2,233.0
Mogilev	538.5	72.3	610.7	67.4	687.1
Vitebsk	640.6	79.4	720.0	72.9	798.5
Total	3,211.1	492.8	3,704.0	583.6	3,719.0

5.5 Georgia

Table 62. Total potential and solar energy production for Georgia

City	Segment A PV capacity (MWp)	Segment B PV capacity (MWp)	Total potential PV capacity (MWp)	Segment B Annual electricity production (GWh)	Segments A&B Maximum theoretical annual electricity (GWh)
Tbilisi	476.7	712.3	1,189.0	1,220.2	2,230.0
Batumi	129.7	75.6	205.3	123.0	328.3
Kutaisi	132.0	146.3	278.3	206.3	288.8
Rustavi	88.1	99.1	187.2	102.3	233.2
Total	822.0	1,033.4	1,855.4	1,651.8	2,321.1

5.6 Moldova

Table 63. Total potential and solar energy production for Moldova

City	Segment A PV capacity (MWp)	Segment B PV capacity (MWp)	Total potential PV capacity (MWp)	Segment B Annual electricity production (GWh)	Segments A&B Maximum theoretical annual electricity (GWh)
Chisinau	142.8	29.5	172.3	29.5	161.1
Balti	17.5	3.4	20.9	3.3	18.8
Cahul	4.5	1.0	5.4	1.1	5.9
Total	164.6	34.0	198.6	33.9	185.8

5.7 Ukraine

Table 64. Total potential and solar energy production for Ukraine

City	Segment A PV capacity (MWp)	Segment B PV capacity (MWp)	Total potential PV capacity (MWp)	Segment B Annual electricity production (GWh)	Segments A&B Maximum theoretical annual electricity (GWh)
Kyiv	3,983.3	488.0	4,471.2	413.1	3,571.7
Odesa	2,039.9	322.4	2,362.3	312.3	2,187.9
Lviv	598.8	142.1	740.9	158.2	618.8
Zaporizhia	524.1	236.5	760.7	242.6	736.2
Total	7,146.1	1,189.0	8,355.1,770. 4	1,126.2	7,114.6

5.8 Peak load mitigation strategies

Finally, the impact of restrictions due to the grid has should also to be taken into consideration. However, in all of the countries considered this is not really a constrain, given the really small size of even the maximum PV potential, compared to the existing grid connections, which are designed based on full conditions covered by conventional and big hydro power plants, not following the load cycles and operating on a regional scale dating from the USSR period.

Still, a very suitable tool to control this for BAPVs, is by applying peak load mitigation controls, which will be discussed in brief.

The typical basic indicator to select optimal roof-tops for PV-installations in urban environments is the sum of the solar global radiation per square meter over a year (“MaxYearlyProd”). A higher sum indicates that the location is better, and the amount of produced energy per area unit can thus be maximised. Moreover, when comparing locations, the area required to fulfil a certain yearly demand and the installed capacity can be minimised. This concept relies on the assumption that all of the produced energy can either be used for self-supply or can be sold through the grid. However, this is not necessarily true if PV-penetration is high: if the amount of generated energy is beyond the local demand and the grid capacity, energy curtailment is necessary to avoid instability of the grid and risks for the security of the supply.

To illustrate to what extent a strategy is best-suited for the energy balance of a certain location, we propose three alternative strategies to select locations based on different optimal criteria. The first strategy, “MinVariability”, consists of selecting locations based on the expected variability of a potential PV-system per average square meter. We understand variability as proposed in Hoff and Perez (2010), i.e., variability is the standard deviation of the change in the power output over time. They evaluated the variability of PV-fleets that consist of PV-power plants dispersed in large regions (the distance between plants could be hundreds of kilometres). In the case of municipalities, the major difference in the variability between installations is caused by the orientation and shadowing conditions of every plant and not by different weather conditions. The lower the variability is, the lower are the reserve requirements to meet reliability standards. Furthermore, Hoff and Perez (2010) proposed an equation to evaluate the variability of the whole fleet. To rate single power plants, we adapted the equation as presented in:

$$\sigma_{\Delta t}^n = \sqrt{\text{Var}[\Delta P_{\Delta t}^n]}$$

where $\Delta P_{\Delta t}^n$ is the time series of changes in supplied power at the potential system n occurring over a time interval of Δt .

The second strategy, “MaxYearlyProdOverMinVar”, rates potential PV-installations based on the factor between the total yearly production

$$\left(\sum_{t=1}^T P_t^n \right)$$

and the variability

$$\left(\sigma_{\Delta t}^n \right)$$

The higher the yearly production is and/or the lower the variability is, the better a certain location would perform. PV-plant sets selected considering this indicator deliver a balanced electricity output, where every Wh added to the yearly production is de-rated by the amount of variability that the potential PV-plant adds to the resulting load.

The third strategy, “ProperP”, consists of a sequential selection of plants based on the amount of energy that is properly supplied and the amount of excess energy generated during every time step in a year. Properly supplied energy

$$(PrSu_t^n)$$

is defined as the energy that is generated by the PV-plant n at the moment it is required. It is described in Eq. (3). Excess energy (Exc_t^n) is the amount of energy generated beyond the demand by the n th PV plant for every time step according to Eq. (4). To prevent plants from generating high levels of excess energy in a proposed solution, the amount of properly supplied energy is divided by the sum of excess energy for the whole year. This decision criterion is called ProperFn and is presented in Eq. (5). The criterion rates installations based on the fit of their energy generation to the local demand. The larger the value of the criterion is, the better it is. A high value means that the amount of properly supplied energy is high compared to the amount of excess energy. This criterion has a value of 0 if the plant does not contribute to a proper energy supply. To avoid that the equation becomes undefined when the PV-installation is very small compared with the demand, which is the case for the initial selection rounds, the criterion is equal to the sum of properly supplied energy when there is no excess energy. In every selection round, ProperFn is calculated for all of the not-yet-selected potential PV-plants against the remaining local demand. The best rated plant is selected, and the remaining unfulfilled demand is calculated by subtracting the output of the chosen plant. The selection loop continues until a certain desired PV-penetration level is achieved. The PV-plant set resulting from this strategy maximises the amount of properly delivered energy and minimises the amount of excess electricity (Camargo et al, 2015).

$$PrSu_t^n = \begin{cases} D_t & \text{if } (P_t^n \geq D_t) \\ P_t^n & \text{if } (P_t^n < D_t) \end{cases} \quad (3)$$

$$Exc_t^n = \begin{cases} P_t^n - D_t & \text{if } (P_t^n > D_t) \\ 0 & \text{if } (P_t^n \leq D_t) \end{cases} \quad (4)$$

$$ProperF^n = \begin{cases} \frac{\sum_{t=1}^T PrSu_t^n}{\sum_{t=1}^T Exc_t^n} & \text{if } (Exc_t^n > 0) \\ \sum_{t=1}^T PrSu_t^n & \text{if } (Exc_t^n = 0) \end{cases} \quad (5)$$

As it will become clear from the following tables, the capacities considered to be feasible in all six countries are rather limited; so is the expected annual production, making the possibility of excess electricity production a rather distant perspective.

Furthermore, especially with respect that we are discussing capacity constraints in the urban environment, constrains would be rather rare in the region. The reasons can be sourced back to the soviet central planning legacy. Though quite inefficient the distribution networks in the cities are far from saturated for two primary reasons. 1) spare capacity of key transformers was always high by design –most often this meant full redundancy. 2) On top of the situation described above

all Former Soviet Union countries have experienced a sharp economic decline (and thus a respective decline in electricity consumption). In most cases the current levels of consumption have not reached the network design assumptions for 1990s.¹⁹

¹⁹ http://data.worldbank.org/indicator/EG.USE.ELEC.KH.PC?locations=GE&name_desc=false&view=chart

6 Synopsis and Conclusions

Assessing the technical and exploitable potential for BAPVs depends on a series of factors, the most important ones being the availability of robust and reliable data for the urban terrain and for the building stock, from the types of roofs to their bearing capacity and from the mutual shading to microclimate conditions.

It also depends on understanding the soft parameters that make the transition from technical to realistically exploitable potential possible: Ownership of buildings and patterns of roof usage are frequently critical for the success of promoting PVs, although they are not always clearly manifested. The people's attitude towards a –still- capital intensive renewable energy systems is important, especially when linked with retail prices of electricity and with the available income, both for private and for commercial applications. The importance of regulatory issues and procedures, most important of which is licensing, should not be underestimated.

Featuring local capacities for the planning, installation and maintenance can be of high significance, especially in the initial steps of the technology. The lack of adequate support, especially in remote areas, can easily discredit the technology.

It is against this background that one should evaluate and utilise the findings of this component, which determined the solar potential and the respective total annual energy production. It should act as a maximum achievable goal under best possible conditions.

Applying the experience obtained since the early 2000s in the EU, and particularly in Southern Europe with its tight funding conditions and it's not always helpful regulatory framework, a realistic strategy would be to aim for utilizing 25% of this potential within a period of 5 to 10 years.

It lies in the assessment of each country's specific regulatory and economic conditions to determine the mixture of policy tools (FiTs, soft loans, subsidies) needed to achieved specific targets (in residential and public buildings, in apartment blocks and in single family houses).

7 References

- Akbari, H., Shea Rose, L., & Taha, H., 2003, Analyzing the land cover of an urban environment using high-resolution orthophotos. *Landscape and Urban Planning* 63 1, pp. 1-14.
- Blaschke, T., Lang, S., Lorup, E., Strobl, J., & Zeil, P., 2000. Object-oriented image processing in an integrated GIS/remote sensing environment and perspectives for environmental applications. In A. Cremers & K. Greve (Eds.). *Environmental information for planning, politics and the public* (Vol. 2, pp. 555–570). Germany, Metropolis-Verlag: Marburg.
- Busch, A., 1998. Revision of built-up areas in a GIS using satellite imagery and a GIS. *The international archives of the photogrammetry. Remote Sensing and Spatial Information Sciences*, XXXII(4), 91–98.
- Carneiro, C., Morello, E., Desthieux, G., 2009. Assessment of solar irradiance on the urban fabric for the production of renewable energy using LiDAR data and image processing techniques. In: *AGILE Conf.* 83–112.
- Deng, C. and Wu, C. BCI: A Biophysical Composition Index for Remote Sensing of Urban Environments. *Remote Sensing of Environment*. 2012. 127; 247-259.
- Digital Globe, 2016, http://www.digitalglobe.com/index.php/48/Products?product_id=27.
- Gadsden, S., Rylatt, M., Lomas, K., Robinson, D., 2003a, Predicting the urban solar fraction: a methodology for energy advisers and planners based on GIS, *Energy and Buildings* 35 1, pp. 37-48.
- Gadsden, S., Rylatt, M., Lomas, K., 2003b, Predicting the urban solar fraction: a methodology for energy advisers and planners based on GIS, *Energy and Buildings* 35 1, pp. 37-48.
- Gagnon, P., R. Margolis, J. Melius, C. Phillips, and R. Elmore. 2016. Rooftop Solar Photovoltaic Technical Potential in the United States: A Detailed Assessment, Technical Report NREL/TP-6A20-65298, National Renewable Energy Laboratory, www.nrel.gov/publications
- Ghosh, S. and R. Vale, 2006, Domestic energy sustainability of different urban residential patterns: A New Zealand approach, *International Journal of Sustainable Development*, 9(1), p16–37.
- Griffiths, P., Hostert, P., Gruebner, O., and Linden, S. 2010. Mapping Megacity Growth with Multi-Sensor Data. *Remote Sensing of Environment*. 114 (2) 426-439.
- Guindon, B., Y. Zhang and C. Dillabaugh, 2004, Landsat urban mapping based on a combined spectral-spatial methodology, *Remote Sensing of Environment*, 92(2), p218– 232.
- Ioannidis, C., Psaltis, C., & Potsiou, C. , 2009. Towards a strategy for control of suburban informal buildings through automatic change detection. *Computers, Environment and Urban Systems*, 33, (1), 64-74.
- Izquierdo, S., Rodrigues, M., & Fueyo, N., 2008. A method for estimating the geographical distribution of the available roof surface area for large-scale photovoltaic energy-potential evaluations, *Solar Energy*, 82, pp. 929-939.

- Jochem, A., Hofle, B., Rutzinger, M., Pfeifer, N., 2009. Automatic roof plan detection and analysis of airborne lidar point clouds for solar potential assessment. *Sensors* 9, 5241–5262.
- Kaimaris, D., P. Patias, 2016. Population Estimation in an Urban Area with Remote Sensing and Geographical Information Systems, *International Journal of Advanced Remote Sensing and GIS*, Vol. 5, No. 6, 1795-1812, Cloud Publications, ISSN 2320 – 0243
- Kaimaris D., Patias P., 2016. Identification and Area Measurement of the Built-up Area with the Built-up Index (BUI), *International Journal of Advanced Remote Sensing and GIS*, Vol 5, No 6: 1844-1858, Cloud Publications, ISSN 2320 – 0243.
- Kamusoko, C., Gamba, J., and Murakami, H. 2013. Monitoring Urban Spatial Growth in Harare Metropolitan Province, Zimbabwe. *Advances in Remote Sensing*. 2; 322-331.
- Karteris M. and Papadopoulos A.M. (2013), Legislative framework for photovoltaics in Greece: a review of the sector's development, *Energy Policy*, 55, 296-304
- Karteris M., Slini T. and Papadopoulos A.M. (2013), Urban solar energy potential in Greece: A statistical calculation model of suitable built roof areas for photovoltaics, *Energy and Buildings*, 62, 459-468
- Karteris M., Theodoridou I., Mallinis G. and Papadopoulos A.M. (2014), Façade photovoltaic systems on multifamily buildings: An urban scale evaluation analysis using geographical information systems, *Renewable & Sustainable Energy Reviews*, 39, 912-933
- Kassner, R., Koppe, W., Schuttenberg, T., Bareth. G., 2008. Analysis of the solar potential of roofs by using official lidar data. *The International Archives of the Photogrammetry, Remote Sensing and Spatial Information Sciences*. Vol. XXXVII. Part B4. Beijing 2008. 399–403.
- Kaufmann, R.K., Seto, C.K., Schneider, A., Liu, Z., Zhou, L., and Wang, W. 2007. Climate Response to Rapid Urban Growth: Evidence of a Human-Induced Precipitation Deficit. *Journal of Climate*. 20; 2299-2306.
- Kraines, S. B., D.R.Wallace, Y. Iwafune, Y.Yoshida, T. Aramaki and K. Kato, 2001, An integrated computational infrastructure for a virtual Tokyo: Concepts and examples, *Journal of Industrial Ecology*, 1, p35–54.
- Kraines, S.B. and D.R. Wallace, 2003, Urban sustainability technology evaluation in a distributed object-based modelling environment, *Computers, Environment and Urban Systems*, 27(2), p143–161.
- Lehmann, H. and Peter, S., 2003. Assessment of roof & façade potentials for solar use in Europe. Institute for sustainable solutions and innovations (ISUSI), Aachen, Germany. <http://sustainable-soli.com/downloads/roofs.pdf>
- Levinson, R., Akbari, H., Pomerantz, M., Gupta, S., 2009. Solar access of residential rooftops in four Californian cities. *Solar Energy* 83, 2010– 2035.
- Lu, D. and Weng, Q. 2006. Use of Impervious Surface in Urban Land-Use Classification. *Remote Sensing of Environment*. 102; 146-160.
- Lukac, N., D. Zlaus, S. Seme, B. Zalik, G. Štumberger, 2013. Rating of roofs' surfaces regarding their solar potential and suitability for PV systems, based on LiDAR data, *Applied Energy* 102, 803–812.

- Masek, J.G., Lindsay, F.E., and Goward, S.N. 2000. Dynamics of Urban Growth in the Washington DC Metropolitan Area, 1973-1996, from Landsat Observations. *International Journal of Remote Sensing*. 21; 3473-3486.
- Melesse, A.M., Weng, Q., Thenkabail, P.S., and Senay, G.B. 2007. Remote Sensing Sensors and Applications in Environmental Resources Mapping and Modelling. *Sensors*. 7; 3209-3241.
- Melgani, F. and Bruzzone, L. 2004. Classification of Hyper-spectral Remote Sensing Images with Support Vector Machines. *IEEE Transactions on Geoscience and Remote Sensing*. 42 (8) 1778-1990.
- Nguyen, H., J. Pearce, 2012. Incorporating shading losses in solar photovoltaic potential assessment at the municipal scale, *Solar Energy* 86, 1245-1260
- Nguyen, H., J. Pearce, 2013. Automated quantification of solar photovoltaic potential in cities, *International review for spatial planning and sustainable development*, Vol.1 No.1, 49-60, ISSN: 2187-3666.
- Pal, M. and Mather, M.P. 2005. Support Vector Machines for Classification in Remote Sensing. *International of Remote Sensing*. 26 (5) 1007-1011.
- Pratt, W. K., 2001. *Digital image processing (3rd ed.)*. New York, USA: John Wiley & Sons Inc (pp. 289–294).
- Psaltis, C., & Ioannidis, C., 2008. Simple Method for Cost-Effective Informal Building Monitoring. *Surveying and Land Information Science*, 68, 65-79.
- Robinson, D., 2006. Urban morphology and indicators of radiation availability. *Solar Energy* 80, 1643–1648.
- Ratti, C. and P. Richens, 1999, Urban texture analysis with image processing techniques. Paper presented at the CAADFutures '99 Conference. Atlanta.
- Rylatt, M., S. Gadsden and K. Lomas, 2001, GIS-based decision support for solar energy planning in urban environments, *Computers, Environment and Urban Systems*, 25(6), p579–603.
- Satellite Imaging Corp. 2016, <http://www.satimagingcorp.com/>
- Seto, K.C. and Liu, W. 2003. Comparing ARTMAP Neural Network with the Maximum-Likelihood Classifier Detecting Urban Change. *Photogrammetric Engineering and Remote Sensing*. 69 (9) 981-990.
- Sorensen, B., 2001. GIS management of solar resource data. *Solar Energy Materials and Solar Cells* 67 (1–4), 503–509.
- Stamou, A., P. Patias, A. Papadopoulos, I. Theodoridou, 2012, Study and Analysis of WorldView-2 satellite imagery for evaluating the energy efficiency of the urban area of Kalamaria, Greece, *South-Eastern European Journal of Earth Observation and Geomatics [SEJoEOG]*, Vol 1, No 1 (2012) pp. 41-54
- Stamou A., Manika S., Patias P., 2013, Estimation of land surface temperature and urban patterns relationship for urban heat island studies, *Proceedings of International Conference on "Changing Cities": Spatial, morphological, formal & socio-economic dimensions*, June 2013, Skiathos, Greece, p.2007-2013, ISBN 978-960-6865-65-7, Grafima Publ.

- Stamou, A., P. Patias, M. Tsakiri-Strati, O. Georgoula, 2014a, Improved urban land cover mapping using WorldView-2 imagery, for estimating the geographical distribution of the available roof surface area for photovoltaic potential applications in urban environments, [SEEJoEOG], Vol 3, No 2S (2014), pp. 355-358
- Stamou, A., P. Patias, 2014b. Analyzing the Relationship between Urban Patterns and Land Surface Temperature Using WorldView-2 and Landsat-ETM+, *Journal of Earth Science and Engineering* 4 (2014) 195-202.
- Taubenbock, H., A. Roth and S. Dech, 2008, Linking structural urban characteristics derived from high resolution satellite data to population distribution. In V. Coors, M. Rumor, E. M. Fendel, & S. Zlatanova (Eds.), *Urban and regional data management* (pp. 35–45). London, Taylor & Francis Group.
- Ukwattage, L.N. and Dayawansa, K.D.N. 2012. Urban Heat Islands and the Energy Demand: An Analysis for Colombo City of Sri Lanka Using Thermal Remote Sensing Data. *International Journal of Remote Sensing and GIS*. 1 (2) 124-131.
- United States Geological Survey, 2016, www.usgs.gov
- Walter, V., 2004. Object-based classification of remote sensing data for change detection. *ISPRS Journal of Photogrammetry and Remote Sensing*, 58(3-4), 225–238.
- Ward, D., Phinn, R.S., and Murray, T.A. 2000. Monitoring Growth in Rapidly Urbanizing Areas using Remotely Sensed Data. *Professional Geographers*. 52 (3) 371-386.
- Weng, Q., 2008: Remote Sensing of Impervious Surfaces: An Overview. In *Remote Sensing of Impervious Surfaces*; Weng, Q., (ed.) Boca Raton, FL, USA: CRC Press, Taylor & Francis Group.
- Wiginton, L., H. Nguyen, J. Pearce, 2010. Quantifying Solar Photovoltaic Potential on a Large Scale for Renewable Energy Regional Policy, *Computers, Environment and Urban Systems* 34, (2010) pp. 345-357. <http://dx.doi.org/10.1016/j.compenvurbsys.2010.01.001>
- Xian, G. and Crane, 2005. M. Assessment of Urban Growth in the Tampa Bay Watershed using Remote Sensing Data. *Remote Sensing of Environment*. 97 (2) 203-205.
- Xian, G. and Crane, M. 2006. An Analysis of Urban Thermal Characteristics and Associated Land Cover in Tampa Bay and Las Vegas using Satellite Data. *Remote Sensing of Environment*. 104; 147-156.
- Xu, H. 2008. A New Index for Delineating Built-Up Land Features in Satellite Imagery. *International Journal of Remote Sensing*. 29; 4269-4276.
- Yang, X. .2011. Parameterizing Support Vector Machines for Land Cover Classification. *Photogrammetric Engineering and Remote Sensing*. 77 (1) 27-37.
- Yuan, F., Sawaya, E.K., Loeffelholz, C.B., and Bauer, E.M. 2005. Land Cover Classification and Change Analysis of the Twin Cities (Minnesota) Metropolitan Area by Multitemporal Landsat Remote Sensing. *Remote Sensing of Environment*. 98 (2-3) 317-328.
- Zhang, Q., Wang, J., Peng, X., Gong, P., and Shi, P. 2002. Urban Built-Up Land Change Detection with Road Density and Spectral Information from Multi-Temporal Landsat TM Data. *International Journal of Remote Sensing*. 23 (15) 3057-3078.


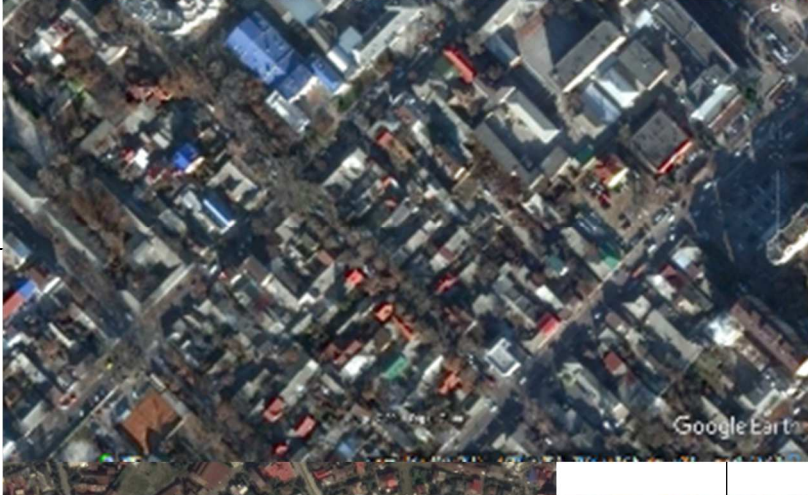
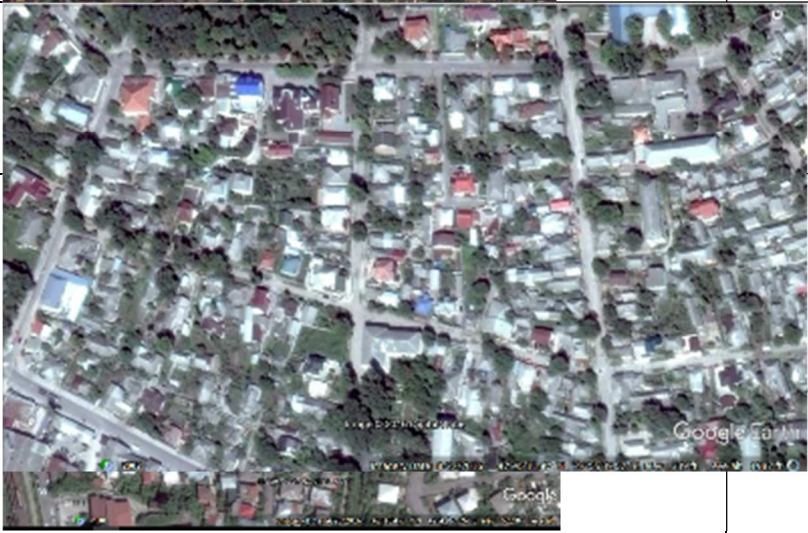
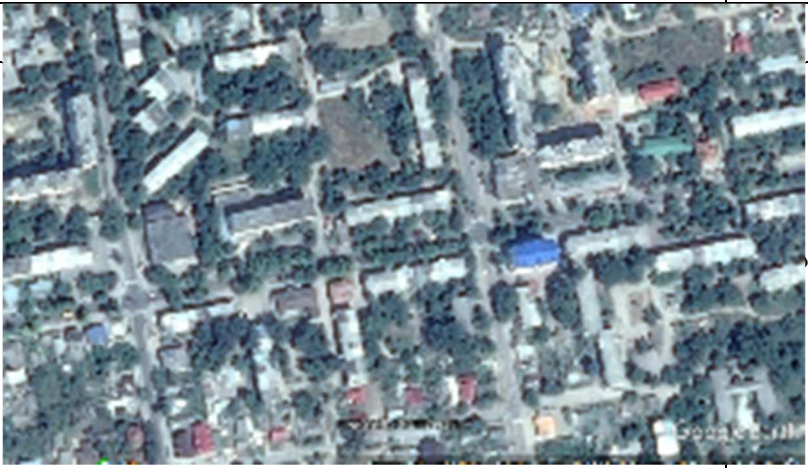
Zhou, X., Jancsó, T., Chen, C., and Veróne, W.M., 2012. Urban Land Cover Mapping Based on Object Oriented Classification using WorldView 2 Satellite Remote Sensing Images. Theme Paper for the International Scientific Conference on Sustainable Development & Ecological Footprint, 1-10, Sopron, Hungary.


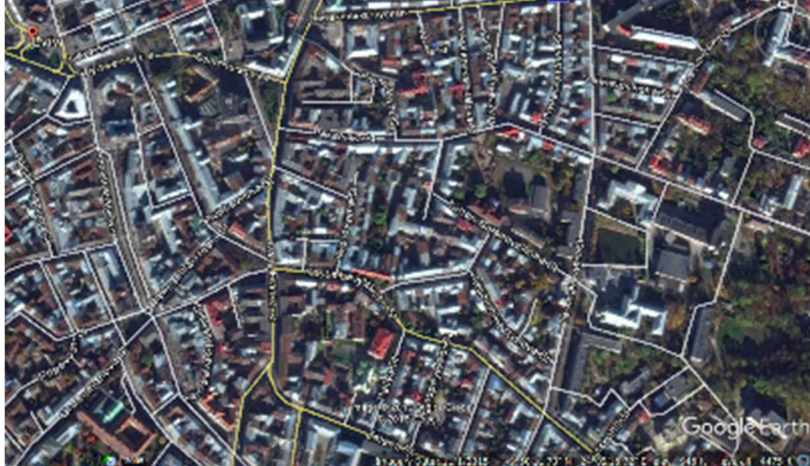

8 Annex: Summary of surface-related findings


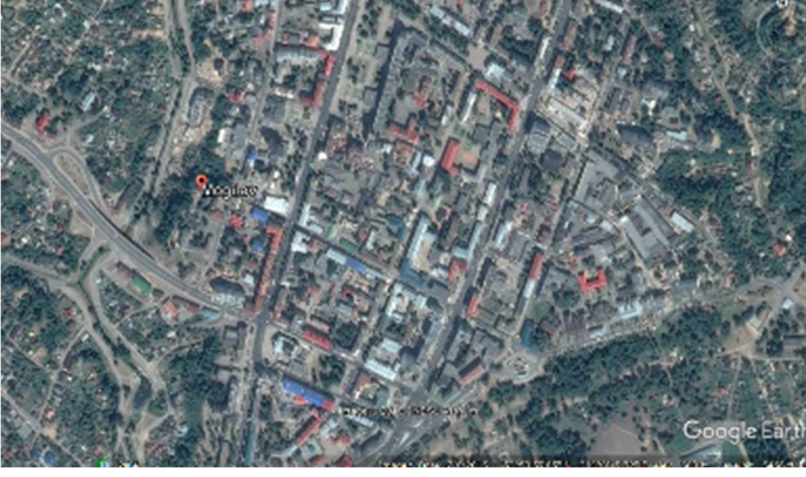
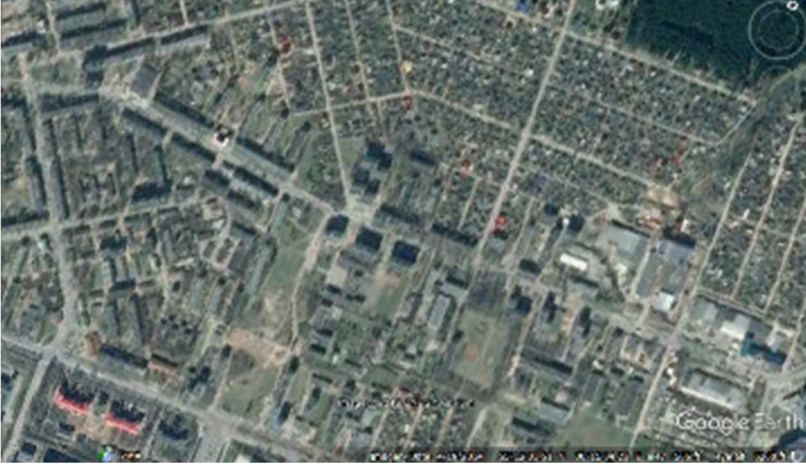
The aggregated results are given in the next table:


Country	City	Total building roof area (m ²)	population (ca)	m ² /ca	Method of calculation	
Georgia	Tbilisi	24,634,075	1,112,000	22	Existing GIS/Cadastre	
	Batumi	2,879,820	153,000	19		
	Kutaisi	4,816,095	201,000	24		
	Rustavi	2,904,118	125,000	23		
Moldova	Chisinau	2,339,686	500,000	5		
	Balti	286,000	78,000	4		
	Cahul	73,000	41,000	2		
Armenia	Yerevan	23,494,972	1,100,000	21		Satellite imagery
	Vanadzor	3,943,260	87,000	45		
	Gyumri	3,263,584	122,000	27		
Azerbaijan	Baku	43,260,600	2,120,000	20		
	Sumgait	4,428,452	300,000	15		
	Ganja	3,808,980	325,000	12		
Belarus	Minsk	41,663,680	2,000,000	21		
	Mogilev	8,822,708	375,000	24		
	Vitebsk	10,496,612	370,000	28		
Ukraine	Kyiv	59,075,200	3,000,000	20		
	Odesa	30,700,548	1,020,000	30		
	Lviv	17,659,260	730,000	24		


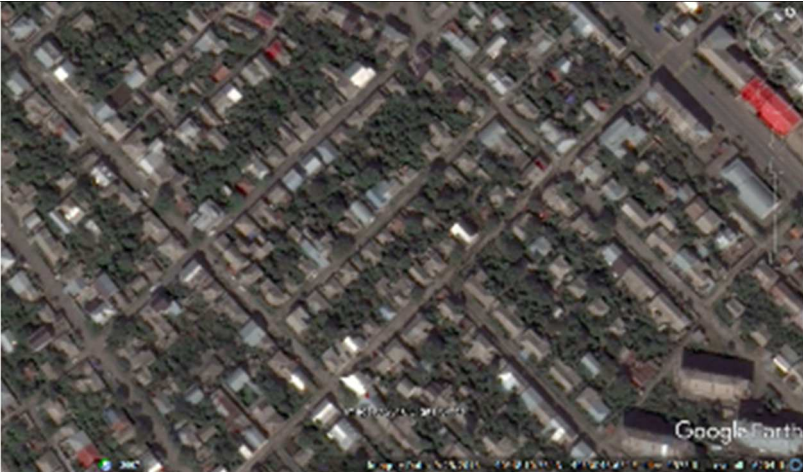
In all above cities the vast majority of the rooftop types is “tilted tiles” with only a small percentage of flat roofs. The following tables show typical urban blocks and typical rooftop types.

Georgia		Estimated % of flat roofs
		
		Estimated % of flat roofs
		< 10%
Tbilisi		<p>Mainly industrial</p> <p>< 20%</p> <p>Mainly industrial and new constructions</p>
Chisinau		
Batumi		
		
Kutaisi		< 5%
Balti		
		
Babtavi		<p>< 20%</p> <p>Mainly industrial and new constructions</p>

	Ukraine	Estimated % of flat roofs
Kyiv		<p>< 50%</p> <p>Mainly industrial and new constructions</p>
Lviv		<p>< 20%</p> <p>Mainly industrial and new constructions</p>
Odessa		<p>< 10%</p> <p>Mainly industrial and new constructions</p>

	Belarus	Estimated % of flat roofs
Minsk		<p>< 20%</p> <p>Mainly industrial and new constructions</p>
Mogilev		<p>< 10%</p> <p>Mainly industrial and new constructions</p>
Vitebsk		<p>< 10%</p> <p>Mainly constructions new</p>

	Azerbaijan	Estimated % of flat roofs
Baku		<p>< 10%</p> <p>Mainly industrial and new constructions</p>
Sumgait		<p>< 5%</p>
Ganja		<p>< 5%</p>

	Armenia	Estimated % of flat roofs
Yerevan		< 5%
Gyumri		< 5%
Vanadzor		< 5%